

UTRECHT UNIVERSITY

Master Thesis

The Technical and Economic Potential of Airborne Wind Energy

Heilmann Jannis

8/30/2012

STUDENT:	JANNIS HEILMANN
CONTACT:	JANNIS.HEILMANN@GMAIL.COM
STUDENT NUMBER:	3558657
COURSE NAME:	RESEARCH PROJECT ENERGY SCIENCE
DEPARTMENT:	DEPT. OF SCIENCE, TECHNOLOGY AND SOCIETY
SUPERVISOR (UU):	DR. WILFRIED VAN SARK
SUPERVISORS (FHNW):	COREY HOULE, PROF. DR. HEINZ BURTSCHER
SUPERVISOR (ALSTOM AG)	DR. GIANFRANCO GUIDATI

CONTENTS

Abstract.....	1
Preface.....	2
1 Introduction.....	3
1.1 Why wind energy?.....	3
1.2 Potential for Innovation.....	7
1.3 Airborne Wind Energy – The Major Variants.....	9
1.3.1 Airborne Wind Turbine.....	11
1.3.2 Pumping Kite Generator.....	12
1.4 Airborne versus Conventional Wind Energy.....	13
1.4.1 Tower versus Tether.....	13
1.4.2 Kite Versus Rotor Blade.....	14
1.5 Assessing a Technology’s Potential.....	14
1.6 Research Questions.....	16
1.7 Limitations.....	16
2 Background.....	18
2.1 Wind Resource Fundamentals.....	18
2.1.1 Wind Speed Distribution.....	18
2.1.2 Wind Shear.....	19
2.1.3 Temporal Variations.....	20
2.2 Aerodynamics Fundamentals.....	21
2.3 Efficiency Considerations.....	21
2.3.1 Material Efficiency.....	22
2.4 Cost of Energy Analysis.....	24
2.5 Electricity Market and Feed-in Tariffs.....	24
2.6 Key References.....	25
3 Methodology.....	30
3.1 System Design.....	30
3.1.1 Assumptions.....	31
3.1.2 Machine Design.....	31
3.1.3 Kite Scenarios.....	32
3.2 Performance Simulation Development.....	34
3.2.1 Performance model.....	34
3.2.2 Implementation.....	36
3.2.3 Output.....	36
3.3 Cost Analysis.....	37
3.3.1 Uncertainty.....	38
3.3.2 Cost Model.....	38

3.3.3	Currency.....	41
3.3.4	Fixed Charge Rate	42
3.3.5	Revenues.....	42
3.4	Wind Modelling and Annual Energy Production.....	44
3.4.1	Wind Data.....	44
3.4.2	Calculation Methods.....	44
3.4.3	Output.....	45
4	Parameter Study Results.....	47
4.1	Design Parameter Study	47
4.1.1	Projected Kite Area.....	47
4.1.2	Nominal Generator Power.....	49
4.1.3	Nominal Tether Force (Scaling).....	51
4.1.4	Optimal Design.....	53
4.2	Operational Parameter Study.....	53
4.2.1	Tether angle.....	53
4.3	Current Kite Scenario.....	54
4.4	Gearbox Option.....	57
4.5	Secondary Parameters Sensitivity.....	58
5	Comparison to Conventional Turbine.....	61
6	Wind Modeling Results	65
6.1	Wind Shear Exponent	65
6.2	Mean Wind Speed	65
6.3	Swiss Mountain Site.....	68
6.4	Variable Tether Angle	68
7	Experimental Results.....	72
8	Summary of Results.....	74
9	Conclusions	76
9.1	Research Questions.....	76
9.2	Consequences.....	76
9.3	Limitations.....	77
10	Future Research	78
11	Appendix	79
11.1	Performance Model.....	79
11.1.1	Matlab Files.....	79
11.1.2	Alternative Performance Model.....	87
11.2	Annual Energy Calculation.....	89
11.2.1	Matlab Files.....	89
11.3	Machine Spacing.....	92

11.4	Component Cost Model	94
11.4.1	Kite	94
11.4.2	Mechanical Systems	97
11.4.3	Electrical Systems	99
11.4.4	Control and monitoring	102
11.5	Balance-of-Station Cost	104
11.5.1	Summary	104
11.5.2	Foundation/support structure	105
11.5.3	Transportation	105
11.5.4	Roads, civil work	106
11.5.5	Assembly and installation	107
11.5.6	Electrical Interface, connections	109
11.5.7	Miscellaneous infrastructure	109
11.5.8	Engineering, Permits	109
11.6	Levelized Replacement Cost	111
11.6.1	Tether	111
11.6.2	Kite	113
11.7	Operation and Maintenance Cost	115
11.8	Land Lease Cost	116
11.9	Calculating Levelized Cost	116
11.10	Electricity Market	117
12	References	118

ABSTRACT

In this thesis, a methodology is developed, to assess the feasibility of airborne wind energy. A particular concept called pumping kite generator (PKG), is analyzed. Previous works on this topic suggest that the cost of energy of such systems can be far lower than for conventional wind energy, mainly because higher altitudes can be reached and material can be saved.

The cost of energy of pumping kite generator designs in the 1 to 2 MW range is calculated. For this purpose, power curves are calculated by using a simple and quick performance simulation. The power curves are then used to calculate the annual energy production based on either a Rayleigh distribution or wind data from a weather model. For each component of the pumping kite generator, two cost functions are developed: A lower and a higher limit for the expected cost. Assuming a normal distribution of component costs, the probability density function for the total cost or total annual cost can be calculated as a function of several design parameters.

The levelized cost of energy of a baseline design is determined and its sensitivity to changes of various design parameters, the site specific wind conditions and the operating altitude is evaluated.

It is shown that the basic design parameters – kite area, nominal generator power and nominal tether force – of the baseline design, are within a robust optimum range for the chosen baseline wind conditions. The kite properties, especially its lifetime and coefficient of lift are shown to be the most important factors for the feasibility of the pumping kite concept.

A comparison to a large onshore wind farm with 1.5 MW horizontal axis wind turbines (HAWTs) shows that PKGs can be cost competitive in this sector. The technology can be economical under current subsidy schemes and at good sites even without government support. However, the comparison also suggests, that the cost of airborne wind energy will stay in a similar range as conventional wind energy in the mid-term.

It is concluded that addressing niche energy markets in remote areas or with complex terrain, where PKGs have great advantages, can play an important role when introducing the technology. Low wind sites and deep offshore projects look the most promising for the long term.

In addition the possibility of increasing the capacity factor of a PKG at low extra cost can be a crucial factor when competing with conventional wind turbines in a free market, without feed-in tariffs in a grid with high wind power penetration.

PREFACE

The present thesis was conducted within the framework of the SwissKitePower-Project in the Electrical Power Processing Group of the Institute of Aerosol and Sensor Technology at the University of Applied Sciences Northwestern Switzerland (FHNW). SwissKitePower is a collaborative research and development project of FHNW, the Swiss Federal Institute of Technology (ETH), the Swiss Federal Laboratories for Materials Testing and Research (EMPA) and Alstom Switzerland AG. The groups from the different institutions meet regularly to exchange knowledge on the involved research areas of mechanical and power engineering, wing design, control algorithms, sensor technology and system design.

I would like to thank all participants of those meetings for their inputs and feedback – especially Dr. Rolf Luchsinger and Sean Costello for their support with developing a performance simulation. Roland Verheul provided valuable advice on cost functions and parameters of current and future kite concepts. Corey Houle, Nick Butcher and Tobias Strittmatter supported the present work through many fruitful and inspiring discussions.

Finally, I owe thanks to my supervisors Dr. Wilfried van Sark from Utrecht University, Dr. Gianfranco Guidati from Alstom Switzerland AG and Prof. Dr. Heinz Burtscher and Corey Houle from FHNW.

1 INTRODUCTION

1.1 WHY WIND ENERGY?

In order to reduce greenhouse gas emissions and the dependency on oil and natural gas imports, many countries are now trying to increase the share of renewable power in their electricity grid. The market for renewable technology is growing rapidly and there are a large number of options which all have their pros and cons. However, there are a number of reasons why many see an especially large potential for wind power in the near future.

In the US and in Europe, there are regions where around 9 m/s average wind speeds and an average power density higher than 1000 Watt per m² of swept area is reached (see Figure 1-1 and Figure 1-2, (U.S. Department of Energy, 2011) and (Risø National Laboratory, 2011)). This is much higher than most other renewable resources such as solar power or biogas.

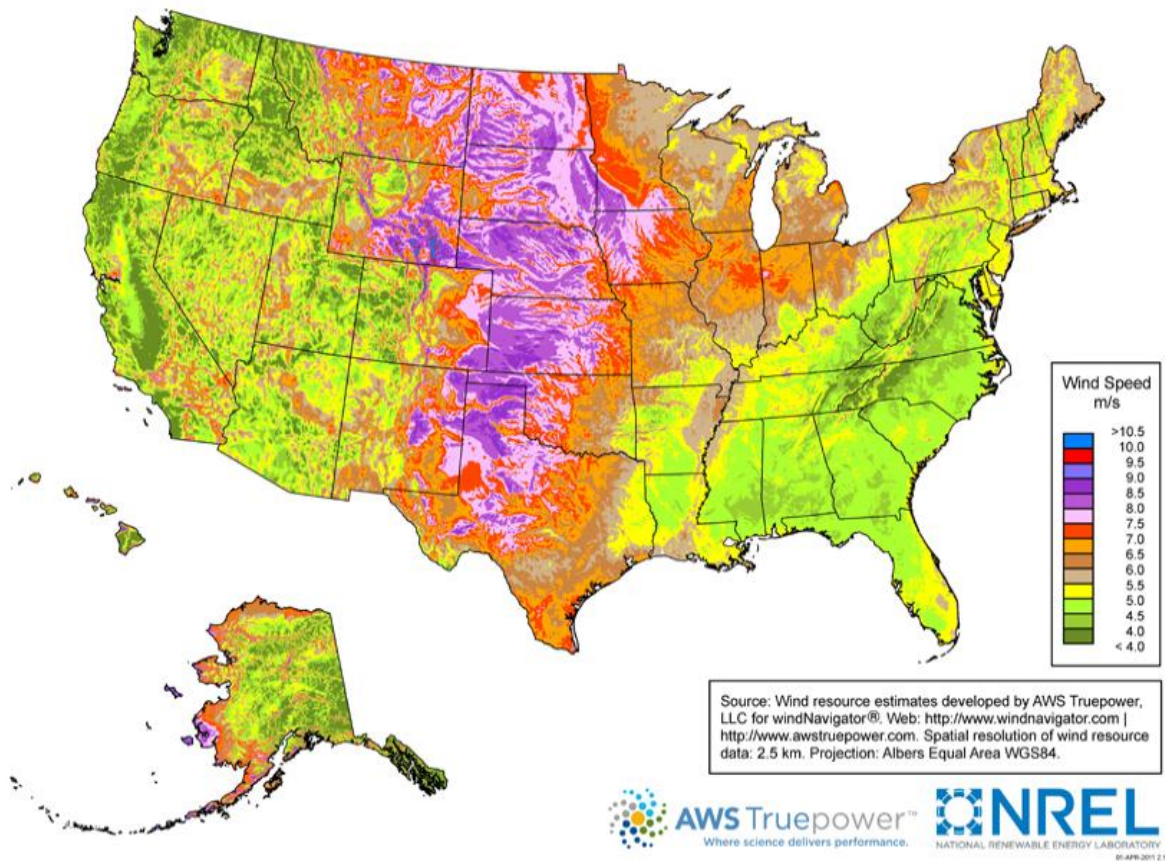
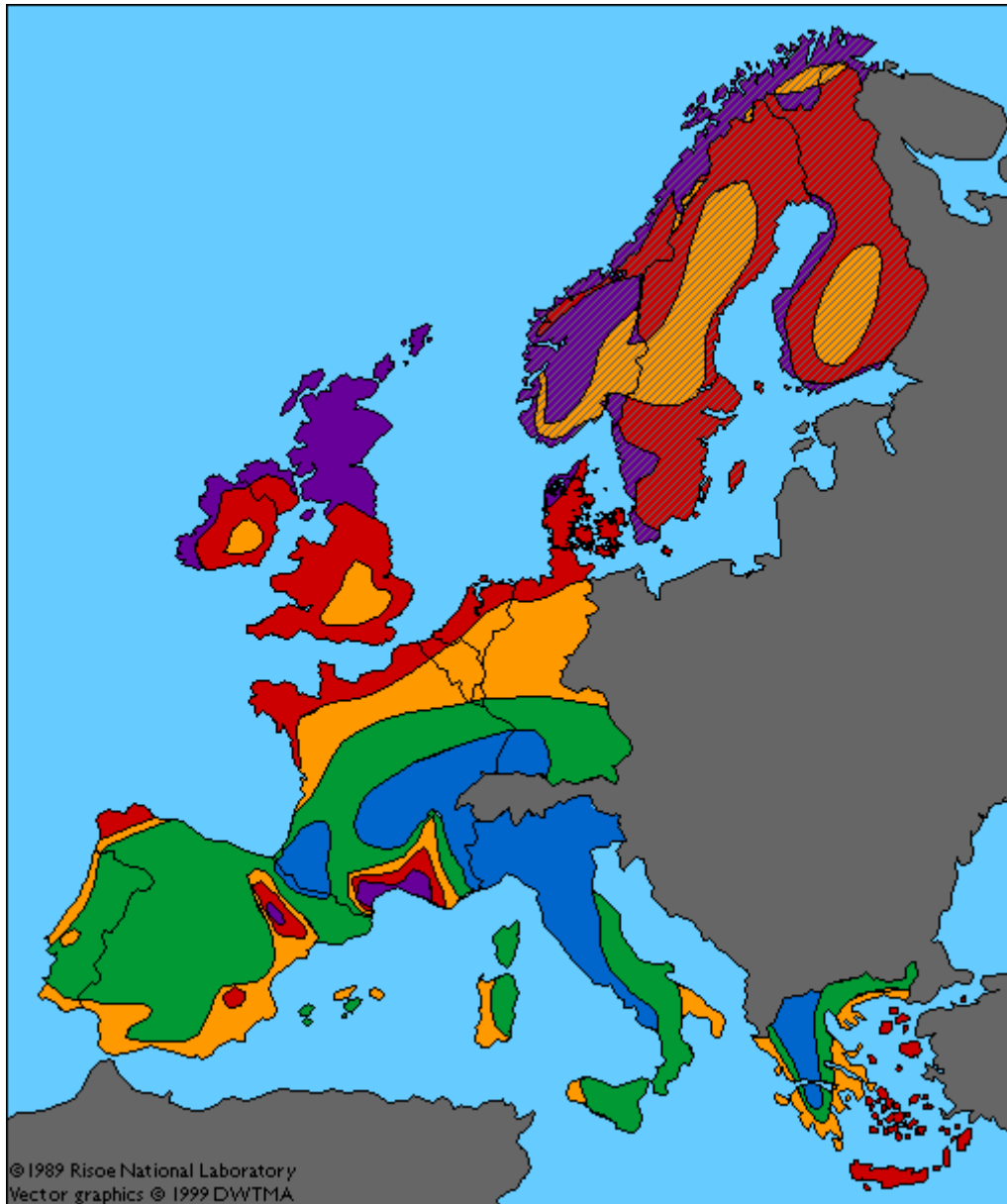


FIGURE 1-1 US WIND RESOURCES, WWW.WINDPOWERINGAMERICA.GOV



Wind resources at 50 meters above ground level for five different topographic conditions:
1) Sheltered terrain, 2) Open plain, 3) At a coast, 4) Open sea 5) Hills and ridges.

	m/s	W/m ²	m/s	W/m ²	m/s	W/m ²	m/s	W/m ²	m/s	W/m ²
	>6.0	>250	>7.5	>500	>8.5	>700	>9.0	>800	>11.5	>1800
	5.0-6.0	150-250	6.5-7.5	300-500	7.0-8.5	400-700	8.0-9.0	600-800	10.0-11.5	1200-1800
	4.5-5.0	100-150	5.5-6.5	200-300	6.0-7.0	250-400	7.0-8.0	400-600	8.5-10.0	700-1200
	3.5-4.5	50-100	4.5-5.5	100-200	5.0-6.0	150-250	5.5-7.0	200-400	7.0-8.5	400-700
	<3.5	<50	<4.5	<100	<5.0	<150	<5.5	<200	<7.0	<400
			>7.5							
			5.5-7.5							
			<5.5							

FIGURE 1-2 EUROPEAN WIND RESOURCES, RISO NATIONAL LABORATORY

The cost of wind power has decreased rapidly during the last 30 years (see Figure 1-3). Bloomberg New Energy Finance recently reported, wind turbine prices fell under 1000 Euros per kW for the first time since 2005 (<http://bnef.com/PressReleases/view/139>). In the windier

parts of the world, wind power becomes competitive with power from fossil fuels without subsidies.

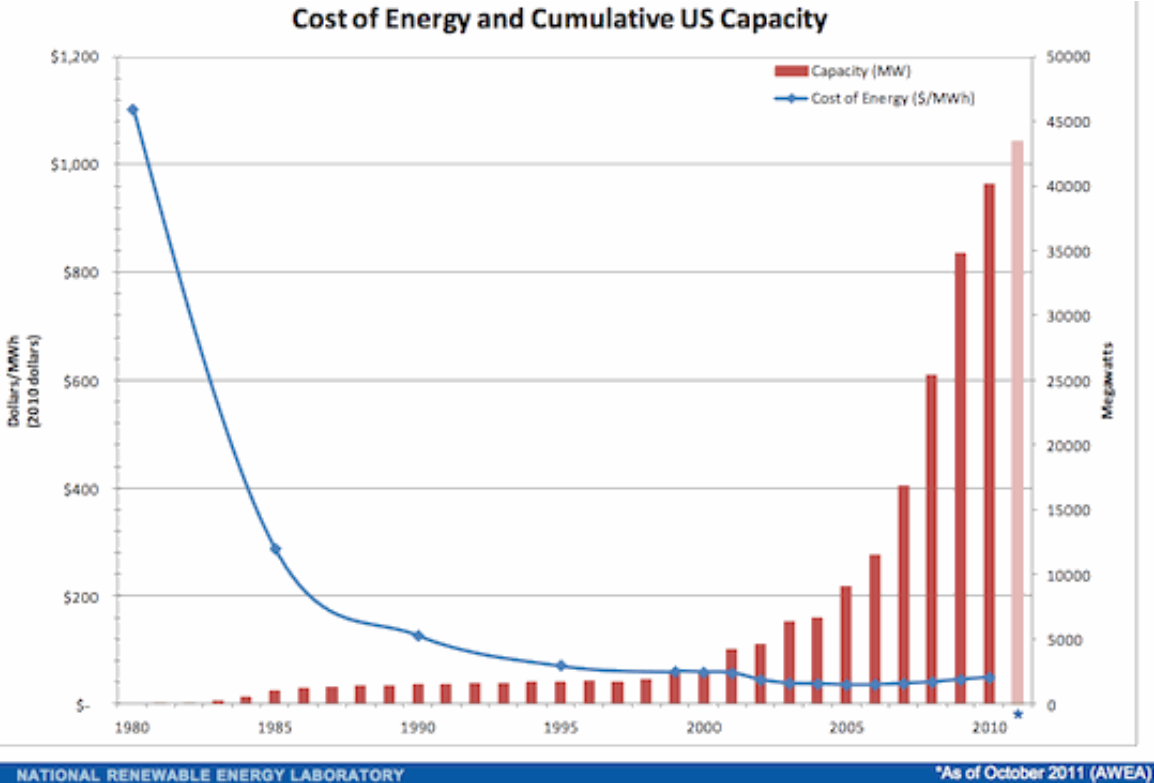


FIGURE 1-3 COE AND CUMULATIVE CAPACITY IN THE US, NREL AS CITED BY ENERGYBULLETIN¹

The largest power consumers are in the northern hemisphere. In these regions, there is generally less sun than in the south. This results in solar technology as well as growing energy crops being less economic. The regions with large wind resources however are relatively close to the regions of largest power consumption (Figure 1-4). For instance the shallow waters on the continental shelf off the east coast of the US between Massachusetts and North Carolina have a great potential for wind energy. The wind resource near this very densely populated region is about four times larger than the regions relatively high energy demand (Kempton, Archer, Dhanju, Garvine, & Jacobson, 2007).

¹ <http://www.energybulletin.net/stories/2012-03-13/nukes-hazard-one-year-after-fukushima-nuclear-power-remains-too-costly-be-major-c>

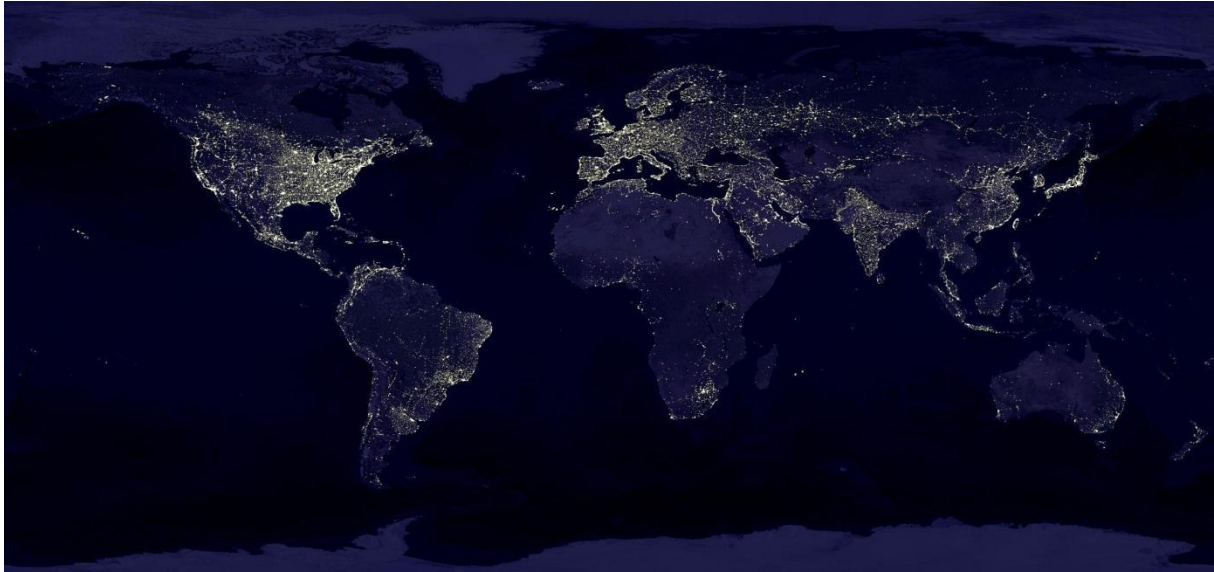
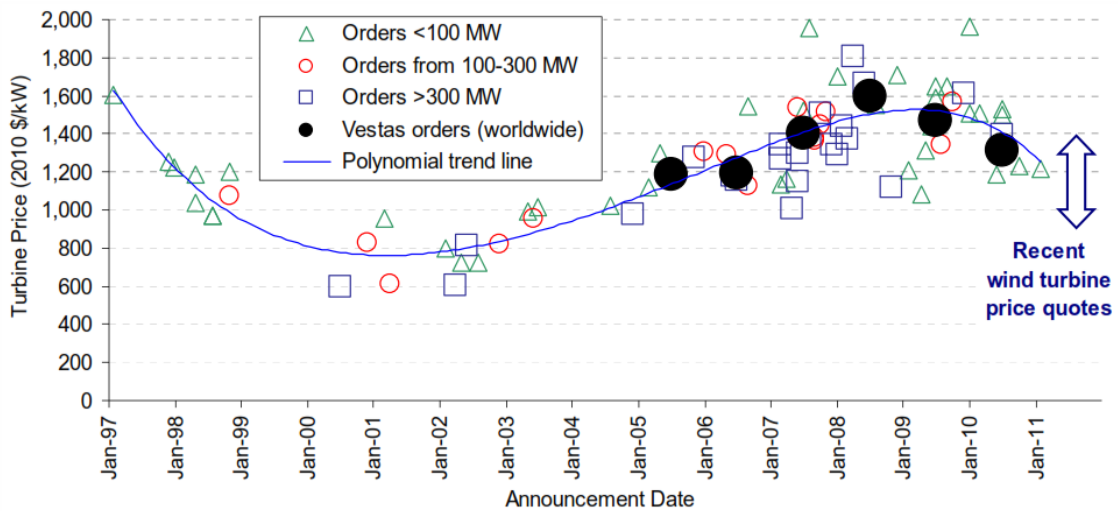


FIGURE 1-4 EARTH AT NIGHT, IMAGE BY CRAIG MAYHEW AND ROBERT SIMMON, NASA GSFC

The global resource is large enough to cover a significant amount of the world's energy needs. The German Advisory Council on Global Change (WBGU) estimates that 39,000 TWh of wind energy could be produced per year in a sustainable way (GWEC, 2009). That is about twice the global electricity demand of around 20,000 TWh (IEA, 2010). Concerning the maximum sustainable extraction rate of wind power from jet streams, researchers published estimates ranging between 7.5 TW (Miller, Gans, & Kleidon, 2011) and 1700 TW (Archer & Caldeira, 2009). The difference is due to different methodologies (free energy balance versus wind speeds as a limiting factor) and the issue is not yet resolved. However, even the lower estimate would result in an extraction limit of around three times the current electricity demand.

1.2 POTENTIAL FOR INNOVATION

Figure 1-3 shows not only that the cost of wind power has declined rapidly, but also that this cost decrease has slowed down in recent years and will almost come to a halt in the near future. Between 2001 and 2009, the prices of wind turbines even increased (Bolinger & Wiser, 2011) (see Figure 1-5). This was due to the strong demand, but also due to increasing raw material cost (BTMConsult, 2008). Some cost increase could also be justified by improvements in performance and reliability of the newer turbines.



Source: Berkeley Lab, Vestas (2011b, 2011c, 2011d), Bloomberg NEF (2011b)

FIGURE 1-5 US WIND TURBINE PRICES FROM 1997 TO 2011 (BOLINGER, 2011)

Still, it seems that wind energy technology is approaching technical and economic limits and the cost cannot decrease much further. This would not be a big problem in the current situation where subsidies are provided in many countries and there is only a small or no penalty for the intermittency of wind power. However, if it should provide a large part of electric power, subsidies will have to decrease and intermittent wind power has to be smoothed out by additional storage facilities or other means. This requires still a significant decrease of cost. In order to reach such a significant change, it seems necessary to switch to completely new approaches – at least for some parts of the turbines – instead of trying to further optimize the current technology.

As the cost increases in recent years have shown, one good opportunity for reducing cost would be to reduce material consumption. Using less material would also make regions like Europe and the US less dependent on imports for the production of wind turbines and a larger part of the added value could be generated locally. Looking at the global wind resource, we can see that the best spots are often situated in deep-sea regions for which current technology is not suited. Floating wind turbines are currently under development (Robertson & Jonkman, 2011), but the combination of dynamic loads from wind and waves poses significant problems and requires changes in many parts of the system. As proven technology is not optimized for this environment and the required adjustments might become expensive, there is a chance that more radical design changes such as the airborne wind energy concepts treated in this thesis may become feasible.

Apart from expanding the usable resource further offshore, there is a strong case for making more onshore sites usable in an economic way. The main reasons why onshore sites are not suited are: too little wind (see average power density at 120m in Figure 1-6), opposition from

residents, nature protection or limited accessibility. If those restrictions could be overcome or reduced by a new technology, wind power could be generated also in regions that are far inland from the shore and the need for energy transportation could be reduced.

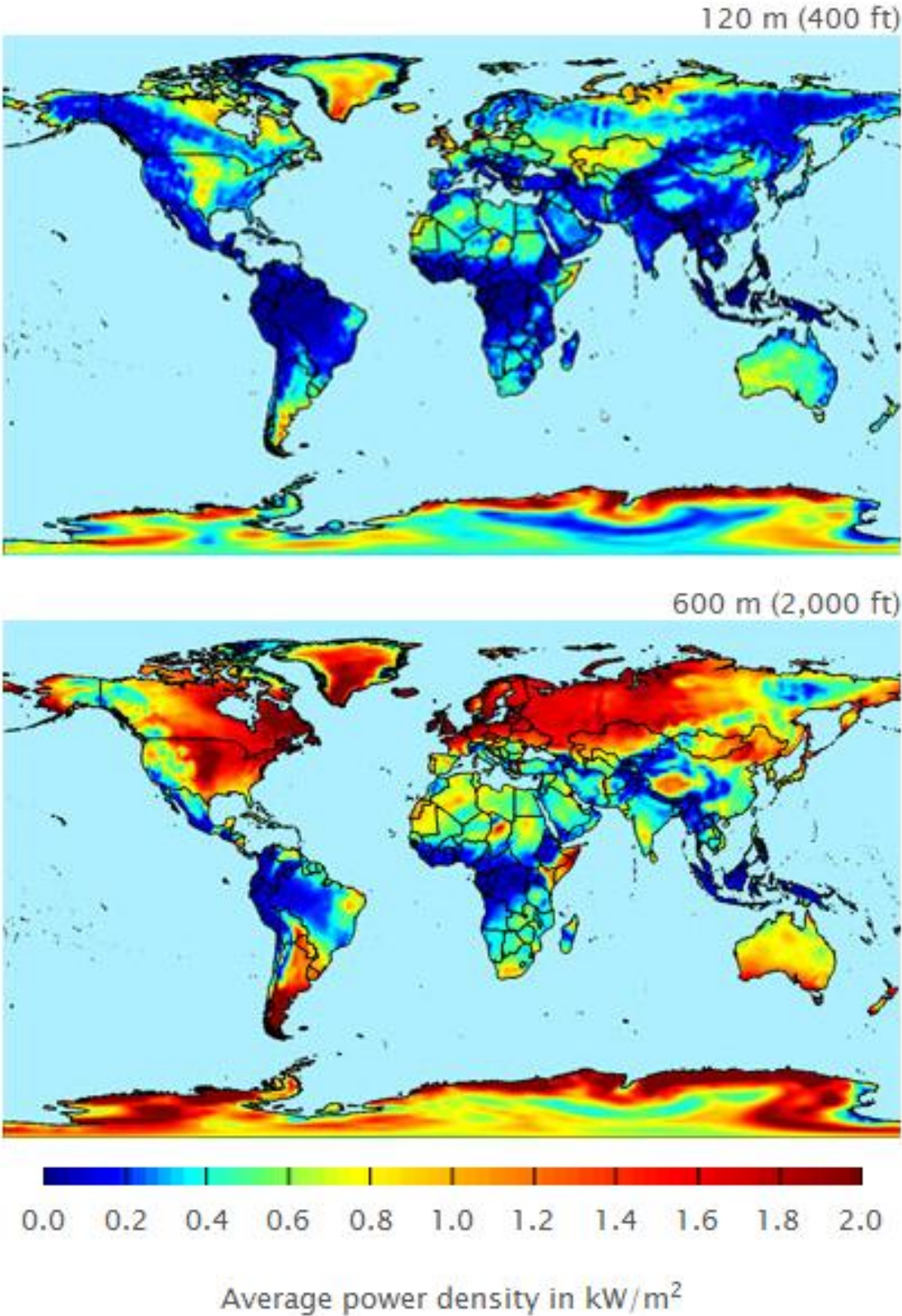


FIGURE 1-6 GLOBAL WIND RESOURCE - ANNUAL AVERAGE (JOBYENERGY.COM)

1.3 AIRBORNE WIND ENERGY – THE MAJOR VARIANTS

Airborne Wind Energy (AWE) stands for a variety of technologies that allow the extraction of wind energy by means of an airborne device, often called kite. All such machines can also be called airborne wind generators (AWGs). A number of properties can be used to categorize them.

- Crosswind motion or stationary
- Generator airborne or ground-based
- Flexible or rigid wing
- High altitude or low altitude

The device that captures the wind energy can either perform a motion perpendicular to the wind direction or stay more or less at one location relative to the ground. The crosswind motion allows drawing power from a much larger area. Most current concepts try to make use of this advantage. However, a stationary operation has the advantage of much simpler control. An example for a stationary airborne wind generator is the Flying Electric Generator, invented and built by Brian Roberts in Australia (Sky Windpower, 2012). The power output per swept area of this machine can still be higher than for a conventional wind turbine, because higher altitudes can be reached where the wind speed is higher.

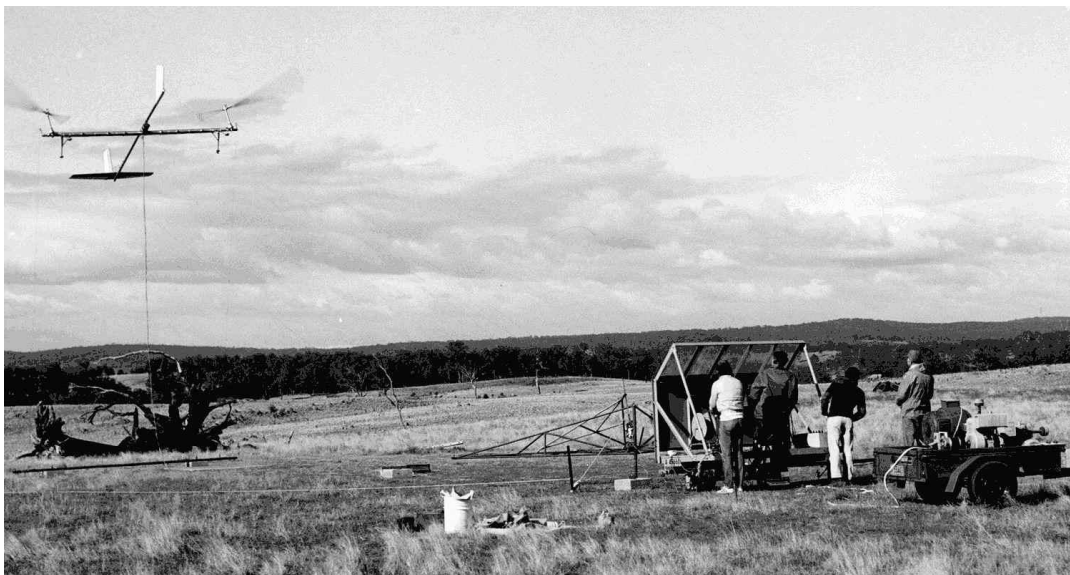


FIGURE 1-7 TESTING A PROTOTYPE 'FLYING ELECTRIC GENERATOR' (SKY WINDPOWER, 2012)

Electricity can be produced with either an airborne generator or a ground based generator. The airborne generator is driven by propellers similar to a conventional wind turbine. However the wind speed on the rotor is usually much higher – especially in the case of crosswind motion. This allows the use of high speed generators which are generally lighter and cheaper and do not require a gearbox. Ground based power generation has the advantage that the kite can be very light and potentially cheaper and that the weight of the drive train is not an issue. It can be realized by making use of the traction force of the kite. This principle will be explained in more detail below.

The kite can be made from flexible material, much like a paraglider. This design is only used when no generators have to be placed on the kite. It usually requires the use of several tether

connection points on the kite in order to spread the traction force over the surface. Alternatively, the tether can be attached on the sides only and the wing bends in direction of the traction force. A flexible wing is for instance planned to be used by the KiteGen group in Italy.



FIGURE 1-8 KITE GEN STEM, KITEGEN, ITALY (KITEGEN.COM)

The bending can be reduced by inflating parts of the wing to obtain a semi-rigid structure. Current kite surf kites use this strategy already. More advanced inflated structures for wings that can withstand much higher forces are being developed at the Center for Synergetic Structures at EMPA, Switzerland (Breuer & Luchsinger, 2010).



FIGURE 1-9 TENSAIRITY KITE FROM EMPA, SWITZERLAND (BREUER & LUCHSINGER, 2010)

Rigid wings are preferred mainly by groups who use airborne generators as those are difficult to install on a flexible structure. But there are also ground-based generator systems that use rigid wings. The project ERC Highwind at KU Leuven aims at using kites similar to glider planes and the research group works on a special launching system with a rotating arm as well as on the operation of several kites on one ground station.

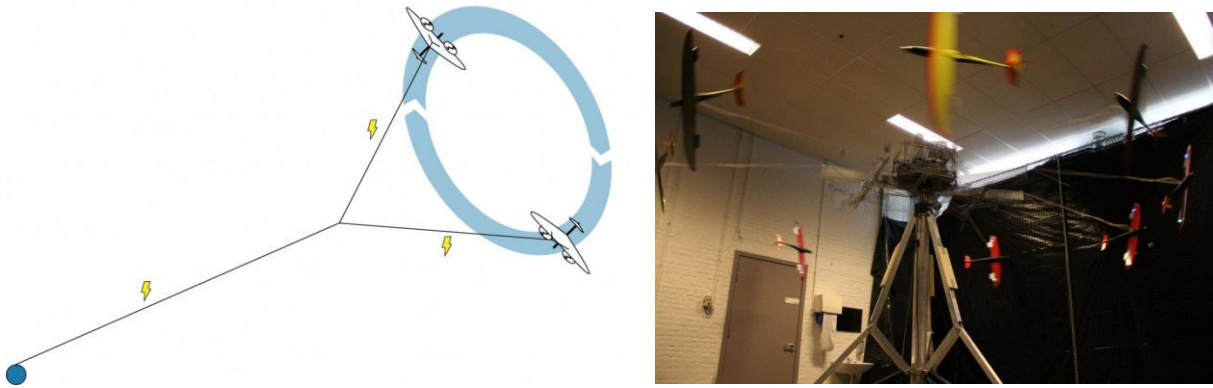


FIGURE 1-10 HIGHWIND, KU LEUVEN, BELGIUM (HIGHWIND.BE)

Concerning the altitude of operation, the focus of the different groups varies a lot. In general, groups focusing on ground-based generator concepts tend to consider lower altitudes around 100 to 500 meters. For systems with stationary operation it makes sense to go to higher altitudes, because tether drag is less important.

Another option that has mainly been proposed for pumping kite systems, but is also applicable to airborne turbines, is the use of stacked or dancing kites. On one tether several kites can be attached. They can either be attached to each other or with a short tether to a common point on the main tether. More information on such concepts can be found in (Houska, 2007).

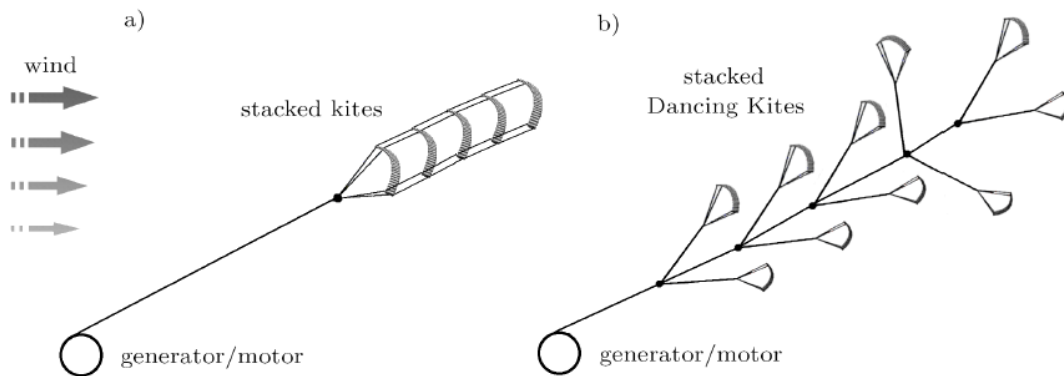


FIGURE 1-11 STACKED AND DANCING KITES, HOUSKA 2007

We will now consider two specific options in more detail: The airborne wind turbine and the pumping kite generator. For the rest of this thesis, only the pumping kite generator will be treated.

1.3.1 AIRBORNE WIND TURBINE

The biggest company working on the concept of airborne wind turbines (AWTs) is the US-based Makani Power. Concerning the properties discussed above, it can be categorized as a crosswind motion, airborne generator, rigid wing, low altitude – concept. It consists of an airplane-like kite with several propellers which produce electricity with small, lightweight generators and conduct it to the ground via the tether which also takes the lift forces of the kite. The tether length stays constant while the kite flies circles. Power is extracted from the wind through the drag of the turbines.



FIGURE 1-12 PROTOTYPE, MAKANI POWER INC., USA (MAKANIPOWER.COM)

1.3.2 PUMPING KITE GENERATOR

This thesis will treat the pumping kite generator (PKG) concept. It consists of a kite which is connected to a winch on the ground. Reeling out the tether, the lift produced by the kite moving crosswind can be used to turn the winch and produce electric power using a generator on the winch drum. Once the tether is completely reeled out, the force on the tether is reduced by stopping the crosswind motion and decreasing the angle-of-attack of the kite. Then the tether can be reeled-in again. As less energy is needed for reeling in than for reeling out, net energy can be produced (see Figure 1-13).

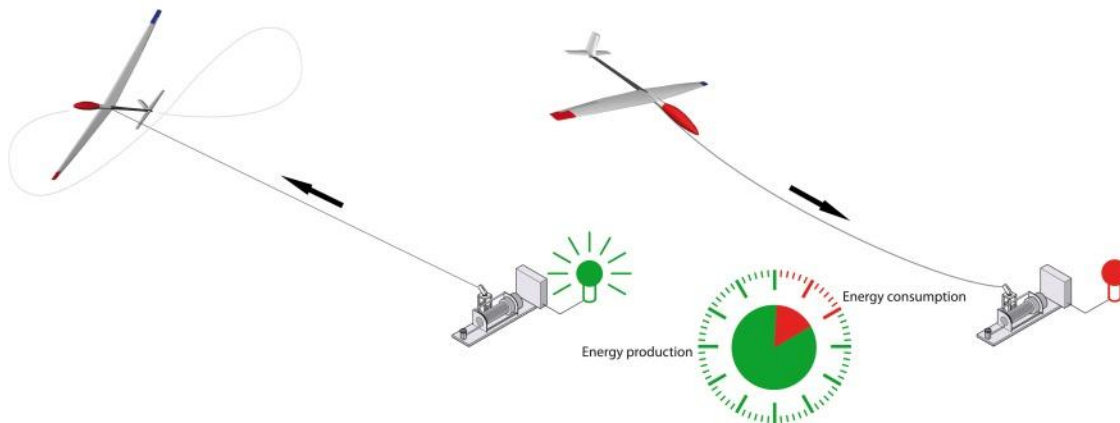


FIGURE 1-13 POWER PLANE SYSTEM BY AMPYX POWER, THE NETHERLANDS (AMPYXPOWER.COM)

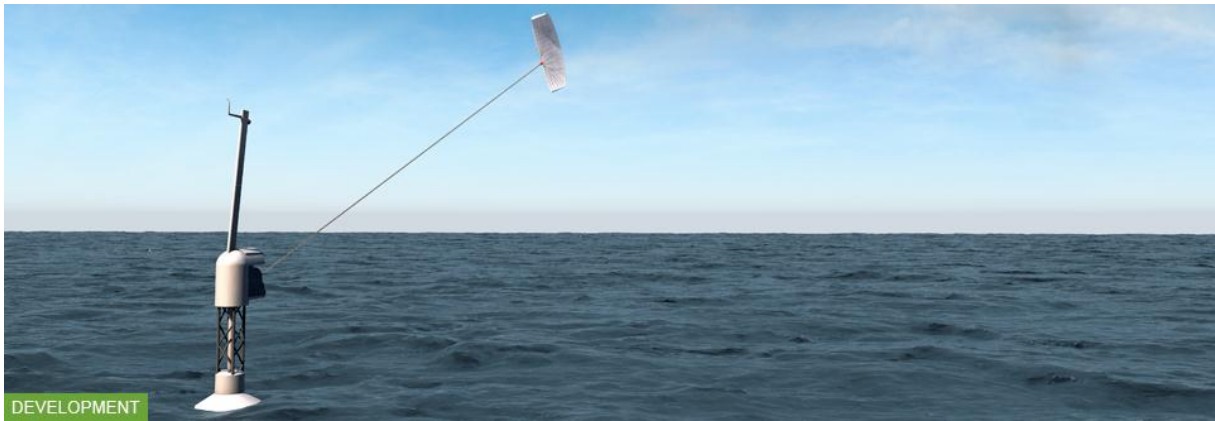


FIGURE 1-14 SKYSAYLS POWER SYSTEM, 1MW OFFSHORE DEMONSTRATOR (SKYSAILS.COM)

Amongst others, the companies SkySails, Ampyx Power, Enerkite and KiteGen are working on this concept. The German company SkySails is already building kite towing systems for large container ships and has succeeded in automating the flight control and launching and landing of a kite. According to their website, they are now planning to build a 1 MW offshore pumping kite generator as a proof of concept (Figure 1-14).

1.4 AIRBORNE VERSUS CONVENTIONAL WIND ENERGY

AWG's have a number of advantages often put forward by its supporters. Most of them refer to conventional horizontal axis wind turbines (HAWT's) as a basis of comparison.

- Access to greater heights and thus stronger winds
- No tower is required
- Easily transportable
- Convenient maintenance at ground level
- Floating offshore systems can be built relatively easily

From a structural point of view, the most important difference between HAWTs and PKGs is the use of a tether instead of a tower and a kite instead of rotor blades.

1.4.1 TOWER VERSUS TETHER

When using airborne systems instead of conventional wind turbines, most of the functionality of the tower can be taken over by the tether. The tether allows the kite to access the wind resource at higher altitudes. Furthermore it can conduct power to the ground – either mechanically or electrically.

The material cost of a tether is much cheaper than for a tower. On the one hand this potentially brings down total system cost, but on the other hand it also allows going much higher and making use of the generally stronger and more consistent winds at altitude. Apart from that, the tower has to be erected, which can be quite troublesome, especially for high towers and difficult terrains. The large overturning moment of the tower makes a large foundation necessary and causes problems when trying to build floating turbines. On an AWG ground station, there is only a minimal overturning moment.

When parts have to be replaced in a conventional wind turbine, a crane is needed and it can take weeks until the weather is calm enough to perform the works. With ground based generators, maintenance would become much easier and cheaper. Even for airborne turbines, the maintenance would probably be cheaper, because the kite would land for maintenance and would be easily accessible.

The tower is also the most visible part of a wind turbine. Replacing it by a tether would significantly reduce the visual impact and might thus reduce the public opposition against wind energy. Furthermore, replacing both tower and rotor blades can turn previously inaccessible sites into viable options for wind energy. Firstly, no wide roads are required as for rotor blades transportation; small, possibly flexible or inflatable kites with compact ground stations could be transported on small paths in forests or on mountains. Secondly, there is no need for strong foundations or for large machinery that are usually needed for the erection of towers. Especially mountainous regions become much easier accessible and, as explained above, floating platforms would not have to resist large moments and could thus be built at relatively low cost. This would allow to access deep-sea offshore sites economically.

1.4.2 KITE VERSUS ROTOR BLADE

Using an aerodynamically optimized, fast moving kite instead of a rotor blade makes it possible to utilize the airfoil's properties more efficiently. Over the length of a rotor blade the apparent wind speed changes a lot, requiring changes in the shape of the blades, which causes suboptimal utilization. A kite can have approximately the same wind speed across its entire span and can always operate at optimal speed. On wind turbine blades, the largest part of the wind loading is applied on the tips. The leverage effect results in high forces close to the hub. A wing as long as the rotor blade would experience a considerably lower leverage effect because the wind loading is more evenly distributed and the distance from any point on the wing to the next bridle point is at maximum half of the span.

Airborne devices for wind energy extraction have the advantage that they can simply be landed for maintenance or replacement.

1.5 ASSESSING A TECHNOLOGY'S POTENTIAL

Most of the advantages mentioned are very plausible and there is not much controversy about them. However, they are not sufficient to prove the potential of the technology. In order to yield overall benefits, airborne wind energy has to compete with alternative means of power generation. The benefits of using wind as a resource were discussed above. Airborne wind energy has to be able to compete with conventional wind harnessing methods in order to prove its technological and economic potential.

The first step in assessing a new wind technology is usually to calculate the efficiency with which the available energy can be extracted. For conventional wind turbines, the aim is to reach the so-called Betz Limit, which is the theoretical limit for extracting wind energy from a given area.

As will be explained later, for airborne wind energy it is not as easy to define the area that energy can be extracted from. Even if enough data is available to make a comparison between the efficiency of airborne wind energy and conventional turbines, the efficiency still does not give enough information to make a judgment. Once it is known how much energy can be drawn

from a given resource, it has to be determined how much it costs to make use of this resource – e.g. the cost per swept area in case of horizontal wind turbines.

A number that is commonly used in energy economics is the *Levelized Cost of Energy* (LCOE) expressed in \$ or € per kWh. Especially when constant feed-in tariffs are available, the LCOE can give good information on the feasibility of a project. The investor is then only interested in the annual energy production and not so much in seasonal or diurnal patterns.

When the actual value of a power plant in an electricity grid is to be assessed, the intermittency of the power source has to be considered. A power plant that mostly operates during off-peak hours has less value than one that always operates during peak hours. The so-called *capacity value* takes this fact into account (Manwell, McGowan, & Rogers, 2009).

Under current market conditions the economic feasibility of an electricity producing system can be estimated fairly accurately by calculating the corresponding LCOE. Comparing AWGs to conventional wind turbines on the basis of LCOE gives much more insight than only comparing possible efficiencies, energy densities or capacity factors. For conventional wind turbines, there are a number of standard tools to estimate the LCOE of a given system at a given location. They have been developed for many years and most authors agree on the same methods. The performance is usually indicated by the power curve which relates wind speed to electrical power output. So-called Weibull distributions are used to describe the annual wind speed distribution at a location with a given average wind speed (see chapter 2.1.1). Wind shear exponents are used to estimate the wind speed increase with height (see chapter 2.1.2) and thus to calculate the wind speed at hub height from the wind speed at for instance 10 meters height. If actual wind farms are to be planned, more accurate measurements and calculations have to be done, but for a first estimate, the described tools are generally considered sufficient.

When trying to do a similar analysis for AWGs, many questions arise – most of which were not yet treated in literature about AWGs. In order to assess the potential of AWGs as a renewable energy source, efficient tools have to be developed, taking into account the specific features of the technology. For promoting the technology to potential investors, it is crucial for the sector to agree on standard methodologies. Also strategic planning by governments is only possible if the required tools are available.

1.6 RESEARCH QUESTIONS

The central question of this research project can be put as follows:

How can the cost of energy produced by a PKG be calculated and how does the outcome depend on the following factors?

- The location where the system is installed (Point of use)
- Design parameters and assumptions (Machine Design)
- The operating height and tether angle (Operation)
- The cost of system components (Cost)

Figures for the cost of energy from a PKG will be calculated in this research. However, the focus is not so much on the exact numbers, but more on the methods to get there and the dynamics that occur when trying to optimize a system for cost of energy. The actual numbers still carry a large uncertainty. Assumptions on the uncertainty of different inputs shall be made and the resulting ranges for the cost of energy shall be calculated.

When evaluating the machine design, it will be important to find out which parameters have the highest impact on cost of energy, what their optimal value is and if their optimal value changes a lot with a change of location. Furthermore, a comparison of the impact of changing primary design parameters, component properties (secondary design parameters) and operational parameters will give insights on where to focus future research.

Another important point for economic analysis of PKGs is the question whether one power curve per machine as used for current terrestrial wind generators is also suitable or if several power curves for the different tether angles should be used. In order to use a power curve, either a fixed operating height has to be assumed or the influence of tether angle on power production has to be neglected for a certain range of tether angles. A similar question arises when trying to analyze the wind data: Does the application of Rayleigh distributions and wind shear exponents yield sufficiently accurate results or is hourly wind data required?

1.7 LIMITATIONS

Point of use: Different locations will be considered only by using different average wind speeds and wind shear exponents. Actual data will be used only for one site on a mountain in Switzerland. More research should be done for coastal areas and offshore, because PKGs are expected to have interesting benefits there. However, mountainous regions are also very interesting, because they usually exhibit strong wind shear.

Machine Design: Only a small number of parameters can be researched in detail. For many parts of the system it is not yet known how exactly they will be constructed. Assumptions on this have to be made and the actual design used in the future will be somewhat different. Still, the chosen parameters will most likely be the most influential ones also in future designs.

Operation: The parameters describing the operation of a pumping kite system had to be simplified a lot in order to reduce the complexity of the analysis. Only the most important parameter is considered: the tether angle, which corresponds to the operating altitude and thus has a major impact on efficiency as well as available wind power. Simplifying the actual shape of the flight trajectory surely has an impact on the maximum obtainable power output, but other studies (Houska, 2007) showed that simple circular or eight-shaped trajectories are quite close to optimal and are thus likely to be used in future systems. The option of using different

elevation angles during traction and reel-in phase is not considered in this thesis. For systems with low depower (see chapter 2.2), this option is important, because it can reduce significantly the power consumption during reel-in. However, future systems will likely use high performance kites with strong depower capabilities and a constant angle will allow for short transition times between traction and reel-in phase. Also for close spacing of machines in a wind farm, constant elevation angles are better suited (see chapter 0).

Cost: As the technology is still very young and no commercial products are on the market yet, it is still hard to estimate technical and economic parameters and there will be significant changes in the coming years. The above research questions shall be answered for a time span of the coming five to ten years. It is assumed that some major technical issues will be resolved, but the technology as a whole will by far not be as mature as conventional wind turbines. Two approaches can be used to estimate the cost of system components. Bottom-up estimates can be made by getting quotes from manufacturers for each component and different sizes. Those quotes can then be used to make cost curves and experience curves could be used to predict costs in a future, more mature market (Junginger, Sark, & Faaij, 2010). Alternatively, cost curves from conventional wind turbine technology can be taken over and adjusted where necessary. As some components of pumping kite generators are more or less identical with those of HAWTs and other are completely different, a mixture between both approaches is used for this analysis. However, experience curves have not been applied: For standard components of HAWTs there is no significant cost decrease expected (an increase is even possible). For new components, there is not yet enough information to make reasonable estimates on learning effects.

2 BACKGROUND

2.1 WIND RESOURCE FUNDAMENTALS

Wind is caused primarily by differing solar radiation on the earth surface and by the rotation of the earth. The power that is contained in wind depends on the wind speed U , the density ρ of the moving air and the projected surface area A that is considered:

$$Power = \frac{1}{2} \rho A U^3$$

The air density ρ is about 1.2 kg/m^3 at sea level and 15°C . It decreases with height and with temperature. The effect of temperature is rather weak. Altitude can have a significant effect: moving from sea level to 1600 meters height can decrease the available power by about 14% only due to changes in air density. Also the humidity has an effect on air density, but this only becomes significant at very high temperatures and high humidity such as in tropical climates.

2.1.1 WIND SPEED DISTRIBUTION

The occurrence of different wind speeds at a given site throughout the year can be described by a probability density function. Experience has shown that the Weibull distribution is well suited to approximate such a function.

$$f(x; \lambda, k) = \begin{cases} \frac{k}{\lambda} \left(\frac{x}{\lambda}\right)^{k-1} e^{-(x/\lambda)^k} & x \geq 0, \\ 0 & x < 0, \end{cases}$$

where k is called the shape parameter and λ the scale parameter. Both are positive. The variable x correspond in this case to the wind speed U . A special case of the Weibull distribution ($k=2$) which often holds for wind distributions is the Rayleigh distribution:

$$f(x; \sigma) = \frac{x}{\sigma^2} e^{-x^2/2\sigma^2}, \quad x \geq 0,$$

The scale parameter σ of the Rayleigh distribution is related to the scale parameter of the Weibull distribution:

$$\lambda = \sqrt{2} * \sigma.$$

And the mean of the Rayleigh distribution, which would be the average wind speed in our case, is:

$$\mu = \sigma \sqrt{\left(\frac{\pi}{2}\right)} \approx 1.253 \sigma$$

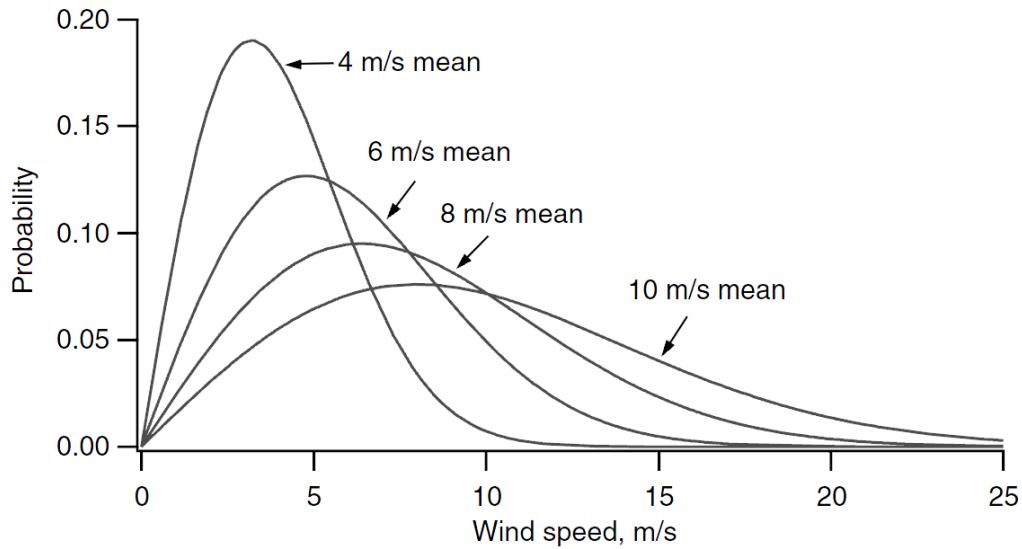


FIGURE 2-1 EXAMPLE OF RAYLEIGH PROBABILITY DENSITY FUNCTION (MANWELL ET AL., 2009)

Both distributions are widely used in wind energy research to make quick estimations of the obtainable annual energy output of a wind turbine at a given site. They usually fit well with actual measured wind speed distributions (Corotis, Sigl, & Klein, 1978; Hennessey, 1977) and make the analysis much simpler. However, before the final decision about building a wind farm, measurements should be taken at the site.

2.1.2 WIND SHEAR

Horizontal or vertical wind speed gradients are called wind shear. For wind energy, mainly the vertical component is interesting. A major cause for this wind shear is the friction on the earth's surface. It generally causes wind speeds to increase with altitude.

For HAWTs, wind shear has a twofold impact: it determines the productivity of the turbine and the lifetime of the rotor. A rotor at higher altitude usually is exposed to stronger winds and thus produces more energy. Strong differences in wind speed between the lower blades and higher blades causes a bending moment. The cyclic loads wear out the blades (Manwell et al., 2009). For AWES, the wind shear mainly affects the productivity. The operating height can in principal be changed relatively easily, but operating at higher altitudes always has disadvantages (see chapters 3.2.1 and 4.2.1). The issue of uneven loadings is less important for kites, because they tend to have spans that are significantly smaller than the rotor diameter of a wind turbine with similar rating.

It is important to note the difference between instantaneous and seasonal variation of wind speed as a function of height. The prior refers to average wind speeds over a few seconds and is described by the similarity theory of boundary layers. The latter refers to long-term averages and must rely on a more empirical approach (Manwell et al., 2009).

Where no measured height profile is available, the following formula is often used to estimate the change of wind speed with height:

$$\frac{U}{U_0} = \left(\frac{h}{h_0}\right)^\alpha$$

where U is the velocity at height h , U_0 is the velocity at height h_0 and α is the wind shear exponent. The wind shear exponent varies with the type of terrain. Typical values are:

- 0.10 for open water
- 0.14 for smooth, grass-covered terrain
- 0.20 for row crops or low bushes with a few small trees
- 0.25 for forests, several buildings or mountainous terrain

2.1.3 TEMPORAL VARIATIONS

Short-term variations of wind speed (turbulence and gusts) in the order of seconds to minutes can have a significant impact on a wind turbine's lifetime and on the power quality. Longer time scale, diurnal variations occur in both tropical and temperate latitudes. Often, the wind speed increases during the day and decreases at night with a minimum between midnight and dawn. Those variations can have a significant impact on the capacity value and thus the system's economics whenever the electricity has to be sold on the market. With high wind speeds during daytime, power production might match well with the typical demand. Seasonal differences also occur in most parts of the world. For example in northern Europe, there is usually more wind in winter than in summer. The same holds for most of northern America. The wind corridors of Oregon, California and Washington show summer and spring maxima. These variations again become important when considering the matching of demand and supply of electricity in a grid with a high share of wind power. Wind speed distributions do of course not only change from season to season but also from year to year. However, statistical analysis has shown that one year of wind data is generally sufficient to estimate seasonal mean wind speeds within an accuracy of 10% with a confidence level of 90% (Manwell et al., 2009).

2.2 AERODYNAMICS FUNDAMENTALS

A flying wing is affected mainly by two forces: The lift force L , which acts perpendicular to the oncoming flow, and the drag force D , acting parallel to the oncoming flow. They both depend on the speed v and the density ρ of the flow. A dimensionless coefficient relates the resulting force to the area A of the wing:

$$L = \frac{1}{2} \rho v^2 A C_L$$

$$D = \frac{1}{2} \rho v^2 A C_D$$

The coefficients of lift and drag depend on the shape of the wing. Often the ratio between them, the lift-to-drag ratio ($\frac{C_L}{C_D} = \frac{L}{D}$) is used to describe the performance of a wing. Some examples of lift-to-drag ratios are:

- Modern sailplanes (45 to 70)
- Hang gliders (~15)
- High performance paraglider (~11)
- Surf kites (up to 6)

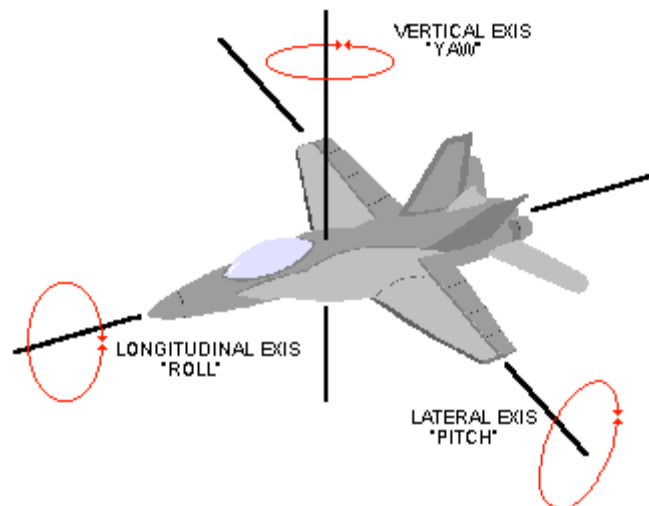


FIGURE 2-2 PITCH, ROLL AND YAW MOVEMENT (ALLSTAR.FIU.EDU)

The state of a kite can be described by the same terms as used for airplanes: the pitch, roll and yaw angle (see Figure 2-2). A roll movement can cause a sideways movement called sideslip. Furthermore, the so-called angle-of-attack (AoA) is used to describe the wing's position relative to the oncoming air flow. It can change the lift force. For kites, a pitch movement that results in a smaller angle-of-attack and thus a smaller lift force, is called depowering. Good depower is important for pumping kite systems, because it allows rapid reel-in with low power consumption. It can be described by the minimum lift coefficient $C_{L \min}$.

2.3 EFFICIENCY CONSIDERATIONS

For HAWTs, the efficiency is limited by the Betz limit, which relates the power available in the wind passing the rotor swept area S to the power that can maximally be extracted by the wind turbine:

$$C_{P,S} = \frac{P_{max}}{P_{wind,S}} = \frac{16}{27} \approx 59.3 \%$$

This ratio is called the coefficient of power per swept area.

Similarly to the Carnot efficiency for heat flows, this method describes the maximally extractable power from a limited wind resource. This makes sense, because a horizontal wind turbine can access only a certain part of the air flow – defined by the rotor’s swept area.

For AWE it is not so simple to define the available area to draw power from. The swept area of the kite depends on its performance (C_L and C_D) and the way it is operated.

Apart from the difficulties to define a swept area for AWE, it is also questionable if energy efficiency is actually a good measure for the potential of a renewable energy technology.

2.3.1 MATERIAL EFFICIENCY

Instead of comparing the extractable power to the available power in the “utilized” area, the extractable power could be compared to the available power in the area that has to be paid for. For HAWTs this mainly relates to rotor blade area, for AWE to the kite’s projected area A .

$$C_{P,A} = \frac{P_{max}}{P_{wind,A}} = \frac{4}{27} * C_L \left(\frac{C_L}{C_D} \right)^2$$

For currently available high performance sports kites with $C_L = 0.9$ and $C_D = 0.15$ ($L/D=6$), this coefficient of power per wing area can reach values of around 5. This means five times the power available in an area as large as the wing area can be extracted by such a wing. The kite would travel at a speed four times higher than wind speed. Future kites, optimized for power production, could have a C_L of 1.3 and C_D of 0.13 and thus a coefficient of power of around 20. The maximum efficiency is defined by C_L and C_D , for which rather practical than theoretical considerations determine the limits. Sail planes and wind turbine blades can reach much higher L/D ratios of 30 to 100. It is however important to note, that for a pumping kite system, this coefficient of power describes only the power produced during the traction phase. The net power production over a complete cycle is significantly lower. At nominal operation, this ratio of net power to maximum traction power will be called pumping efficiency (PE). Furthermore, it has to be noted that the tether adds drag and thus has to be considered when calculating the drag coefficient C_D .

A comparison to HAWTs can be done by using the solidity σ of the rotor to relate the swept area S of an HAWT to its blade area A_{wing} .

$$\sigma = \frac{B c}{2 \pi r} = \frac{A_{wing}}{S}$$

The solidity is defined by chord length c , number of blades B and rotor radius r . A typical value for modern, fast spinning wind turbines, is $\sigma = 5 \%$. The coefficient of power per blade area of a HAWT operating at maximum theoretical efficiency is thus:

$$C_{P,A} = \frac{P_{max}}{P_{wind,A}} = \frac{C_{P,S}}{\sigma} = \frac{16}{27 * \sigma} \approx 12$$

While the values for HAWTs are well known and the theoretical limits are already closely approached in reality, realistically achievable performances of kites for power production can only be very roughly estimated. Also the price that has to be paid for better performance is still very hard to estimate. At the same time, already small changes of C_L and C_D have a large impact on the efficiency of the wing (see Figure 2-3).

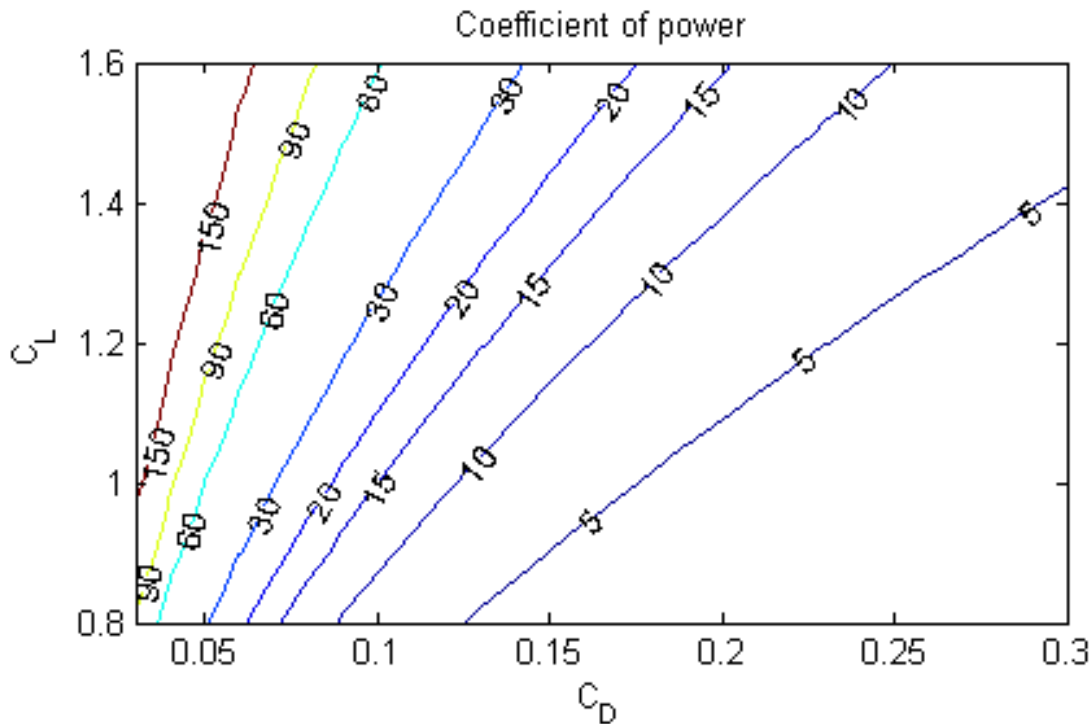


FIGURE 2-3 A KITE'S COEFFICIENT OF POWER

From this comparison, it seems that HAWTs have quite an advantage in terms of wing area efficiency as compared to currently available kites. However, in order to access a part of the wind resource (swept area), a HAWT does not only need the blades, but also a tower: The material used to be able to access high altitudes must also be considered. As in airborne wind energy, only a tether is needed for this purpose, the advantage would again shift to airborne systems. Of course this comparison becomes only economically meaningful when considering the cost related to each unit of material. For a rough estimation, we could consider a 3 MW wind turbine with about 6000 m² of swept area (90 m rotor diameter), a solidity of 5% and thus a useful blade area of 300 m². Assuming turbine costs of 1000 €/kW, the square meter of useful area would cost about 10,000 €. If we would build an airborne wind energy system with a kite of 150 m² for 1M€, the square meter of useful area would cost 6,666 €. That would mean that the kite would have to be at least 2/3 as efficient as a wind turbine blade in extracting energy from the wind. For pumping kite generators, the kite would probably have to reach even higher coefficients of performance than wind turbine blades to be cost competitive, because energy is lost during the reel-in phase.

In fact, there are a large number of other costs and benefits that all have to be considered. In the end, the economic feasibility of a technology can only be determined by comparing the sum of all costs to the expected energy production. The result of this calculation is called the levelized cost of energy (LCOE) of a given system.

2.4 COST OF ENERGY ANALYSIS

The most common methods in US wind industry for calculating the cost of energy are the EPRI TAG method (Electric Power Research Institute, Technical Analysis Group) and the cash flow method. Both are described in (Manwell, McGowan, & Rogers, 2009). The EPRI TAG method was chosen for the calculations in this thesis, because it is significantly simpler and does not require assumptions on the exact cash flow each year. The cost of energy COE [\$/kWh] is calculated as a function of the specific installation cost C_{spec} [\$/kW] normalized by rated power, the capacity factor CF , the fixed charge rate FCR , the annual operation and maintenance cost and the annual replacement cost:

$$COE = \frac{FCR * C_{spec} + C_{O\&M} + C_{replacement}}{8760 * CF}$$

Note that the definition of capacity factor used for PKGs in this thesis differs from the one for wind turbines and the CF in the formula above, has to be replaced by $CF*PE$. See chapter 3.4.3 an explanation and the reasons for this definition.

The FCR is the percentage of the initial capital cost that is needed every year to cover the capital cost. A value of 11.58% for wind farm financing was found in (Fingersh, Hand, & Laxson, 2006) where it includes “construction financing, financing fees, return on debt and equity, depreciation, income tax, and property tax and insurance”. It depends on many factors like the country, the size of the project, the economic lifetime of the project, the maturity of the used technology and the global economic situation. It is questionable if the same FCR as for conventional wind farms also would apply for AWE farms, but using the same FCR allows for an assessment of the technology itself – apart from financing issues (see 3.3.4). Finding a realistic FCR especially for AWE requires more research.

2.5 ELECTRICITY MARKET AND FEED-IN TARIFFS

In many countries, there are subsidy schemes for the support of renewable energy and specifically for wind energy. In Germany, the current feed-in tariffs are about 89 €/MWh for at least the first 5 years. This period can be prolonged for machines with a low annual energy production. After that period, the tariff drops to 49 €/MWh. Those tariffs will drop to 79 and 43 €/MWh respectively till 2020 (BMU, 2012).

If no feed-in tariff is provided, the electricity can be sold on the electricity market. As an example, the APX day-ahead market in the Netherlands can be considered. The average market prices are shown in Figure 2-4, as well as the weighted average prices for a typical wind turbine of 600 kW contracted at the company Windunie Trading B.V (Windunie, 2012).

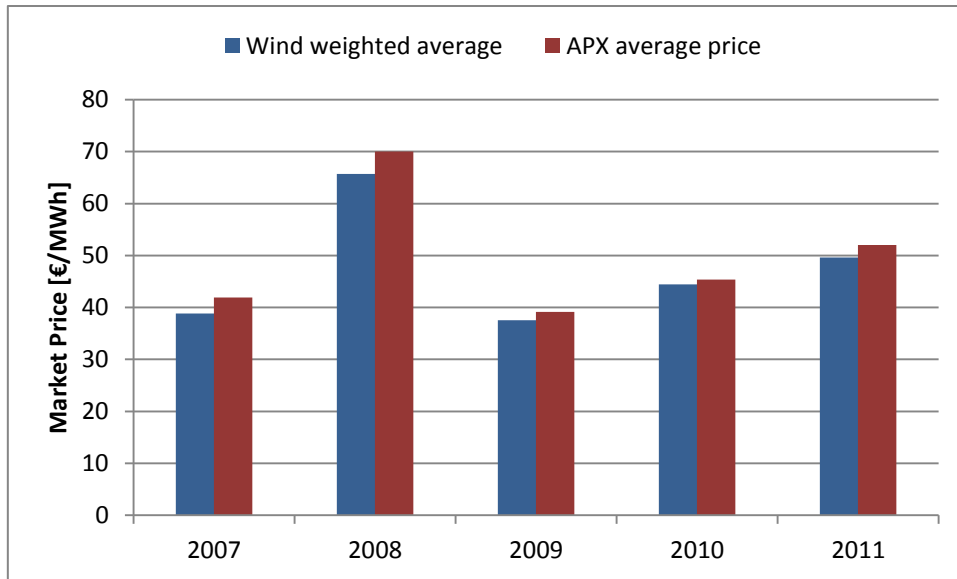


FIGURE 2-4 WIND ENERGY ON THE ELECTRICITY MARKET IN THE NETHERLANDS

The difference between the two prices has (at least) two possible reasons: At the times when this wind turbine produces power, many other wind turbines in the country also produce power, so depending on the share of wind power, the supply of electricity tends to be larger at those times. This can lead to lower prices and thus to a weighted average that is lower than the market average. Apart from that, it is possible that wind power production often coincides with a low demand. For instance, the wind always blows harder in the night. This depends very much on the location. For The Netherlands, the opposite is true: There is generally more wind power during daytime (see appendix 11.10).

The first factor will very likely become more and more important as the share of wind power in electricity grids grows and wind power producers will have to sell their electricity on the market instead of receiving feed-in tariffs. A high capacity factor can potentially counteract this effect.

On the other hand, the integration of different renewable energy sources and of wind farms that are located very far from each other can help to smooth out the fluctuating supply.

2.6 KEY REFERENCES

In this chapter the content of the key references is briefly summarized. Those references are mainly used for developing a performance model for a pumping kite generator. That is why the focus of this chapter lies in explaining the kite performance models described in the references.

The first peer-reviewed paper on kite power was written by Miles L. Loyd in 1980 (Loyd, 1980). Loyd showed that there are basically three different ways of extracting from the wind using a tethered wing: The “simple kite” mode, the “lift” mode and the “drag” mode. In the simple kite mode, the kite does not move in crosswind direction but only in the wind direction. By reeling out the tether, power can be produced. In the other two modes, the kite moves crosswind and can thus intercept the wind from a much larger area compared to the simple kite mode. In lift mode, the lift produced by the fast moving kite is used to reel out the tether. In drag mode, turbines on the kite are used to generate power. Lift and drag mode both have the same

maximum power production. It is higher than that of the simple kite by a factor of approximately $(L/D)^{2/2}$. Loyd uses the equation

$$P = P_w A C_L F$$

with the function F indicating energy extraction efficiency and the power density P_w of the wind:

$$P_w = \frac{1}{2} \rho V_w^3$$

to compare the three modes to each other. For the lift mode - which is the one being treated in this thesis - he finds F to be:

$$F = \left(\frac{L}{D}\right)^2 * \frac{v_T}{v_w} * \left(1 - \frac{v_L}{v_w}\right)^2$$

with a maximum of:

$$F_{max} = \frac{4}{27} * \left(\frac{L}{D}\right)^2$$

which occurs at

$$\frac{v_L}{v_w} = \frac{1}{3}$$

Loyd then develops a more detailed model in which half of the tether weight is added to the weight of the kite. The tether drag is considered by assuming a straight tether and integrating the incremental moment from the tether drag over the length of the tether (the part near the kite moves faster than the one close to the ground). He then simulates the flight of a kite based on the properties of the C-5A aircraft and calculates an average power output of 6.7 MW in drag mode. The peak tether tension is determined to be 3.2 MN.

Houska (Houska, 2007) developed a more detailed, three dimensional model. He included the weight, elasticity, internal friction and drag of the tether. Furthermore parasitic as well as induced drag is considered. Houska also developed a model for dancing kites - that is two or more kites connected to one main tether.

In Jérôme Marchand's Master Thesis (Marchand, 2011) the formulas from Houska are used to develop a kite simulation. He also included a model of the winch, generator and gearbox in order to simulate the drive train efficiencies and mechanical dynamics. As can be seen in Figure 2-5, the major parts of the system are the kite model, the ground station model and the controller. The aerodynamic model allows for all three translational degrees of freedom and one rotational degree of freedom - the roll angle. The yaw angle is directly connected to the velocity vector of the kite, so that sideslip can never occur. The kite is always aligned with its direction of movement. The angle-of-attack is not explicitly used in the model. Instead, it is assumed that the lift coefficient can directly be controlled.

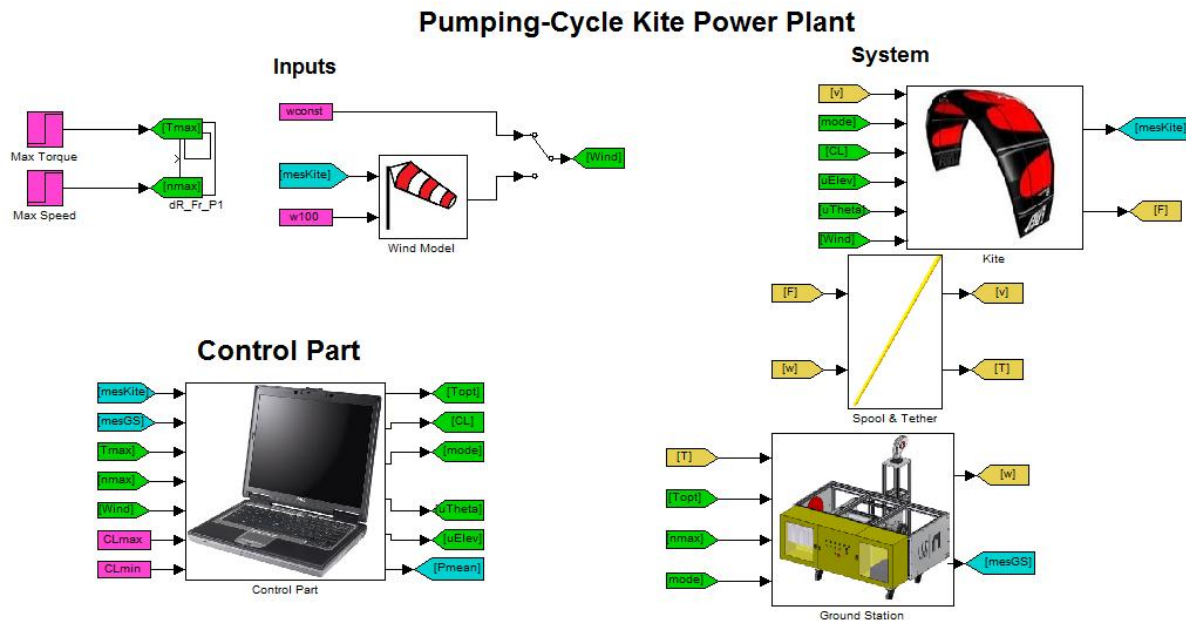


FIGURE 2-5 KITE SIMULATION IN SIMULINK, MARCHAND 2011

In the simulation, the pumping cycle consists of 5 phases: The power production phase, where the kite flies figure eights and the tether is reeled out; the transition to reel-in, where the kite flies out of the power zone and the tether is still reeled out; the recovery phase, where the kite has minimum lift and the kite is reeled in; the transition to the power production phase. Several controllers were implemented: A kite trajectory controller, a winch controller and a power controller.

The trajectory controller aims at keeping the kite in a given trajectory described by a Bernoulli Lemniscate (a figure-eight) in a polar coordinate system. It is realized as a PD-controller that works with the following two inputs: the distance δ between kite and the closest point on the target trajectory and the angle difference Δ between the kite's velocity vector and the tangent on the closest point on the target trajectory. The first one represents the proportional gain and the second one the derivative gain.

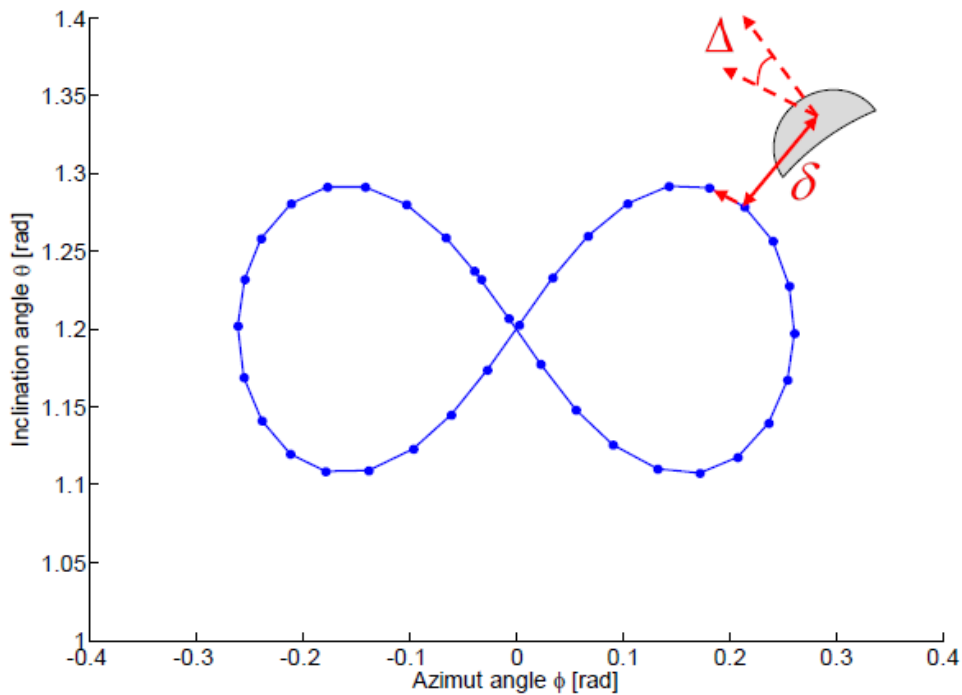


FIGURE 2-6 TRAJECTORY CONTROLLER STRATEGY, MARCHAND 2011

The output is applied to the roll angle of the kite and thus changes its direction of flight. The two gain parameters have to be chosen manually and the optimal values generally change with kite properties like lift coefficient and projected area. However, once appropriate gains are chosen, the controller is able to keep the kite very close to the target trajectory.

The winch controller is responsible for keeping the winch rotational speed at some set speed. This is done by checking the difference between set and actual speed (traction speed error) and then increasing or decreasing the generator torque accordingly. The set speed is determined by the power controller.

The power controller is used to set the traction speed to a value that maximizes the power production. For high wind speeds, the speed can simply be set to the nominal generator speed. However, the winch controller can only reduce the speed by increasing the generator torque up to the point where maximum torque is reached. In the model, the generator is able to provide torques exceeding the nominal value for short times, but in those cases, other means are used to decrease the tether force: The lift coefficient can be reduced or the elevation angle can be increased. Both options are used, but the lift coefficient changes faster while changing the elevation takes some time. The two changes are both driven by the traction speed error. The increase of the elevation angle however lasts until the lift coefficient goes back to its maximum value.

At rather low wind speeds, there is a range of possible traction speeds that all do not violate the force or speed limit. But there is a certain speed that leads to maximum power production. The power controller tries to find this speed by estimating power production for several speeds with a simple formula and picking the optimum. The following formula is used:

$$P(v_T) = \frac{1}{2} \rho A \frac{C_L^3}{C_D^2} \left(1 + \frac{C_D^2}{C_L^2}\right)^{\frac{3}{2}} * \cos(\theta)^3 * (v_w - v_T)^2 v_T$$

It is equal to the formula by Loyd, but a factor $\cos(\theta)^3$ is added to take the elevation angle θ (angle between tether and ground) into account.

At medium wind speeds, the lift coefficient is not reduced, but the traction force is limited to its nominal value by modulating the reel-out speed.

Luchsinger (R. Luchsinger, 2012) derived explicit formulas to calculate the power production and consumption and used those to determine an upper bound for the average power production of a pumping kite generator. As opposed to the simple formulas from Loyd, he also took the tether angle into account. Neglecting the weight of the kite and weight and drag of the tether, he derived the following formulas for the traction phase:

$$P_T = \frac{1}{2} \rho A v_w^2 * C_D * \left(\left(\cos(\theta) - \frac{v_T}{v_w} \right) * \left(\left(\frac{L}{D} \right)^2 + 1 \right) + 2 \frac{v_T}{v_w} \sin(\theta) * (\sin(\theta) - 1) \right)^{\frac{3}{2}} * \sqrt{\cos(\theta) - \frac{v_T}{v_w}} * v_T$$

and for the reel-in phase:

$$P_R = \frac{1}{2} \rho A v_w^2 * C_D * \sqrt{\left(\frac{L}{D} \right)^2 + 1} * \left(\left(\frac{v_R}{v_w} \right)^2 + 2 \frac{v_T}{v_w} \cos(\theta) + 1 \right) * v_T$$

Those formulas are suitable to estimate the maximum possible power production of a pumping kite generator with perfect controllers and an idealized tether with neither drag nor weight. However, the impact of tether drag could be approximated by adding a fraction of the tether's drag coefficient to the drag coefficient of the kite (see 3.2.1).

3 METHODOLOGY

In order to answer the above stated research questions, a method is needed to:

- derive a complete pumping kite system design from some key parameters
- describe the performance of this system (i.e. generate power curves)
- calculate the annual power production (wind modeling)
- estimate the cost of the system

The performance of a given system will be calculated with a relatively simple model that determines the maximum obtainable power output assuming an ideal flight path. For the calculation of annual energy production, several methods will be used: A method assuming constant elevation angle throughout the year will be compared to one that takes into account possible optimization using varying operating heights.

Most of the calculations were done with Matlab and Matlab/Simulink. Some functions were also applied in Excel-Spreadsheets.

3.1 SYSTEM DESIGN

Power, Force and Area are chosen as the primary design parameters to define a pumping kite generator. The power (P) is defined as the nominal generator power. Force (F) is the force that acts on the tether when the generator works at nominal torque and speed. Area (A) is the projected area of the kite. The coefficients of lift and drag as well as the kite costs are related to this area. Any value can be assigned to those parameters; it is a design choice which is independent of the technological possibilities or other uncertain factors. The combination of those parameters is expected to have a major impact on performance of the system and finally on its cost of energy.

A number of other parameters have to be chosen in order to calculate the theoretically obtainable performance. They are called secondary design parameters. Their values are expected to depend very much on the current state of the technology. For some of the secondary design parameters, the impact on power production and on cost of energy will be evaluated.

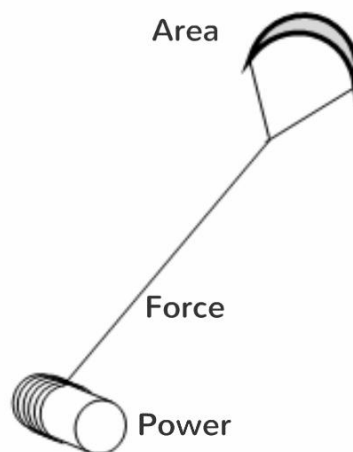


FIGURE 3-1 SYSTEM DESIGN

3.1.1 ASSUMPTIONS

Concerning the flight trajectory, it is assumed that, during the traction phase, the kite moves in circles or figure-eights. It moves over the last 20% of the tether during one cycle. Both the pumping movement and the crosswind movement are small enough (compared to total tether length and elevation angle, respectively) to assume a constant altitude and thus constant wind speed. The fact that wind data is only available for few altitudes (see chapter 3.4.1) also suggests this approach. In order to reel-in at the same (low) angles as reeling out, the kite has to be able to be strongly depowered – the lift coefficient has to be reduced to a very small value. Although this requires special design considerations for the kite, it has a significant effect on pumping efficiency and will thus most probably be incorporated into future pumping kite generators.

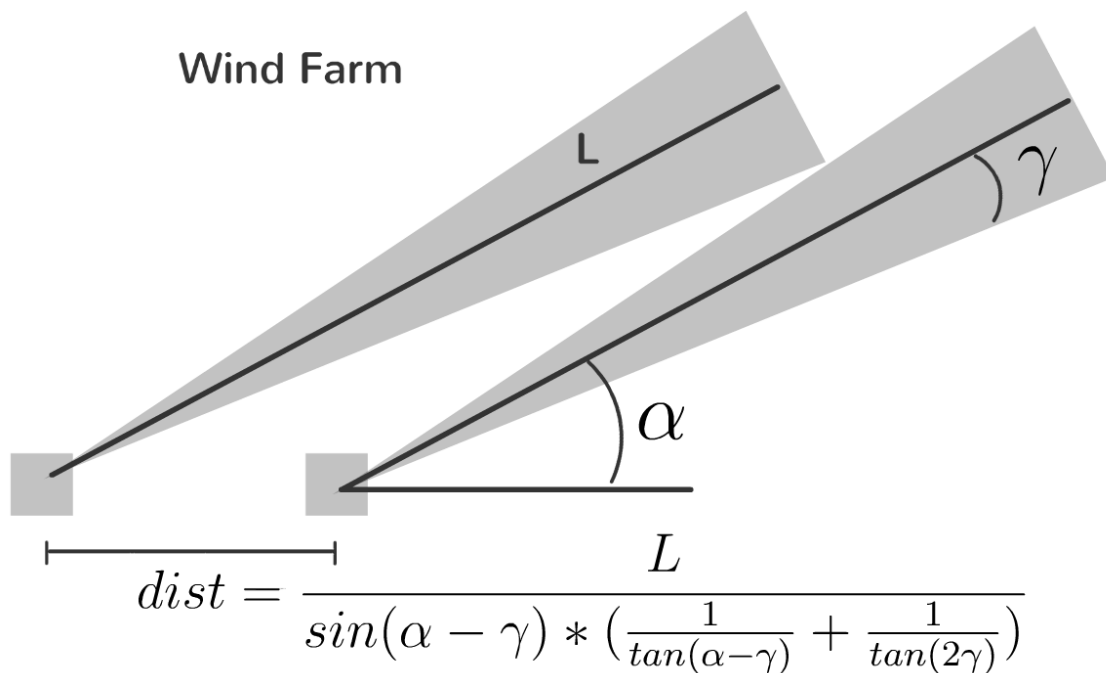


FIGURE 3-2 WIND FARM MACHINE SPACING

The pumping kite generator considered in the following is assumed to be part of a wind farm with a total of 50 MW installed capacity. The machines have a distance *dist* from each other (see Appendix 11.3 for the derivation) to make sure that the kites do not touch each other when operating at the minimum tether angle of $\alpha = 10^\circ$ in a non-synchronized flight pattern limited by the tether angles $\alpha - \gamma$ and $\alpha + \gamma$, with $\gamma = 3.7^\circ$. The maximum tether length is $L = 600\text{ m}$ in the baseline design (see 3.1.2). When space is a limiting factor, the minimum angle α could be increased. This leads in general to lower energy production per machine, but might increase the energy production per land area (see chapters 5 and 4.2.1). In the baseline design, the machines are 326 meters apart from each other.

3.1.2 MACHINE DESIGN

For the PKG, a baseline design is used, of which then single parameters are changed. The following primary design parameters are used for the baseline design:

- Nominal Generator Power $P=1200\text{ kW}$
- Nominal Tether Force $F = 200\text{ kN}$
- Kite Projected Area $A = 150\text{ m}^2$

This corresponds to a nominal tether speed of 6 m/s and a kite area loading of 133 kg/m². The kite area of 150 m² might be reached by a high aspect ratio wing with about 36 meters span and 4 meters chord. This is about the same length as the rotor blades of the wind turbine that will be used for comparison in the following (see chapter 5). Alternatively, a low aspect ratio wing with for instance 20 by 7.5 meters could be used. In the baseline design, the generator is a permanent magnet generator with 93 pole pairs which is directly connected to the winch drum, without the use of a gearbox. A gearbox design with a medium speed generator (289 rpm) and a gear ratio of 9:1 is also evaluated.

Apart from this, secondary parameters have to be chosen. Their baseline values are depicted in Table 3-1. The purple range indicates the parameters which have to be changed for the different kite scenarios (see chapter 3.1.3); in this case the baseline values for the future kite scenario are shown. The efficiency of the drivetrain is assumed to be 90% during traction and during reel-in.

C _{L_max}	1,5	[-]
C _{L_min}	0,05	[-]
C _D	0,15	[-]
Kite lifetime at full loading	10000	[hours]
Kite nominal loading	2	[kN/m ²]
Asymmetry factor	4	[-]
Pumping fraction	0,20	[-]
Maximum tether length	600	[m]
Kite area density	1,50	[kg/m ²]
Winch-tether diameter ratio	100	[-]
Traction drivetrain efficiency	0,90	[-]
Reel-in drivetrain efficiency	0,90	[-]

TABLE 3-1 SECONDARY DESIGN PARAMETERS

The tether diameter is chosen according to the nominal tether force based on a nominal force of 200 N/mm². This has been found to allow for reasonable tether lifetimes (see appendix 11.6.1). The winch drum diameter is then made 100 times larger than the tether diameter (Winch-tether diameter ratio) - also a value that allows for reasonably long tether lifetimes. From the nominal tether speed, the generator speed can be derived.

3.1.3 KITE SCENARIOS

As the development of kites for power production is still in the very beginning and the performance of kites will change a lot in the coming years, two different scenarios are considered:

- A *current kite* scenario, which relates to current technology for sports kites. The maximum lift coefficient $C_{L_{max}}$ is assumed to be 1, with a lift-to-drag ratio of $\frac{L}{D} = 6$ and a minimum lift coefficient $C_{L_{min}} = 0.2$. The lifetime of current kites is very short; it is estimated to be 1000 hours at full area loading. The area loading is 50 kg/m².
- A *future kite* scenario, which relates to technology that might be developed in the coming 3 to 7 years. $C_{L_{max}}$ is set to 1.5 and $\frac{L}{D}$ is 10. $C_{L_{min}}$ is assumed to be improved to 0.05. The

lifetime is estimated to be 10,000 hours at full area loading, which is increased to 200 kg/m².

More information on the two scenarios can be found in the Appendix (11.4.1).

3.2 PERFORMANCE SIMULATION DEVELOPMENT

The power production of a given system is calculated as a function of the elevation angle at which it is operating and the wind speed at the corresponding height. The result can be described by several power curves – one for each angle, or by a power surface. It then serves as an input to the calculation of annual power production. Furthermore, the effect of parameter changes on the shape of the power curves can be analyzed. The model used in this thesis to calculate the power production of a given pumping kite system, is described in the following section.

3.2.1 PERFORMANCE MODEL

The performance model is based on the formulas from Luchsinger (R. Luchsinger, 2012) described above. Apart from the two functions that use aerodynamics to derive power production and power consumption during traction and reel-in phase from the corresponding speeds, a limitation of speed and force is introduced. This limitation is made in order to take the properties of the ground station, namely its nominal power and nominal speed, into account. Furthermore, the tether drag is taken into account by using a simple rule-of-thumb proposed by (Houska, 2007):

$$C_D = C_{D\ kite} + \frac{1}{4} * C_{D\ tether} * \frac{L * d_{tether}}{A_{kite}}$$

Considering the traction phase, the operation of the pumping kite system (or the corresponding power curve) can be described by three different modes: At low wind speeds, it operates in an “unconstrained phase” where the traction speed follows the wind speed in order to maximize power output. At higher wind speeds, the optimal traction speed would cause the traction force to exceed its limit, set by generator moment and/or tether strength. From this point on, the traction speed has to be increased in order to limit the traction force (“speed de-rating”). This mode can be called “force limiting phase”. For even higher wind speeds, the traction speed reaches nominal generator speed and the force cannot be limited by further increasing traction speed. Nominal power production during the traction phase is reached. In this case, the simulation limits the traction force by decreasing the angle-of-attack (“AoA de-rating”) and the phase is called “power limiting phase”. In reality, de-rating can also be done by operating at a different tether angle (e.g. increasing the elevation angle). This strategy is implicitly incorporated by calculating optional power curves for other elevation angles. However, during one power cycle the simulation assumes a constant elevation angle, i.e. the tether angle cannot be changed from traction to reel-in phase.

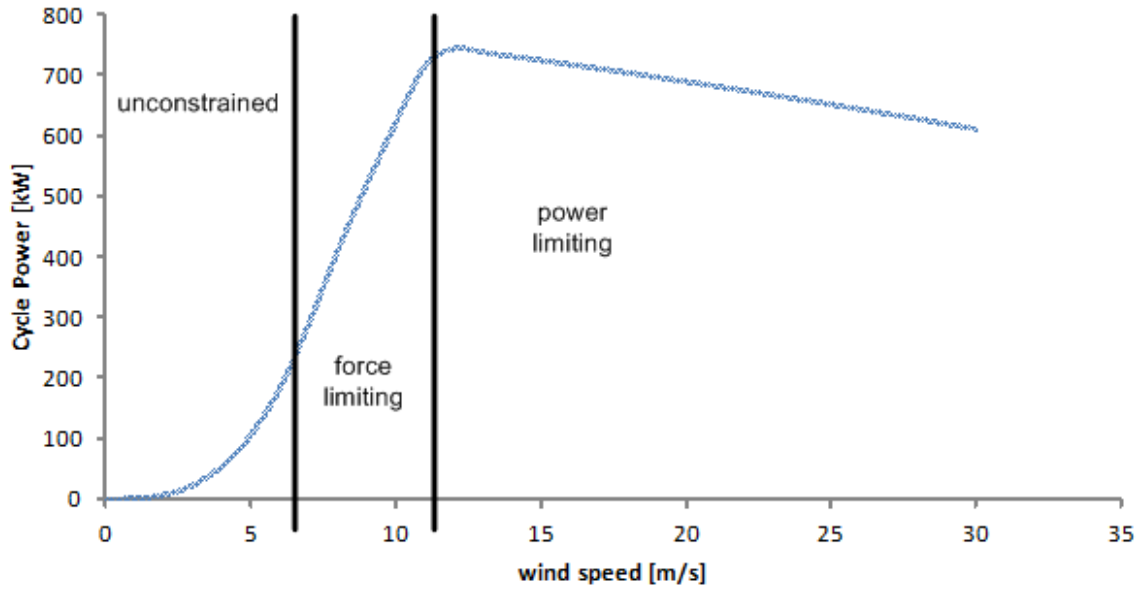


FIGURE 3-3 THREE MODES OF PUMPING KITE OPERATION

The reel-in phase has only two different modes: The theoretic optimal reel-in speed can either be within the limits, set by nominal generator speed and asymmetry factor, or it can exceed this limit. When the limit is exceeded, the system has to reel-in at a suboptimal speed – the maximum possible speed, defined by:

$$v_{R\ max} = AF * v_{nom}$$

where AF is the asymmetry factor. There is a range of traction speeds (from zero to v_{nom}) and reel-in speeds (from zero to $v_{R\ max}$) that can be used. There is a combination of the two, where a maximum average cycle power can be produced. However, there is no separated optimal value for each of them, but only an optimum combination. The optimal speed for traction depends on the reel-in speed and vice versa. In order to find the optimum, the matlab function 'fmincon' is used. It can find minima of constrained nonlinear multivariable functions. There is a choice of different algorithms used for the optimization. It is recommended to first use the 'interior-point' algorithm and to try the others for quicker computation of small- to medium-sized problems. However, the other algorithms are not able to recover from NaN or Inf -results and occasionally stop at local minima. The 'interior-point' algorithm produces reliable results. The constraints used by the optimizer, are a lower and an upper bound for both traction and reel-in speed. The lower bound is zero for both traction and reel-in; the upper bound is the maximum traction speed (defined by the nominal generator speed) and the maximum reel-in speed $v_{R\ max}$, respectively. They both have to be positive.

The target function that is maximized by the optimizer is the average cycle power. It can be derived by considering the net energy E produced during one cycle and the time T needed to complete the full cycle:

$$P_C = \frac{E_T - E_R}{T_T + T_R} = \frac{\frac{P_T}{v_T} - \frac{P_R}{v_R}}{\frac{1}{v_T} + \frac{1}{v_R}}$$

Drivetrain efficiencies are included by assigning an efficiency to the conversion from mechanical power at the tether to electrical power at the grid connection during the traction phase (η_T) and one for the reconversion during the reel-in phase (η_R).

The following matlab functions are created to implement the model (see appendix 11.1):

- *P_C_opt.m*
- *opt_v_R_v_T.m*
- *fun_P_C.m*
- *fun_P_T_limCL.m*
- *fun_P_R.m*

The function *opt_v_R_v_T.m* determines the best possible values for v_R and v_T using the optimizer described above. *fun_P_R.m* determines the reel-in power consumption as a function of reel-in speed. *fun_P_T_limCL.m* does the same for the traction power. However, it also contains a force limitation: When the traction force for a given traction speed exceeds the nominal force, the coefficient of lift C_L is reduced so that the traction force is equal to the nominal value. The function *P_C_opt* uses the other functions to determine the maximum possible power production for a given angle and wind speed under the given constraints for power, force and speed.

This simulation takes about 0.04 seconds to simulate a full pumping cycle and the corresponding power production with a 3.16 GHz Intel Core Duo CPU. This means a full description of a pumping kite generator for 20 wind speeds and 5 elevation angles takes about 4 seconds. The simulation can thus be used to quickly check the influence of a large range of parameters on power production.

Another simulation was planned to be used for comparison. It is based on the simulation developed by Jérôme Marchand. The work that has been done to make this simulation suitable for a parameter study is described in the appendix (11.1.2). Unfortunately, it was still not possible to use it for the specific systems and operation modes considered in the present thesis (for more information on the reasons, see appendix 11.1.2).

3.2.2 IMPLEMENTATION

The following Matlab functions are used to calculate the power production of a given system with different tether angles and wind speeds:

- *MakePowerSurface.m*

The tether angles and wind speeds for which power production should be calculated are required as an input to the function. A loop runs the chosen simulation for each combination of tether angle and wind speed and saves the result in a two-dimensional array.

3.2.3 OUTPUT

The output of the performance simulation is a matrix with cycle power production values for each combination of elevation angle and wind speed (at the corresponding altitude). It can be visualized as a number of power curves (Figure 3-4). Alternatively, a colored surface (power surface) can be used to show the power production as a function of wind speed and elevation angle (FIGURE 3-5). The highest value on this power surface is called pumping efficiency (PE). Together with the capacity factor (see 3.4), it can be used to calculate the annual energy production. The pumping efficiency is lower than one, because the nominal generator power can

only be utilized during the traction phase. It is thus a measure for how well the generator can be utilized under optimal wind conditions.

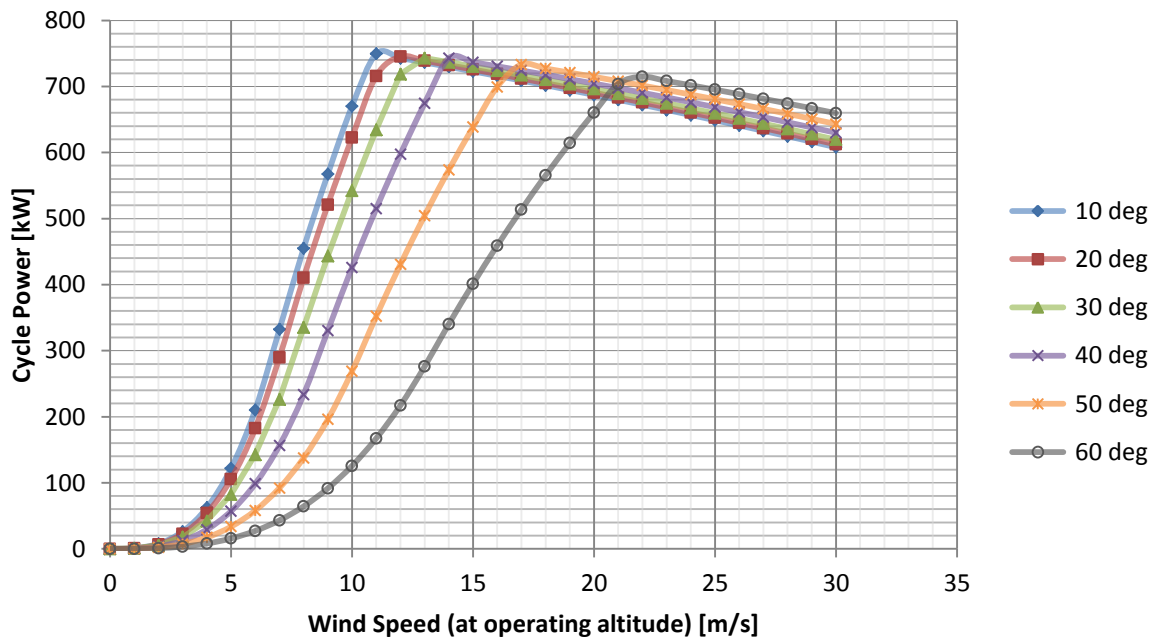


FIGURE 3-4 POWER CURVES FOR DIFFERENT ELEVATION ANGLES

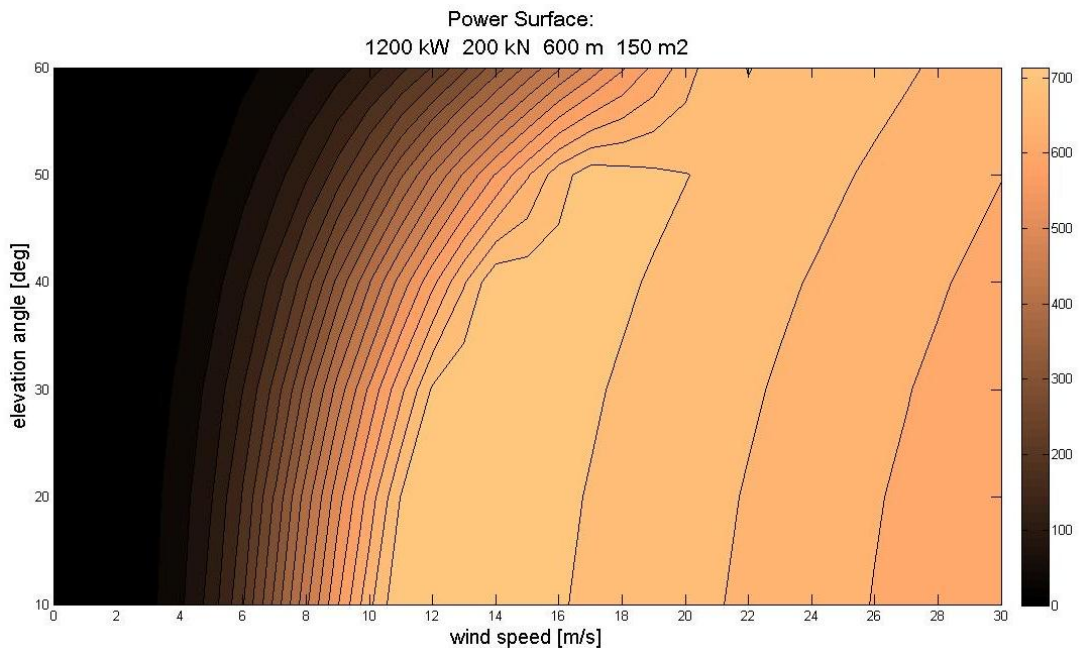


FIGURE 3-5 POWER SURFACE (COLOR BAR: CYCLE AVERAGE POWER IN KW)

If the pumping kite generator is to be operated at variable angles depending on the actual wind profile, the whole power surface is needed to calculate the system's power output. If it is operated at a constant angle throughout the year, only one power curve is needed.

3.3 COST ANALYSIS

The figures calculated for the machine design can then be used to make estimates on the cost of all system components, on the balance-of-station cost and on levelized replacement cost. The costs are estimated by using cost functions that relate a system parameter like nominal force or nominal power to the cost of a component.

3.3.1 UNCERTAINTY

Some cost factors are very hard to estimate, because either the exact construction is not yet known or the product is not yet available and no similar products and their costs are known. To take this uncertainty into account, two cost functions are developed for those cost factors: A lower cost limit that is based on rather optimistic assumptions; and an upper limit that is based on rather pessimistic assumptions. The aim of this method is that experts could agree that it is unlikely that the actual cost will be below the lower or above the upper limit. This range can then be interpreted as a 68% confidence interval and a normal distribution can be derived with standard deviation σ and mean value μ :

$$\sigma = (C_{high} - C_{low})/2$$

$$\mu = C_{low} + \sigma$$

We will assume that the probability for different cost values for one component is normally distributed. This assumption does not take into account that some costs might be more likely to be close to the upper or to the lower bound. However, as there is not much information available to estimate a distribution, a normal distribution seems the most reasonable and most neutral choice. The total cost is then calculated by using the Monte-Carlo-method. If the total cost is a simple sum of all the component costs X_i and the component costs are not correlated, the resulting distribution Y is a normal distribution with mean $\mu(Y)$ and variance $\sigma^2(Y)$:

$$\mu(Y) = \mu(\sum_{i=1}^n X_i) = \sum_{i=1}^n \mu(X_i)$$

$$\sigma^2(Y) = \sigma^2\left(\sum_{i=1}^n X_i\right) = \sum_{i=1}^n \sigma^2(X_i)$$

In that way, a range for the resulting LCOE can be obtained. This range can again be interpreted as a range where the real cost will be in with a likelihood of about 68%.

3.3.2 COST MODEL

Cost curves for all parts of a pumping kite generator have been developed. Basically three different sources were used: Conventional (HAWT) wind turbine components, prototype experience and products currently used in other sectors. A lot of cost curves for conventional wind turbines can be found in the Cost and Scaling Model by NREL (Fingersh et al., 2006) or in related studies (Bywaters et al., 2005; Global Energy Concepts, 2001; Griffin, 2001; Malcolm & Hansen, 2006; Poore, Global, & Concepts, 2003; Shafer et al., 2001; Smith, 2001; Street, 2004). At FHNW, a 10 kW prototype of a pumping kite generator has been built. The cost for parts of this prototype can be used as a starting point to estimate cost curves for larger systems. Furthermore, cost figures of a somewhat larger prototype built by Crosswind Power Systems were used for comparison (see 11.4.1).

The cost functions for PKG components are listed in Table 3-2. They include cost factors (indicated by "C_" plus an abbreviation for the cost item) which are listed in Table 3-3. The cost

factors usually have two alternative values for the lower and upper cost limits. Details on how the cost curves were derived can be found in the Appendix (11.4). For the kite cost factor, the values depend on the scenario (see 3.1.3). For the kite and tether replacement, the following terms are used: P_{cyc} is the maximum cycle power; k_{lf} is the kite loading factor which describes the kite loading at nominal operation as a fraction of the maximum possible kite loading (50 or 200 kg per m² depending on the kite scenario); N is the number of bending cycles the tether can survive; $cycles\ per\ h$ is the number of pumping cycles that are done when operating at nominal traction speed and maximum reel-in speed. Furthermore the term $dist$ is used to describe the distance between ground stations in a farm setting.

Kite Cost [€]	$Cost_{Kite} = C_{Kite} * A^{3/2}$
Kite Replacement [€/a]	$Cost_{KiteReplacement} = Cost_{Kite} * k_{lf} / (lifetime[h] * P_{cyc}) * AEP$
KCU Cost [€]	$Cost_{KCU} = C_{KCU} * (F[kN] + 100 + 2500)$
KCU Replacement [€/a]	$Cost_{KCUReplacement} = Cost_{KCU} / 4$
Mast Cost [€]	$Cost_{Mast} = C_{Mast} (M_{Kite} + 100) * \sqrt{A}$
Tether Cost [€]	$Cost_{Tether} = C_{Tether} * L * (F[kN] + 1000) / 200$
Tether Replacement [€/a]	$Cost_{TetherReplacement} = \frac{Cost_{Tether}}{\frac{N}{h} * P_{cyc}} * AEP$
Winch Drum Cost [€]	$Cost_{Drum} = 2 * M_{Drum} * C_{Alu} + D * C_{Drum}$
Line Handling Cost [€]	$Cost_{LineHandling} = C_{LH} * \sqrt{F[kN]}$
Winch Bearings Cost [€]	$Cost_{Bearings} = C_{Bearings} * \sqrt{F[kN]}$
Generator Cost [€]	$Cost_{Gen} = C_{Gen} * P[kW] + w_{nom}^{-0.57}$
Power Electronics Cost [€]	$Cost_{PowerElec} = C_{PE} * P[kW]$
Yaw Drive Cost [€]	$Cost_{YawDrive} = C_{YD} * P[kW]^{1.657}$
Hydraulic&Cooling Cost [€]	$Cost_{HydrCooling} = C_{HC} * P[kW]$
Ground Station (Cover & Frame) [€]	$Cost_{GS} = C_{GS} * (P[kW] * 11 + 30.5 * P[kW]^{0.8360} + 3671.8)$
Control & Monitoring [€]	$C_{ControlMonit} = P[kW]^{0.2}$
Transportation [€]	$Cost_{Transportation} = C_{Transportation} * P[kW]$
Roads [€]	$Cost_{Roads} = C_{Roads} * dist$
Electrical Interfaces [€]	$Cost_{ElecInterfaces} = C_{EI} * P[kW]$
Miscellaneous, Lighting [€]	$Cost_{MiscLighting} = C_{ML} * P[kW]$
Engineering, Permits [€]	$Cost_{Permits} = C_{Permits} * P[kW] * (0.005 * P[kW] + 10)$
Annual O&M [€/a]	$Cost_{AOM} = C_{AOM}$
Variable O&M [€/a]	$Cost_{VOM} = C_{VOM} * AEP$
Land Lease [€/a]	$Cost_{LL} = C_{LL} * AEP$

TABLE 3-2 COMPONENT COST FUNCTIONS (INVESTMENT COST IN BLUE, ANNUAL COST IN RED, BOS IN PURPLE)

		min	max
Kite Cost factor	C_{Kite}	20	48
KCU Cost factor	C_{KCU}	1	2
Mast Cost factor	C_{Mast}	6	12
Tether Cost	C_{Tether}	0.04	0.15
Winch drum (extra labor)	C_{Drum}	0	20000
Cost of Aluminum	C_{Alu}	1.54	1.54
Line Handling Cost	C_{LH}	2000	6000
Winch Bearing Cost	$C_{Bearings}$	50	100
Generator Cost	C_{Gen}	1152	1267.2
Power Electronics	$C_{PowerElec}$	94	103.4
Yaw Drive	$C_{YawDrive}$	0.21	0.23
Hydraulic&Cooling Cost	$C_{HydrCooling}$	11.4	12.54
Ground Station C&F	$C_{GroundStation}$	1	1.1
Control & Monitoring	$C_{ControlMonit}$	9538	12400
Transportation	$C_{Transportation}$	9.5	19
Roads	C_{Roads}	157	157
Electrical Interfaces	C_{EI}	76	95
Miscellaneous, Lighting	C_{ML}	15	29
Engineering, Permits	$C_{Permits}$	0.95	2.86
Annual O&M	C_{AOM}	7500	20000
Variable O&M	C_{VOM}	5	10
Land Lease	C_{LL}	1.03	1.03

TABLE 3-3 COMPONENT COST FACTORS (PURPLE FIELDS ARE CHANGED IN CURRENT KITE SCENARIO)

The cost model is implemented in a spreadsheet. Also the design parameters (3.1.2) have to be inserted in this spreadsheet and the derived design properties are directly calculated. The performance simulation software that was implemented in Matlab, reads the design parameters from the spreadsheet and writes the values of pumping efficiency (PE) and capacity factor (CP) back into the spreadsheet. Those two values are multiplied with the nominal generator power to calculate the annual energy production. This is sufficient information to determine the levelized cost of energy. A cost summary from the spreadsheet is shown in Table 3-4 and a list of component costs in Table 3-5.

Initial Capital Cost	low	high	mid	sigma	sigma^2
Kite	59.242	133.182	96.212	28.072	7,88E+08
Mechanical Systems	88.402	316.218	202.310	57.705	3,33E+09
Electrical Systems	372.267	409.494	390.881	11.292	1,28E+08
Balance of station	199.277	288.749	244.013	24.223	5,87E+08
<i>Total ICC</i>	719.189	1.147.643	933.416	69.514	4,83E+09
<i>Specific ICC</i>	599	956	778	57,93	3,36E+03
Levelized Replacement Cost [€/MWh]	4,21	9,67	7	2	5
Operation & Maintenance [€/year]	32.502	65.564	49.033	12.031	1,45E+08
Annual Energy Production [MWh]	4.112	4.112	4.112	4.112	4.112
Levelized ICC [€/MWh]	21	33	27	2	4,01E+00
Levelized O&M [€/MWh]	8	16	12	3	9
LCOE [€/MWh]	33	59	46	4	18

TABLE 3-4 SCREENSHOT OF COST MODEL SPREADSHEET, COST SUMMARY

Initial Capital Cost	low	high	mid
Kite	59.242	133.182	96.212
Wing	36.742	88.182	62.462
KCU	22.500	45.000	33.750
Mechanical Systems	88.402	316.218	202.310
Mast	23.883	47.765	35.824
Tether	24.000	90.000	57.000
Winch Drum	2.235	73.600	37.918
Line handling	28.284	84.853	56.569
Bearings	10.000	20.000	15.000
Electrical Systems	372.267	409.494	390.881
Generator	191.345	210.479	200.912
Power electronics	112.800	124.080	118.440
Yaw drive and bearing	26.129	28.742	27.435
Hydraulic and cooling systems	13.680	15.048	14.364
Ground station cover	28.314	31.145	29.729
Control and Monitoring	39.382	51.199	45.290
Balance of station	199.277	288.749	244.013
<i>Total ICC</i>	719.189	1.147.643	933.416
<i>Specific ICC</i>	599	956	778

TABLE 3-5 SCREENSHOT OF COST MODEL SPREADSHEET, COMPONENT COSTS

3.3.3 CURRENCY

All cost curves derived from data in the NREL Cost and Scaling Model (Fingersh et al., 2006), are in 2002-US-Dollars. In order to get an idea of what the calculated LCOE's would mean in the current market, it does not make sense to use 2002-US-Dollars.

Firstly, inflation must be taken into account. This can be done by looking up the Producer Price Index (PPI) for each component at the U.S. Department of Labor, Bureau of Labor Statistics (<http://www.bls.gov/ppi/>). The required NAICS codes are given in the NREL escalation model (Fingersh et al., 2006). This approach would allow taking into account relative changes between costs of key materials such as steel and copper. A simpler method is to just

use the change of GDP as an indicator for general inflation. Both approaches were compared by Fingersh et al. for different wind turbine design and a currency conversion between 2002 and 2005 – dollars. The results were errors in the range of 5%. Because the conversion from cost for HAWT components to cost for PKG components carries quite some uncertainty anyways, it was not considered worth the effort of doing the detailed conversion. The GDP was used to convert 2002 to 2012 dollars. The *IMPLICIT PRICE DEFLATORS FOR GROSS DOMESTIC PRODUCT (IPD_{GDP})* can be found in the NIPA Tables made by the Bureau of Economic Analysis in the U.S. Department of Commerce (www.bea.gov).

$$\frac{IPD_{GDP2002}}{IPD_{GDP2012}} = 1.24$$

Secondly, since most research groups and companies that work on pumping kite generators are situated in Europe, it makes sense to convert the 2012-US-Dollars to 2012-Euros using the current conversion rate.

$$\frac{Euro}{USD} = 1.30$$

The overall conversion rate is thus:

$$\frac{Euro_{2012}}{USD_{2002}} = 1.048$$

The outcome examples in the NREL study are given in 2005-Dollars. To convert 2005 Dollars to 2012 Euros, the PPI component escalation factor for conversion from 2002 to 2005 Dollars ((Fingersh et al., 2006), Chapter 3.3, Table 1) is used:

$$\frac{Euro_{2012}}{USD_{2005}} = \frac{Euro_{2012}}{USD_{2002}} * \frac{USD_{2002}}{USD_{2005}} = 1.048 * 0.86 = 0.90$$

3.3.4 FIXED CHARGE RATE

The fixed charge rate in the baseline is chosen to be the same as in the Cost and Scaling Model by NREL (Fingersh et al., 2006):

$$FCR = 11.58\%$$

$$lifetime = 20 \text{ years}$$

This allows a direct comparison of the outcomes of this thesis to the numbers calculated by NREL for conventional wind turbines, assuming similar financing conditions. Of course the conditions for financing a wind energy project can vary significantly over time and for different countries, technologies, and types of ownership.

3.3.5 REVENUES

For the analysis done in the following chapters, it is assumed that a feed-in tariff is provided, which guarantees a certain price for the produced electricity. A constant feed-in tariff of 50 €/MWh over the whole lifetime of 20 years is used as a reference in the following consideration.

This is a rather conservative estimate, considering actual feed-in tariffs Germany (see chapter 2.5).

The assumed reference tariff is not too far away from actual market prices (also see chapter 2.5). If market prices further increase in the future (e.g. due to scarcity of resources or CO₂ taxes), this price could become a realistic reference for judging the feasibility of wind power projects without subsidies.

The main result of the analysis conducted in this work – the LCOE – is independent of feed-in tariffs, but it can be compared to any feed-in tariff or (average) electricity prices in order to predict a system's feasibility in a specific market situation.

3.4 WIND MODELLING AND ANNUAL ENERGY PRODUCTION

3.4.1 WIND DATA

In the baseline scenario a Rayleigh distribution with an average wind speed of 7.25 and a wind shear exponent of 0.143 is used to generate wind data for the altitude of about 200 meters, where the (baseline) kite is operating at, and all other altitudes required for the parameter sweeps. This specific distribution was chosen, because it corresponds to the wind resource assumed by (Fingersh et al., 2006) for the calculation of the cost of energy of a typical 1.5 MW wind turbine and thus allows a direct comparison (see chapter 5).

For estimating the effect of a variable, hourly optimized tether angle, detailed wind data from different heights is used to model the operation of the pumping kite generator over one year. From a probability density function like the Rayleigh distribution, one cannot derive the actual wind profile for each hour of the year. Those profiles are however crucial for the optimization of the tether angle. This is why hourly wind data has to be used for this part of the analysis. The wind data is taken from the weather model COSMO 2 by meteoswiss (Consortium for Small Scale Modeling, 2011; MeteoSwiss, 2012) and contains horizontal and vertical wind speed on several height levels up to more than 2 km (see TABLE 3-6) for Switzerland and adjacent regions. The mesh size is 2.2 km and values for each hour are available. The model is validated by measurements: Each day, the model data is assimilated with about 120 vertical soundings, 8000 aircraft observations, 28000 surface observations and 1000 wind profiler measurements.

3.4.2 CALCULATION METHODS

The following matlab files are used for calculating the annual energy production:

- *Calculate_EnergyProduction.m*
- *P_optim.m*
- *angle2wind.m*
- *'M','dates','hlevels'*

The function *Calculate_EnergyProduction.m* contains a loop that can calculate the annual energy production for several designs defined by their power curves. The power curves have to be provided to the function. In addition, the data file *'M'* has to be provided. It contains horizontal wind speeds for a specific site in the form of a two dimensional array with the dimension of time, described by *'dates'*, and the dimension of altitude, described by *'hlevels'*.

2'478	2'216	1'971	1'741	1'527	1'328	1'145	978	825	688
565	456	361	279	210	151	101	61	31	9

TABLE 3-6 METEOSWISS MODEL HEIGHTS, HEIGHT ABOVE GROUND IN METERS

The possible operating angles have to be given in the array *'angles'*. The accuracy of the calculation will depend on the number of wind speeds in the array *'winds'*. Both arrays are taken over from the calculation of the power surface.

The function *angle2wind.m* calculates the wind speed for a given tether angle, tether length and date, using the wind data in *'M'*. As the pumping length is assumed to be small relative to the maximum tether length, the maximum tether length is used to determine the altitude of the kite. Because the wind speed is only given for a few altitudes, it would not make sense to do the calculation more accurately. The actual wind speed at the calculated altitude is estimated by a linear interpolation between the given altitudes. Then the wind speed from the array *'winds'*

which is closest to the calculated wind speed is determined and set as the actual wind speed. $P_{optim.m}$ then calculates a value for power production for this wind speed and elevation angle. After all angles are calculated, the highest power value is determined. This power production is assigned to the actual date and time. Also the corresponding optimal angle and the wind speed are saved.

The process of finding the optimal elevation angle for a given wind profile is visualized in FIGURE 3-6. The fat white line shows the wind profile predetermined by the wind data. The other two white lines indicate the range of angles in which a maximum cycle power can be reached. In this case, the kite could fly at an angle between 21 and 29 degree and the power output would approximately be the same. For larger or smaller angles, the power output would be lower.

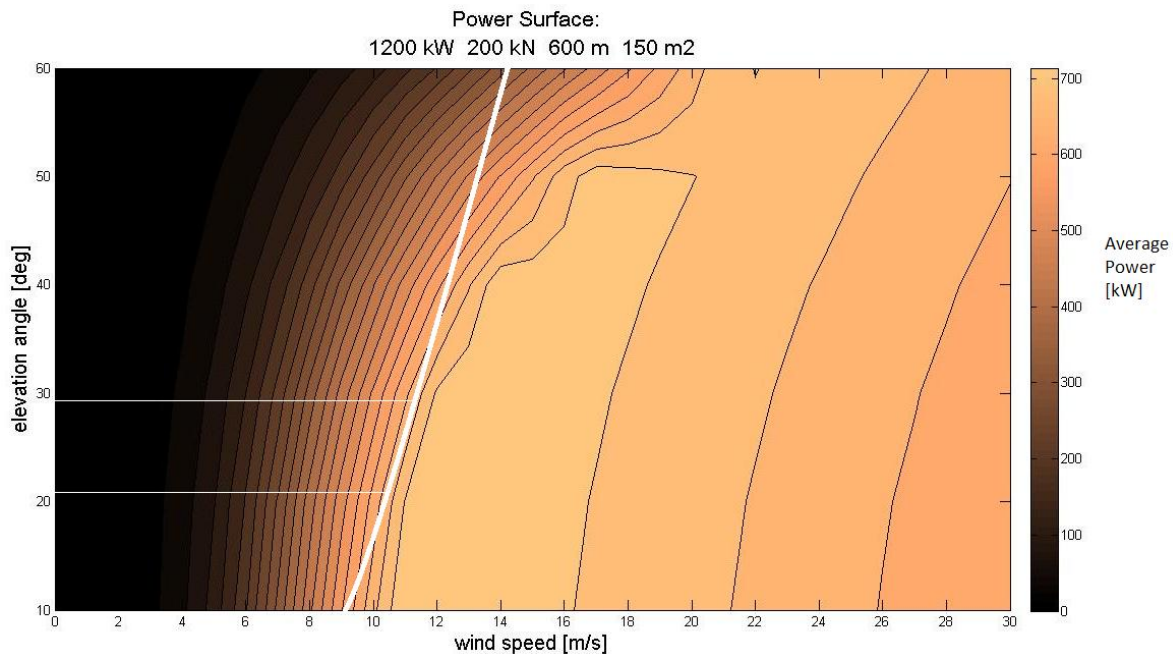


FIGURE 3-6 DETERMINATION OF OPTIMAL OPERATION WITH POWER SURFACE

The annual energy production for the location of Chasseral, Switzerland will be calculated in different ways:

- Allowing for variable angles from 10 to 50°
- With a fixed angle of 10, 20, 30, 40, 50 and 60°

The resulting values for the LCOE will show (for the chosen example) if it is important to simulate the angle optimization or if the difference between a fixed angle and a variable angle is small enough to neglect it.

3.4.3 OUTPUT

The main result from the above described calculations is the annual energy output (AEP). In addition, the operational state of the pumping kite system for each hour is recorded: The wind speed, tether angle and power production.

Apart from this, the capacity factor (CP) of the system is determined. The capacity factor for the pumping kite generator has a different meaning than for a wind turbine. Under optimal wind conditions, a wind turbine produces its rated power. In this work, the rated power of the

pumping kite system was defined as the maximum traction power. This power can never be produced over a whole pumping cycle, because the reel-in phase consumes energy and time. The actual maximum cycle power is defined by the rated power P multiplied by the pumping efficiency PE .

$$P_{cycle,max} = P * PE$$

For the annual energy production, the pumping efficiency has to be taken into account as well:

$$AEP = P * PE * CP * 8760 \text{ hours}$$

Alternatively, the pumping efficiency could have been included in the capacity factor so that CP would actually be the ratio between rated power P and net average power production over a year. With such a definition however, the CP would not only describe the intermittency of the power source, but also the efficiency of the system. It was preferred to separate those two properties. For comparisons with conventional wind turbines, the *effective capacity factor* can be used:

$$CP_{eff} = CP * PE$$

The annual energy production can then be calculated as:

$$AEP = P * CP_{eff} * 8760 \text{ hours}$$

4 PARAMETER STUDY RESULTS

The aim of the parameter study is to show what a change in the basic system parameters means for the energy production and for the cost of energy. Also some secondary design parameters and operational parameters are analyzed. Only one parameter is analyzed at a time, all others are set to the baseline value. The calculations are done with kites according to the future kite scenario (see 3.1.3) if not otherwise stated. A Rayleigh distribution with average wind speed of 7.25 and wind shear factor of 0.143 is used to model the wind resource. Those values are taken over from (Fingersh et al., 2006) (see 3.4.1) in order to make the results comparable to the LCOE values calculated in this study.

4.1 DESIGN PARAMETER STUDY

The primary design parameters nominal force F , nominal generator power P and projected kite area A are varied in order to evaluate the effect on power and energy production as well as on the system economics.

4.1.1 PROJECTED KITE AREA

The kite area A defines to a large degree the wind power that can be captured. Larger kites can capture a lot of wind, but they are more expensive and lead to higher power consumption during reel-in.

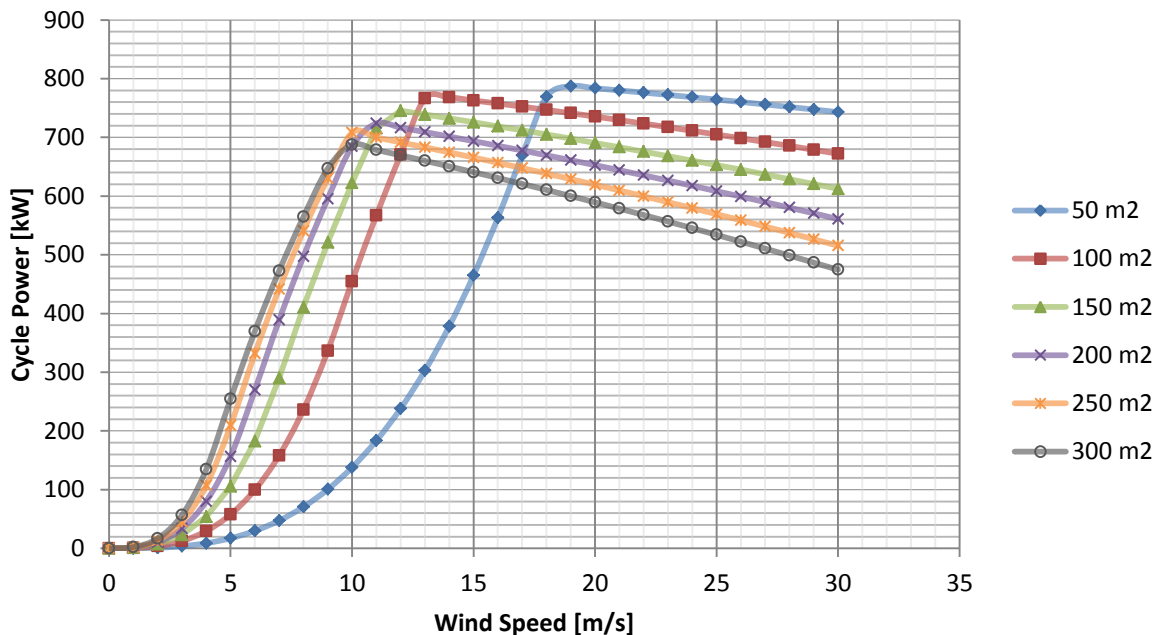


FIGURE 4-1 POWERCURVES FOR DIFFERENT KITE AREAS

Power curves for kites between 50 and 300 m² are shown in the diagram above. The power curves rise earlier for larger kites due to their generating more lift at a given apparent wind speed. The power curves of smaller kites finally reach higher maximum cycle power values and afterwards the power decreases more slowly than for big kites. This is in both cases due to the higher drag of large kites. The reel-in phase requires more energy for large kites and this effect is already visible at rather low wind speeds.

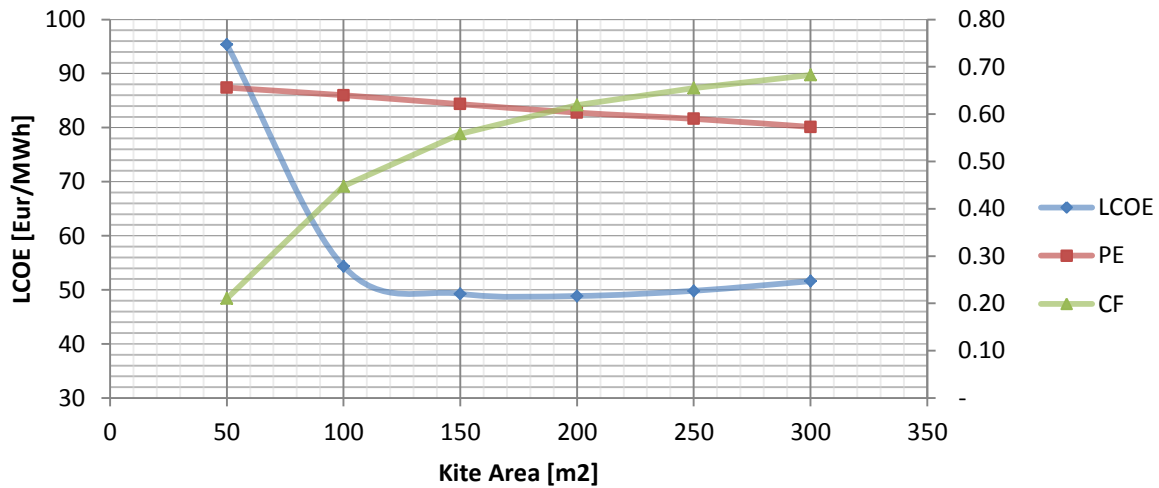


FIGURE 4-2 IMPACT OF KITE AREA ON LCOE, PUMPING EFFICIENCY AND CAPACITY FACTOR

The LCOE is the lowest in a range between 150 and 250 square meters of kite area. Using a kite of 100 square meters would result an area loading of 200 kg/m², which is the maximum allowed value according to the assumptions made. The pumping efficiency PE, which is the maximum possible average power over a pumping cycle divided by the nominal generator power, decreases with increasing kite sizes. This is due to the higher power consumption during the reel-in phase. The capacity factor CF, however, rises for larger kites, approaching a value of about 65%. It is measured based on the maximum average power, which decreases for larger kite areas as a result of increased reel-in power consumption. The annual energy production (which is equal to the generator power P multiplied with PE and CP) thus only increases very slowly. The graph illustrates that a high capacity factor is not always economically beneficial. The advantage of a high capacity factor cannot make up for the higher costs when using kites larger than 200 m². However, increasing the kite area allows to somewhat smooth out diurnal and seasonal variations at rather low cost. The capacity factor can be increased from 52% to 64% for 2 €/MWh. In the absence of a fixed feed-in tariff this might become an interesting option.

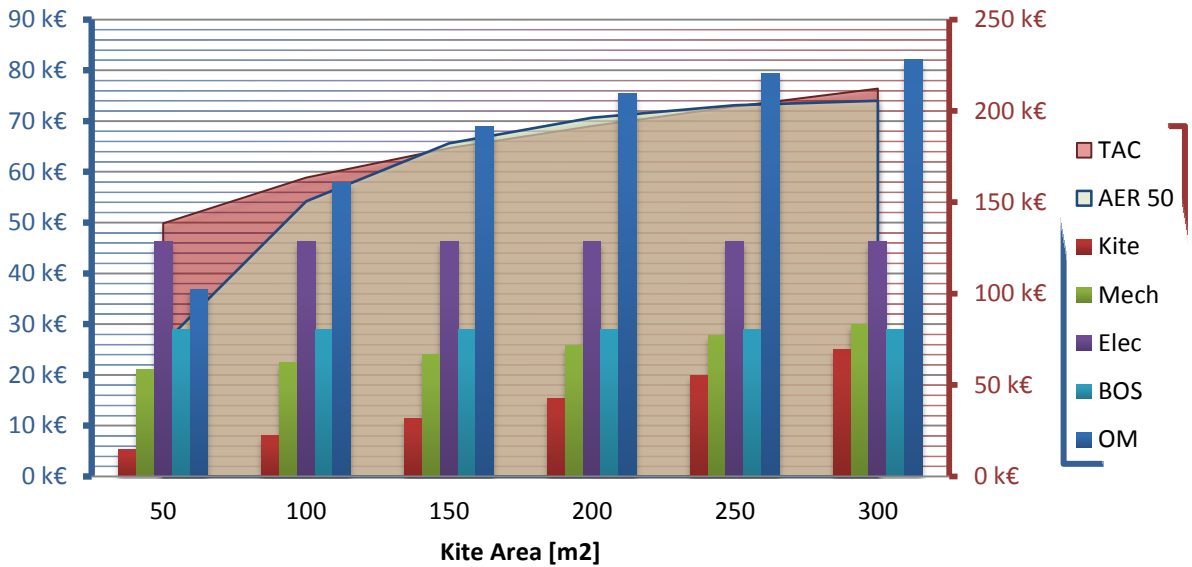


FIGURE 4-3 COST² AND REVENUES³ AS A FUNCTION OF KITE AREA

Figure 4-3 shows all annualized costs as bars (left axis) and their sum (total annual cost) as a surface (right axis). As a reference, the annual revenues at an assumed feed-in tariff of 50 €/MWh (see 3.3.5) are also shown (blue surface, right axis). The cost increase for larger kites is mainly driven by the higher initial costs and replacement costs for the kite, but also the cost of the launching and landing system increases, because a larger structure is required. The annual revenues from selling the produced energy are higher than the total annual costs for kite sizes between 150 and 200 square meters.

4.1.2 NOMINAL GENERATOR POWER

An increase in nominal generator power with fixed kite area and tether force results in a higher nominal tether speed, which means that nominal traction power is reached only at higher wind speeds.

² TAC: Total annual cost, initial costs are annualized with a fixed charge rate of 11.85%

³ AER 50: Annual revenues energy marketing at a tariff of 50 €/MWh

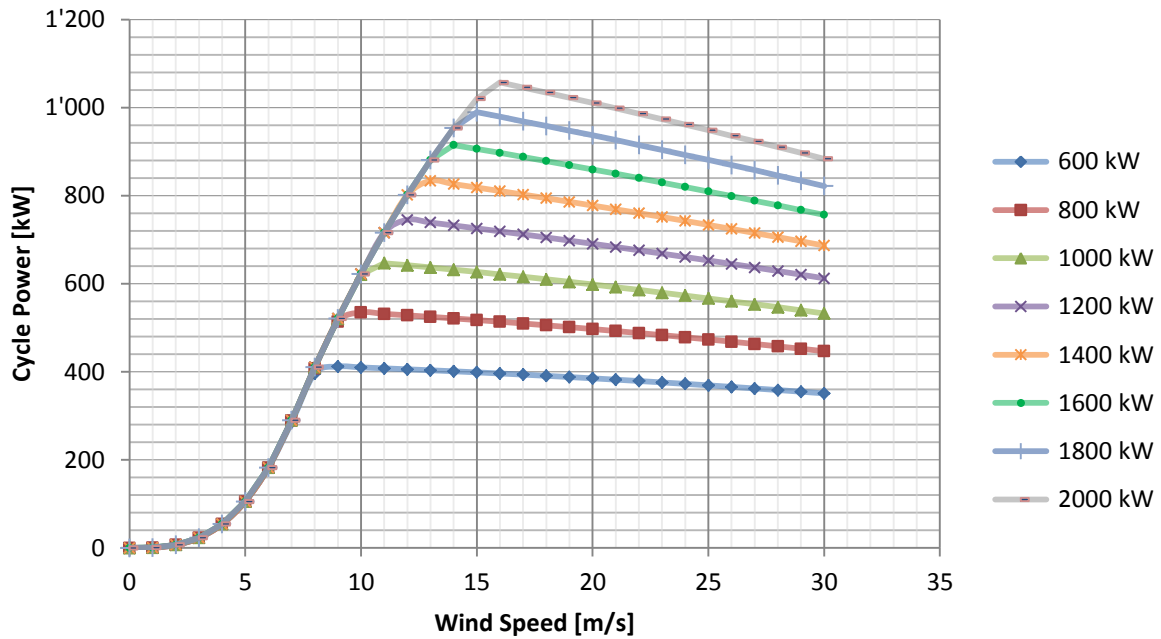


FIGURE 4-4 POWER CURVES FOR DIFFERENT GENERATOR RATINGS

The power curves of different generators (with constant force of 200 kN and kite area of 150m²) have the same slope in the beginning, but the point where they reach their maximum and the power starts to decrease again, differs. This point is reached, when the power produced during the traction phase is equal to the nominal generator power. When moving to higher wind speeds, the traction power still stays at this value, but the power consumption during reel-in rises.

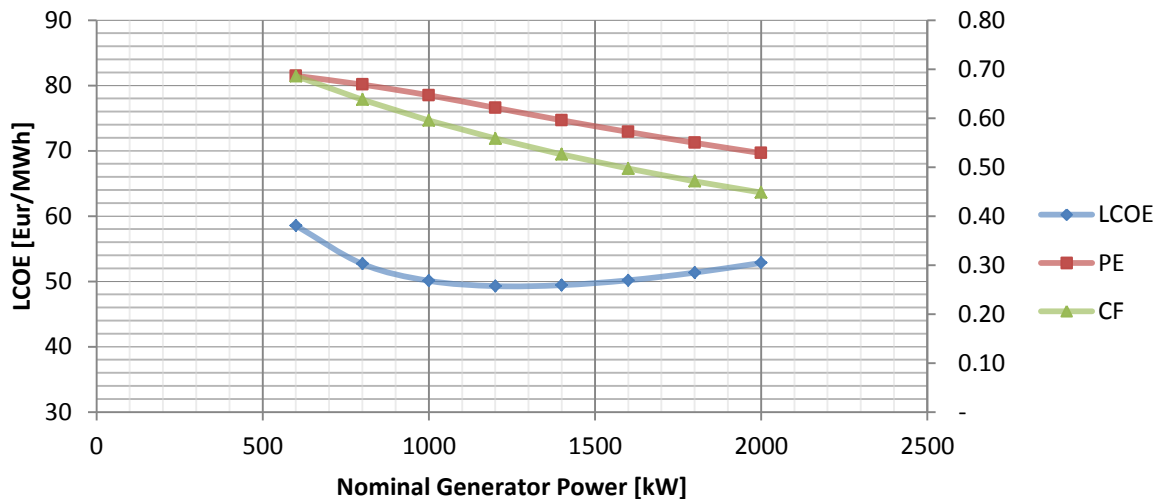


FIGURE 4-5 IMPACT OF NOMINAL GENERATOR POWER ON LCOE, PUMPING EFFICIENCY AND CAPACITY FACTOR

Both, the pumping efficiency and the capacity factor decrease for larger generators. The maximum cycle power can only increase by a fraction of the increase in generator rating, because the nominal tether force is held constant and speed de-rating has to be applied at medium to high wind speeds. The capacity factor decreases, because the maximum cycle power can be reached only at relatively high wind speeds and thus less frequently. Also, for large

generator ratings, the cycle power drops rather quickly at higher wind speeds. An optimum for the LCOE can be found around 1200 kW for nominal tether force of 200 kN, kite area of 150 m². The LCOE does not change much between 1000 and 1600 kW.

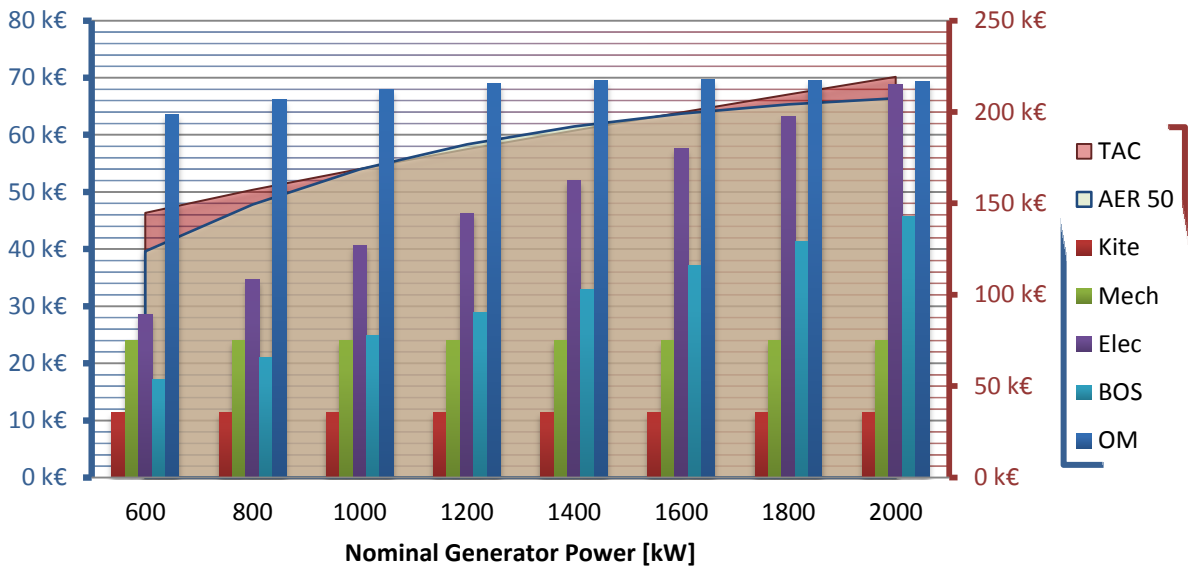


FIGURE 4-6 COSTS AND REVENUES AS A FUNCTION OF NOMINAL GENERATOR POWER

4.1.3 NOMINAL TETHER FORCE (SCALING)

The variation of F is done with constant values for nominal tether speed and kite area loading. This means that P and A are varied proportionally to F and the result is a scaling of the complete system.

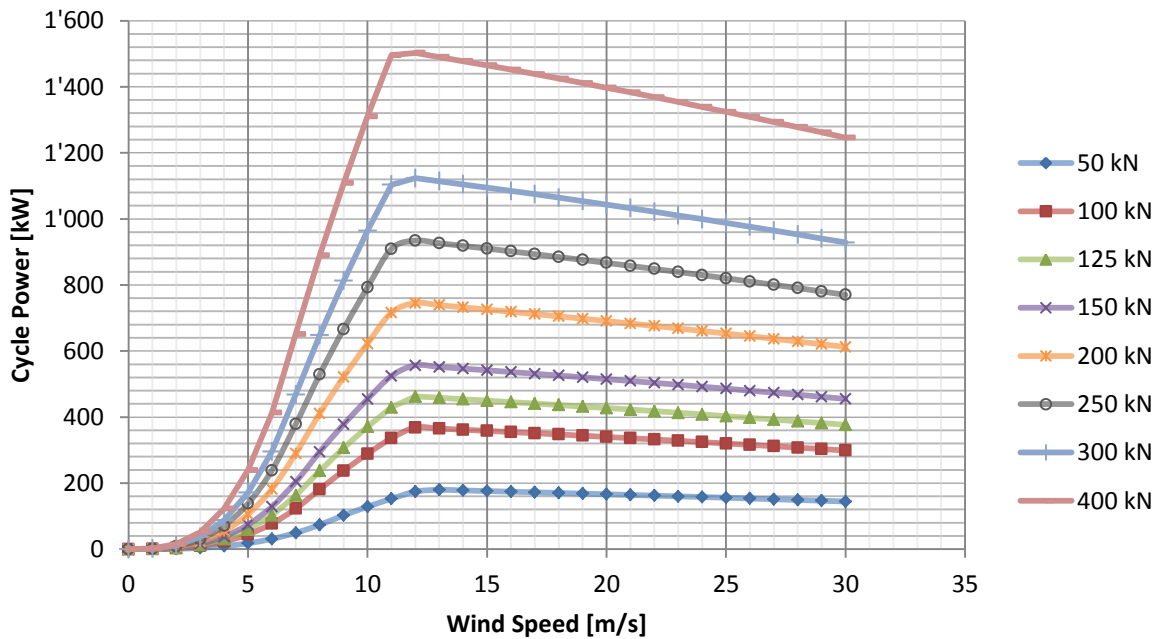


FIGURE 4-7 POWER CURVES FOR DIFFERENT SYSTEM SIZES FROM 50 TO 400 kN

The power curves for systems with 50 to 400 kN show that scaling changes both the slope for low wind speeds and the maximum cycle power; but the wind speed at which maximum cycle power is reached, stays constant. This point depends mainly on the nominal reel-out speed, which is held constant when scaling.

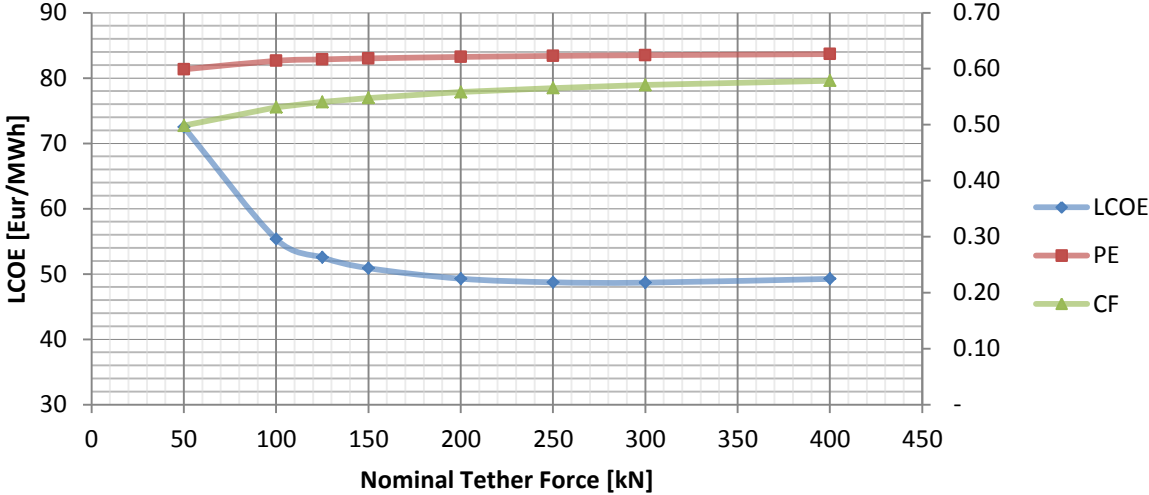


FIGURE 4-8 EFFECT OF NOM. FORCE ON LCOE, PUMPING EFFICIENCY AND CAPACITY FACTOR

Very small systems tend to be significantly less economic. However, from about 150 kN (900 kW) onwards, there is not a large effect of further increasing the system size. The cost of energy again increases very slowly for systems above 300 kN (1800 kW). This is mainly due to a relative cost increase for the kite and the larger drum diameter which requires a slower and thus more expensive generator in the direct-drive design. It might be possible to reduce the generator cost increase by using a gearbox, although this option was only evaluated for the baseline machine (see chapter 5).

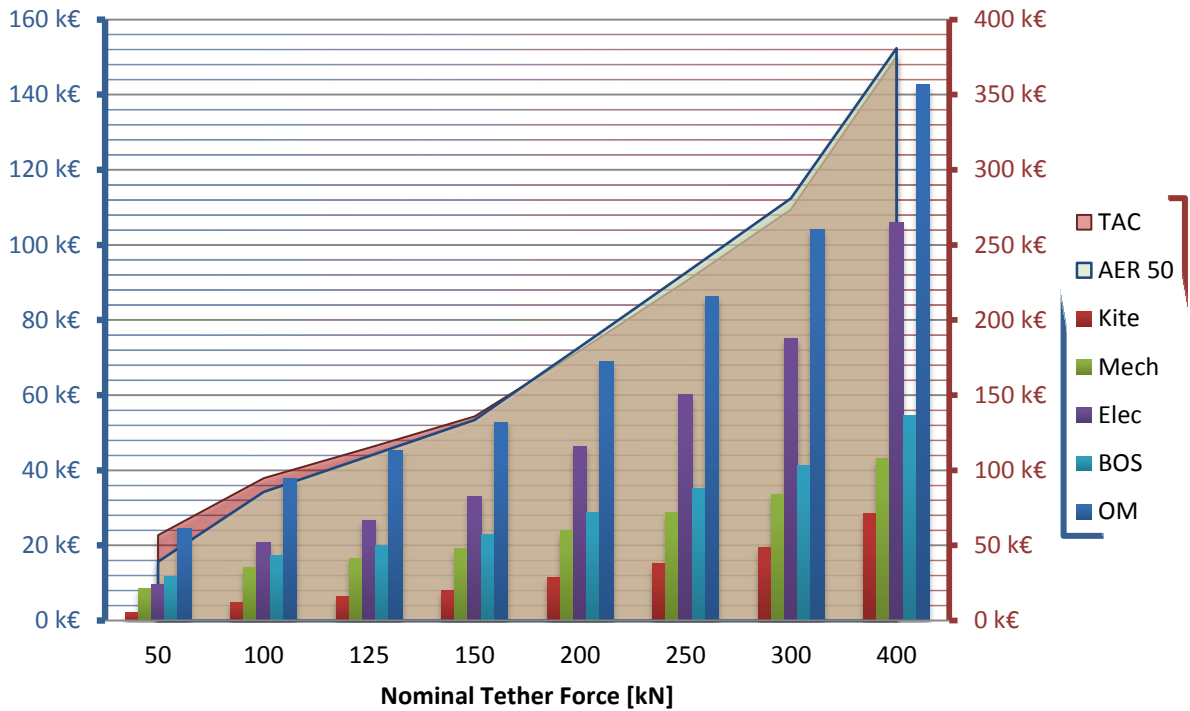


FIGURE 4-9 COSTS AND REVENUES AS A FUNCTION OF NOMINAL TETHER FORCE

4.1.4 OPTIMAL DESIGN

The size of the system seems not to be extremely important, as long as it is somewhere between 150 and 350 kN tether force. When using a 200 kN system, the kite area should be somewhere between 75 and 200 m², corresponding to an area loading of 2.7 and 1 kN/m², respectively. As the limit is 2 kN/m², the kite should have an area of 100 to 200m². The nominal tether speed should best be around 6 to 8 meters per second. With the 200 kN system this would be a generator with nominal power of about 1200 to 1600 kW.

4.2 OPERATIONAL PARAMETER STUDY

As the flight path of the kite is not explicitly modeled in the performance simulation, only the angle at which the kite is operating can be considered. The distance over which the pumping motion is done (related to the pumping fraction), is treated as a secondary parameter (see 4.5) as it is assumed to be fixed over the lifetime of the machine.

4.2.1 TETHER ANGLE

The effect of the tether elevation on average cycle power is depicted in FIGURE 4-10. Elevation angles between 10 and 60 degree in steps of 10 degree are used. Depending on the kite design, tether length and the surroundings, a tether angle of 10 degree might not be possible, because there would be some danger of the kite or the tether hitting the ground, especially during retraction, when the force is low.

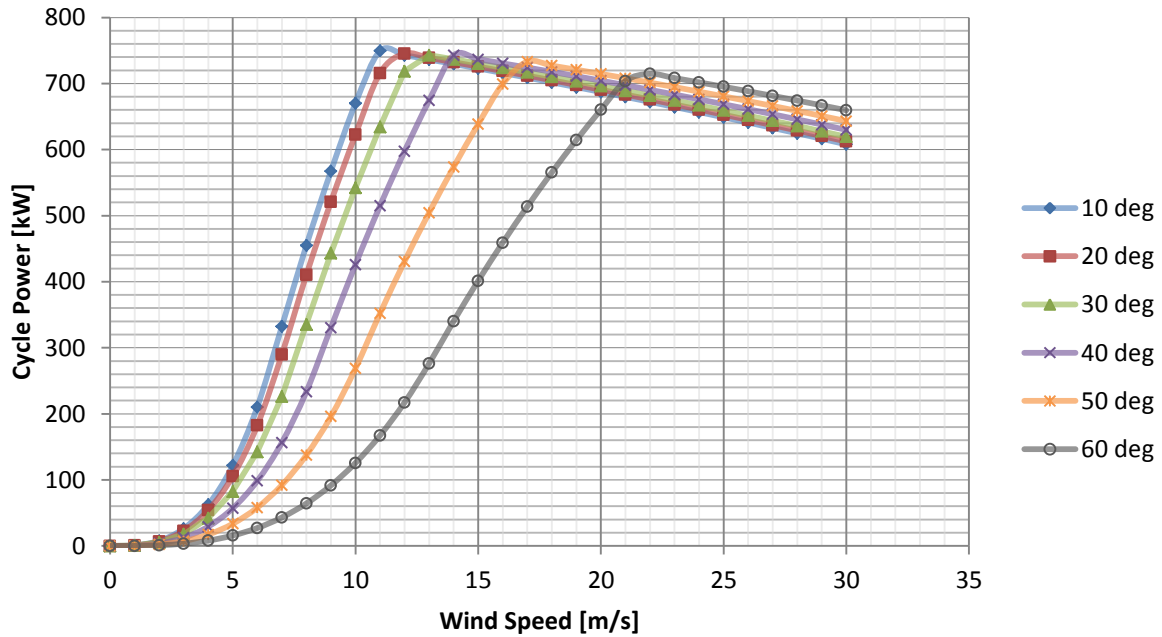


FIGURE 4-10 POWER CURVES FOR DIFFERENT TETHER ANGLES

The power curves show that the same cycle power can be reached only at higher wind speeds as the elevation angle rises. The effect is stronger for larger angles. Maximum cycle power can be reached also for an angle of 50 degree, but only at 17 m/s wind. At 10 degree, the same power is already reached at 11 m/s. For this machine it would thus make sense to operate at 50 degree tether angle only if the wind speed at the according altitude is at least 17 m/s. The optimal operating altitude is dependent on the length of the tether and on the actual wind profile. The wind shear formula might give a first idea of what the profile looks like.

The magnitude of the maximum cycle power varies only by about 35 kW. The variation is due to the differing wind speeds and thus differing power consumption during the reel-in phase.

4.3 CURRENT KITE SCENARIO

As it is still uncertain what future kites would look like, the LCOE is also calculated for kites that are currently available. The nominal tether force is decreased to 100 kN and the nominal generator power to 1000 kW.

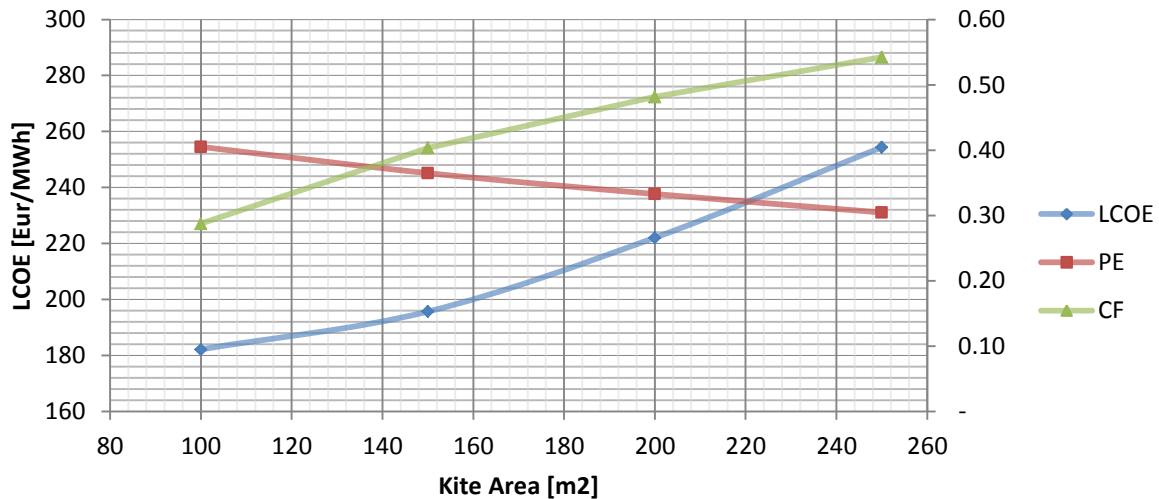


FIGURE 4-11 KITE AREA VARIATION FOR CURRENT KITE SCENARIO

The shape of the LCOE curve in Figure 4-11 shows that smaller kites make the LCOE decrease and that the optimal kite area is probably even smaller than 100 m². However, the maximum kite loading is limited to 50 kg/m², which means that at a tether force of 100 kN, the kite area can actually not decrease below 200 m².

In Figure 4-12 we can clearly see that by far the largest part of the cost is O&M. The reason is that the kite has to be replaced very often as it only has a lifetime of 1000 hours at its nominal loading of 50 kg/m². At the same time it produces relatively little average power even when operating at maximum traction power: The pumping efficiency is only between 30 and 40%. The capacity factor on the other hand is relatively large. It reaches around 50% for the kite areas that are actually possible to use. This is again due to the low nominal kite loading, which requires kites that are quite large in relation to the ground station. The high capacity factor does not have a great benefit however, because not only the energy production but also the main cost factor increases proportionally.

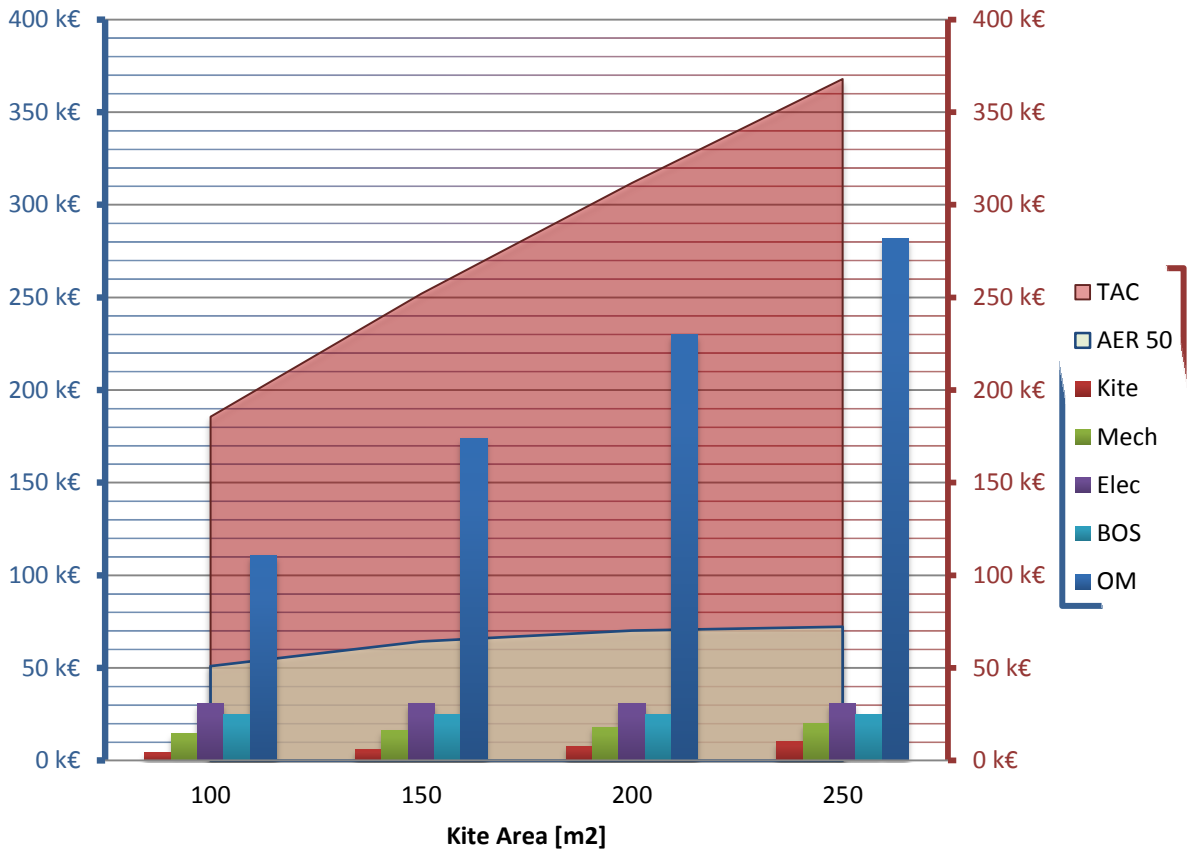


FIGURE 4-12 COST AND REVENUES FOR DIFFERENT KITE AREAS

It can be concluded that the main issues that research should focus on to make pumping kite generators economical, are the kite area loading and the kite lifetime. Using a scaled kite that is based on conventional materials and construction techniques from the kite surfing industry, the LCOE can be expected to be around 220 €/MWh.

C_L_max	1	[-]
C_L_min	0,2	[-]
C_D	0,166667	[-]
Kite lifetime at max. loading	1000	[hours]
Kite maximum area loading	0,5	[kN/m²]

TABLE 4-1 KITE PARAMETERS FOR CURRENT KITE SCENARIO

4.4 GEARBOX OPTION

The baseline design uses a permanent magnet – low speed generator without a gearbox. Those generators are highly efficient, but also very large, heavy and expensive. Mass and size are not a very important issue in a pumping kite ground station (In a wind turbine hub, this causes more serious problems). The cost of the generator could be reduced by using a gearbox. As an example, a design with a single stage gearbox and a medium speed generator with 10 pole pairs will be analyzed. The gear ratio is 9:1 and the nominal generator speed is 289 rpm.

The gearbox cost as a function of nominal generator power was taken from (Fingersh et al., 2006):

$$\text{Gearbox Cost [Euro]} = \frac{74.1 \text{ [USD]}}{1.048 \left[\frac{\text{USD}}{\text{Eur}}\right]} * P = 70.6 * P$$

The reduction in generator cost shows to be larger than the added cost of the gearbox and the LCOE can thus be reduced from approximately 49 to 47 €/MWh. However, in this simple calculation, the negative effect of the gearbox on the drive train efficiency (especially at speeds below rated) and the extra maintenance is not accounted for. As the calculated financial benefit is rather small, those factors could make the LCOE again about equal to the one of the baseline design. Depending on the efficiency reduction, the LCOE could even increase significantly (see drivetrain efficiency in chapter 4.5). Apart from this, the cost uncertainty (about +/- 4 €/MWh) is larger than the calculated difference between the two designs.

4.5 SECONDARY PARAMETERS SENSITIVITY

The impact of the choice of the secondary parameters on the LCOE is evaluated.

Table 4-2 shows the nominal values for all parameters and for each parameter two smaller and two larger, still plausible values. Values above or below these ranges are considered very unlikely. Looking at the resulting ranges for the LCOE (depicted in Figure 4-13, Figure 4-14 and Figure 4-15) gives insights on how big the impact of the uncertainty of each parameter is on the uncertainty of the LCOE.

Secondary parameters			xs	s	base	l	xl
C_L_max	1,50	[-]	0,9	1,3	1,5	1,7	1,9
C_L_min	0,05	[-]	0,01	0,03	0,05	0,1	0,2
C_D	0,15	[-]	0,05	0,1	0,15	0,2	0,25
Kite lifetime at full loading	10000	[hours]	2000	7000	10000	14000	20000
Kite Nominal Loading	2	[kN]	1	1,5	2	3	4
Asymmetry Factor	4	[-]	1	2	4	6	8
Pumping Fraction	0,20	[-]	0,1	0,15	0,20	0,25	0,3
Maximum tether length	600	[m]	200	400	600	800	1000
Kite density	1,50	[kg/m ²]	1	1,25	1,50	2	4
Winch-tether diameter ratio	100	[-]	50	75	100	150	200
Traction Drivetrain Efficiency	0,90	[-]	0,7	0,8	0,90	0,95	0,97
Reel-in Drivetrain Efficiency	0,97	[-]	0,7	0,8	0,90	0,95	0,97

TABLE 4-2 RANGE OF SECONDARY PARAMETERS

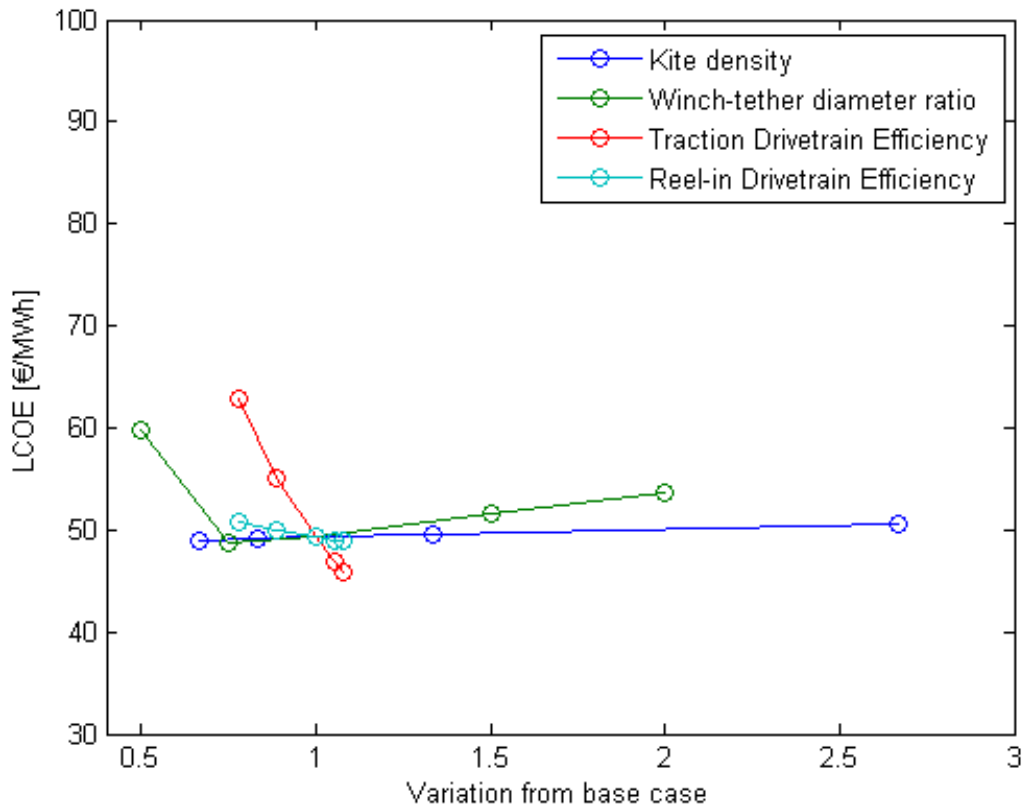


FIGURE 4-13 SENSITIVITY CHART: KITE AREA DENSITY, WINCH-TETHER DIAMETER RATIO AND DRIVETRAIN EFFICIENCIES

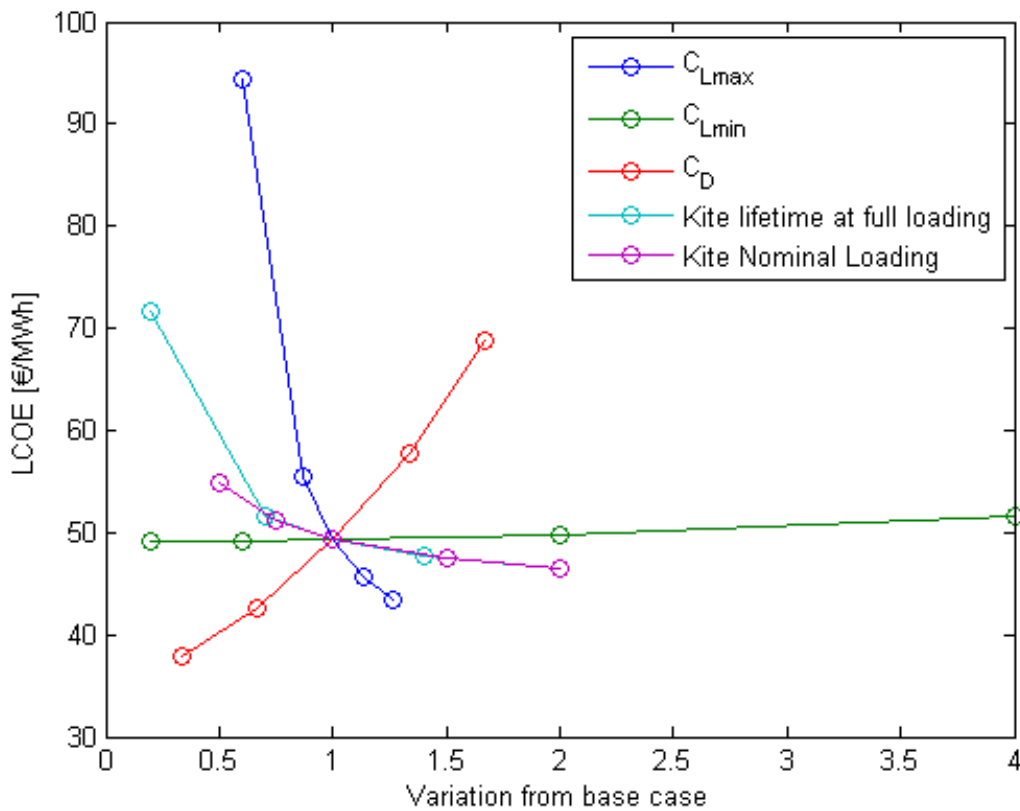


FIGURE 4-14 SENSITIVITY CHART: KITE PROPERTIES

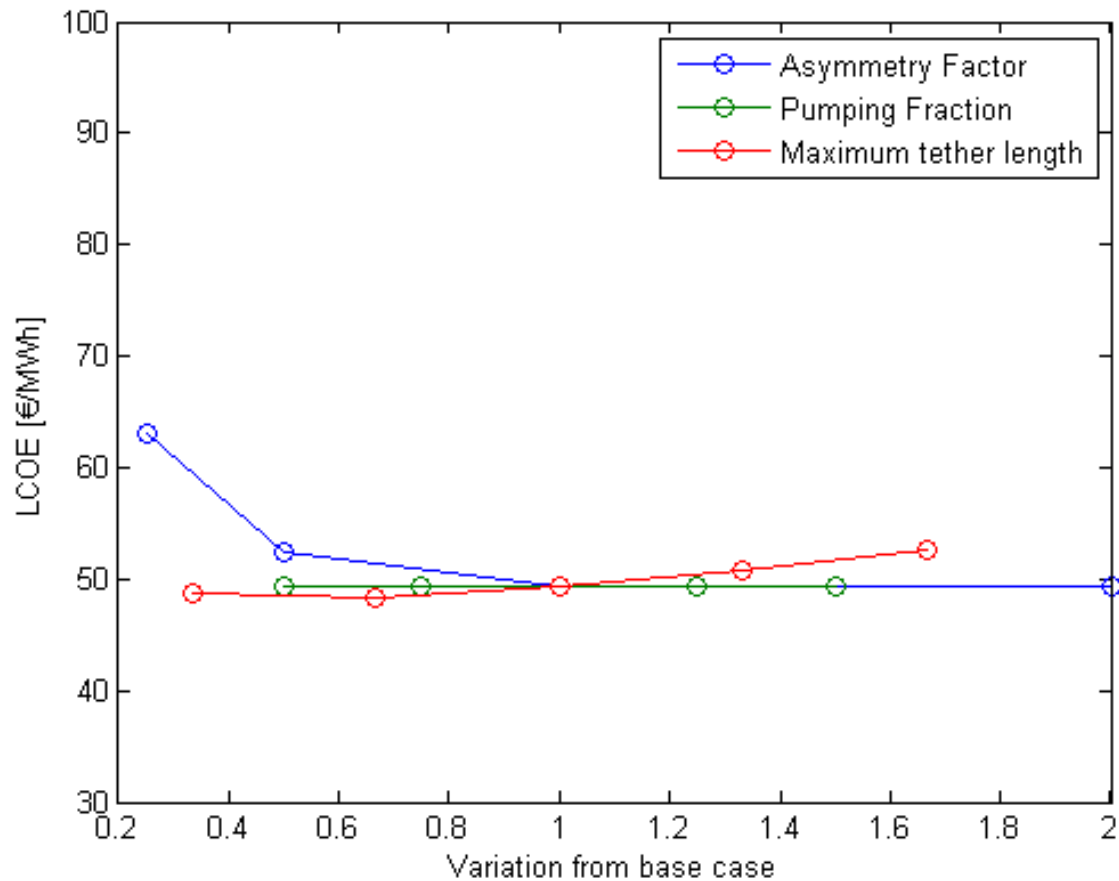


FIGURE 4-15 SENSITIVITY CHART: ASYMMETRY FACTOR, PUMPING FRACTION AND MAXIMUM TETHER LENGTH

The most influential parameters seem to be the following:

- CL_max
- CD
- Kite lifetime at full loading
- Traction drivetrain efficiency,
- Asymmetry factor
- Winch-tether diameter ratio

The traction drivetrain efficiency directly affects the energy production during the traction phase, which is also crucial to the average cycle power as the traction phase usually takes significantly more time than the reel-in phase. The ratio of winch and tether diameter determines the diameter of the winch and thus the number of pole pairs of the generator, because no gearbox is used. The number of pole pairs (relates to nominal speed of the generator) is very important for the cost of the generator (see appendix 11.4.3). A small winch should be preferred from this point of view. However, if the winch-tether diameter ratio becomes too small, the tether wears out very quickly and the replacement cost leads to a strongly increasing LCOE. Both the CL and the CD are important because they have a strong impact on power production during the traction phase. The nominal loading of the kite determines how quickly the kite has to be replaced, because the wear of the kite is a function of the relative kite loading at maximum power production (kite loading factor, see chapter 3.3.2

and 11.6.2). Also the kite lifetime has a direct impact on the replacement cost of the kite, which constitutes an important cost factor within the whole system. The kite area density determines the weight of the kite, but the performance simulation does not take the kite mass into account. It is only important for the cost of the launching system, which makes up for only a small fraction of the initial capital cost. In reality, the kite mass will also have a strong impact on the kites performance and thus on annual energy production (R. H. Luchsinger, 2010).

The influence of the minimum lift coefficient is surprisingly low. The reason might be that the drag coefficient of tether and kite combined, dominate the power consumption during reel-in. It might however also be underestimated by the performance model.

The pumping fraction is not properly accounted for in the performance model. Transition phases between traction and reel-in phases are not considered; neither are changes of wind speed during one phase. A larger pumping fraction only leads to higher cost, because the winch has to be larger in order to accommodate the tether used for pumping on the top layer.

Increasing the tether length does not have a significant effect. The benefit of stronger winds at higher altitudes seems to be outweighed by increased tether drag.

5 COMPARISON TO CONVENTIONAL TURBINE

In the NREL Cost and Scaling Study (Fingersh et al., 2006), where most cost functions are taken from, the LCOE of a typical 1.5 MW horizontal axis wind turbine (HAWT) in a 50 MW farm is calculated (FIGURE 5-3). By simulating the power output of a pumping kite generator of similar size, one can get a first impression of both technology's pros and cons. The currency used in outcomes section of the NREL study (2005-USD) can be converted to 2012 Euros by multiplication with $1/0.9=1.11$ (see chapter 3.3.3).

The mean wind speed was stated to be 7.25 m/s at 50 meters altitude with a power law shear exponent of 0.143 and a Weibull K parameter of 2 (equal to a Rayleigh distribution). This information was used to calculate mean wind speeds for all required heights and produce random numbers for all hours of a year based on the according Rayleigh distribution. The random numbers for different heights are not correlated. In reality, there is some correlation, which is however hard to estimate. So the hourly wind profiles do not describe reality, only their mean value does. If a variable tether angle would be used, the capacity factor would be extremely high, because there is a probability for finding a high wind speed at least at one of the altitudes. By using a fixed tether angle, the error resulting from this can be avoided.

The baseline design (1200 kW, 200 kN, 150 m²) is used for the calculation of the pumping kite energy production. The result is a capacity factor of 56% and a pumping efficiency of 62%, corresponding to an effective capacity factor of about 35% (see 3.4.3). The LCOE is 49 €/MWh, with a lower and upper bound of 45 and 54 €/MWh, respectively. The annual energy production is 3645 MWh.

The 1.5 MW wind turbine produces 4312 MWh and the capacity factor is 33%. The effective capacity factor of the pumping kite system is still slightly higher than the one of the wind turbine, even if the pumping efficiency is only 62%. This is partly due to the fact that the operating height of the PKG is about 205 meters while the wind turbine hub height is only 65 meters. The expected specific investment cost for the PKG is 778 €/kW and for the wind turbine 935 \$/kW (1039 €/kW). The resulting LCOE of 48 \$/MWh (53 €/MWh) for the wind turbine coincides roughly with the upper bound for the PKG. The initial investment for the PKG is

relatively small, but the annual costs are high, so the LCOE ends up in a similar range as for the NREL wind turbine. The cost uncertainty is mainly due to the annual costs.

Another interesting number to compare is the land area used by the wind farm per annual energy production or per installed capacity. The conventional wind farm considered here has 1.5 MW turbines located in squares with a distance of 7 times their rotor diameter (490m) from each other in both directions. This leads to a land use of 0.16 km²/MW of installed capacity or a land area productivity of 18 GWh/a/km². The spacing is rather conservative; spacing rules of 5x5 or 3x7 rotor diameters are also common, with an occupied land area ranging between 0.04 and 0.3 km²/MW (Manwell et al., 2009). The machine distance in the PKG wind farm depends on the minimum tether angle that can be operated at. Figure 5-2 shows the land area productivity of PKG wind farms for different operating angles. The productivity can be strongly increased by increasing the kite's (minimum) operating angle, while the cost of energy only increases little for angles above 20 degrees. The used spacing rule (see 11.2 for details) is however derived without considering potential aerodynamic interference between the kites.

LCOE Comparison

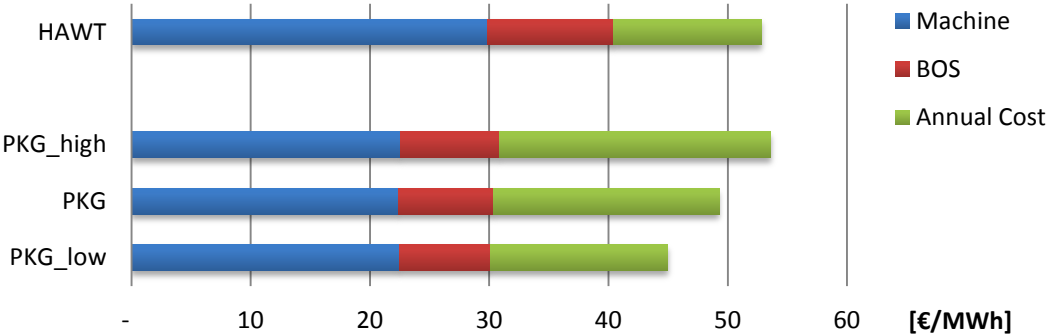


FIGURE 5-1 LCOE OF PUMPING KITE GENERATOR AND HORIZONTAL WIND TURBINE

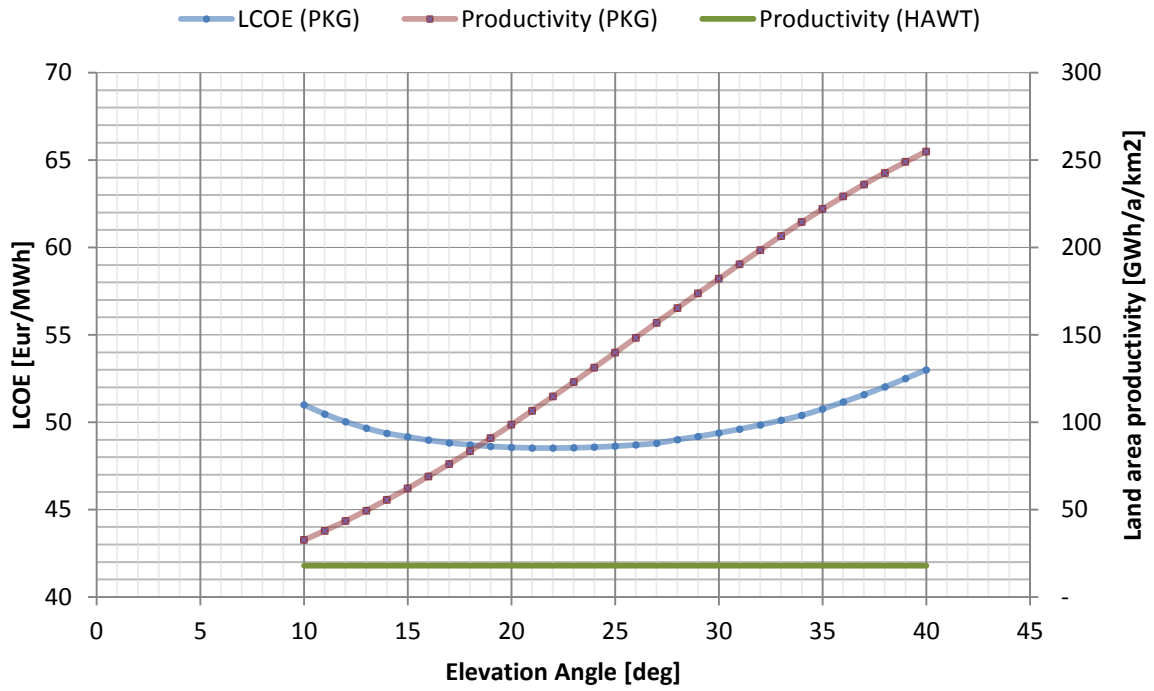


FIGURE 5-2 ANNUAL ENERGY PRODUCTION PER LAND AREA

Component	Component Costs \$1000	Component Mass kgs
Rotor	237	28,291
Blades	152	13,845
Hub	43	10,083
Pitch mechanism & bearings	38	3,588
Spinner, Nose Cone	4	775
Drive train, nacelle	617	43,556
Low speed shaft	21	3,025
Bearings	12	679
Gearbox	153	10,241
Mech brake, HS coupling etc	3	
Generator	98	5,501
Variable speed electronics	119	
Yaw drive & bearing	20	1,875
Main frame	93	19,783
Electrical connections	60	
Hydraulic, Cooling system	18	120
Nacelle cover	21	2,351
Control, Safety System, Condition Monitoring	35	
Tower	147	97,958
	0	
TURBINE CAPITAL COST (TCC)	1,036	169,804
Foundations	48	
Transportation	50	
Roads, Civil Work	79	
Assembly & Installation	38	
Electrical Interface/Connections	122	
Engineering & Permits	32	
	0	
	0	
	0	
BALANCE OF STATION COST (BOS)	367	0
	0	
Initial capital cost (ICC)	1,403	169,804
Installed Cost per kW (cost in \$)	935	113,203
Turbine Capital per kW sans BOS & Warranty (cost in \$)	691	113,203
Levelized Replacement Cost \$ per year	18	
O&M \$ per turbine/yr	30	
Land Lease Cost	5	
CAPACITY FACTOR	32.82%	
Net ANNUAL ENERGY PRODUCTION Energy MWh (AEP)	4312	
Fixed Charge Rate	11.85%	
COE \$/kWh	0.0476	

FIGURE 5-3 COST OF ENERGY CALCULATION OF 1.5 MW WIND TURBINE, NREL

6 WIND MODELING RESULTS

A Rayleigh distribution and the wind data for Chasseral in Switzerland (see chapter 3.4.1) are used to research the effects of using different methodologies and assumptions to calculate the annual energy production of a pumping kite generator. In addition the effect of changes in the wind shear exponent and in the annual mean wind speed at 50 meters altitude is examined. This is done with a Rayleigh distribution.

6.1 WIND SHEAR EXPONENT

At constant mean wind speed (e.g. at 50m), a change of the wind shear exponent can significantly change the wind speed at the operating height of the kite and in turn the annual energy production. For a kite that operates at higher altitudes, this effect is even stronger than for a wind turbine. The baseline design (with a tether length of 600 meters) and a mean wind speed of 7.25 m/s at 50m altitude are used to evaluate, how big the impact could be of changing the wind shear exponent between 0.1 and 0.25.

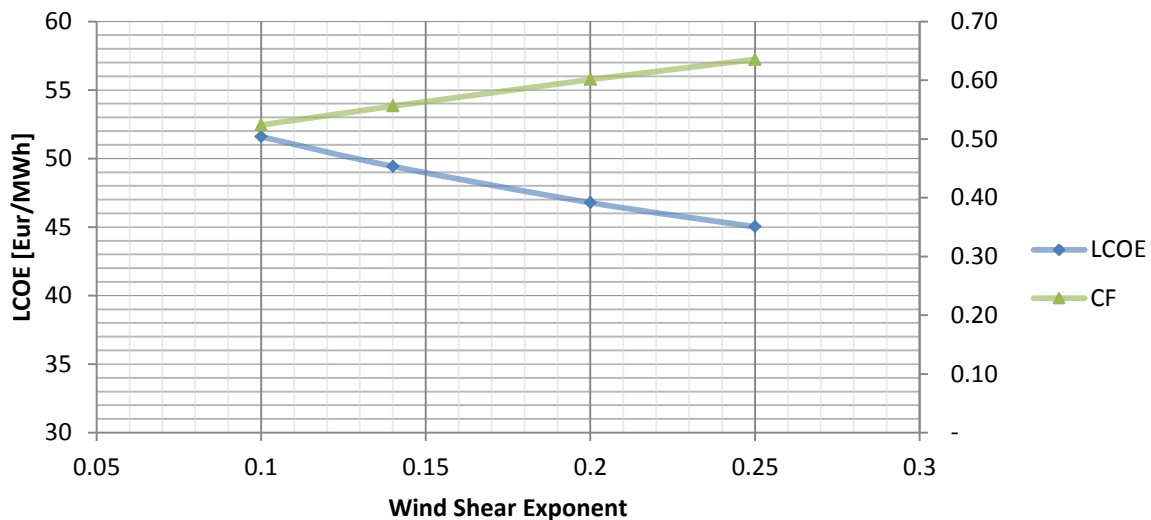


FIGURE 6-1 IMPACT OF WIND SHEAR EXPONENT ON LCOE AND CAPACITY FACTOR

Changes within this range of frequently occurring wind shear conditions (see 2.1.2) can be responsible for changes in LCOE of up to 6.5 €/MWh. At constant mean wind speed, the capacity factor increases about linearly with the wind shear exponent.

6.2 MEAN WIND SPEED

The available wind resource is a crucial factor for the feasibility of wind energy projects. The mean wind speed is often used as a first indicator. The locations with good wind conditions are not always accessible or close enough to the electricity consumers. As the wind energy sector grows, more and more good spots are already taken and locations with lower mean wind speeds have to be used. It is thus interesting to find out, how big the effect of a change in mean wind speed on the cost of energy might be.

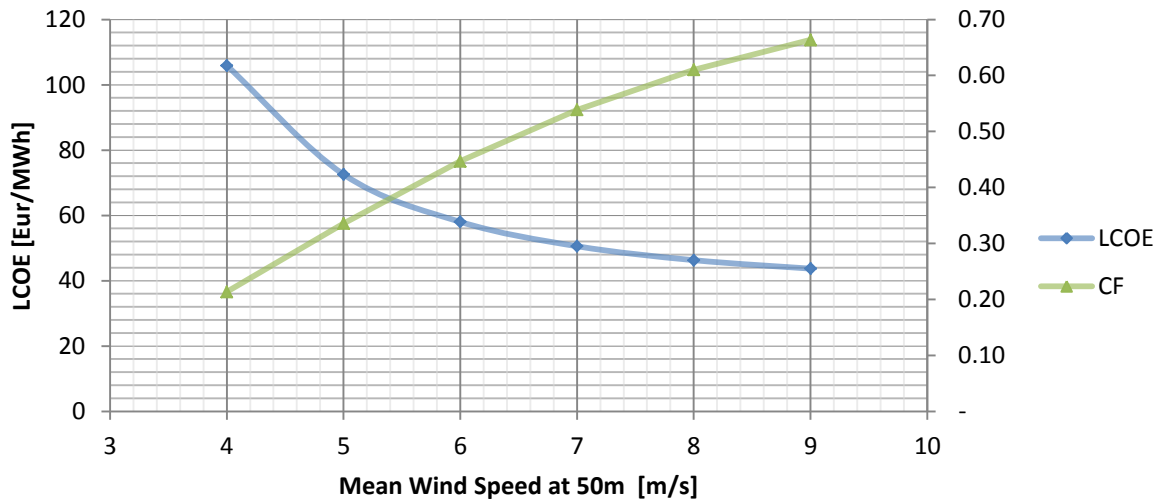


FIGURE 6-2 LCOE AND CAPACITY FACTOR FOR DIFFERENT MEAN WIND SPEEDS

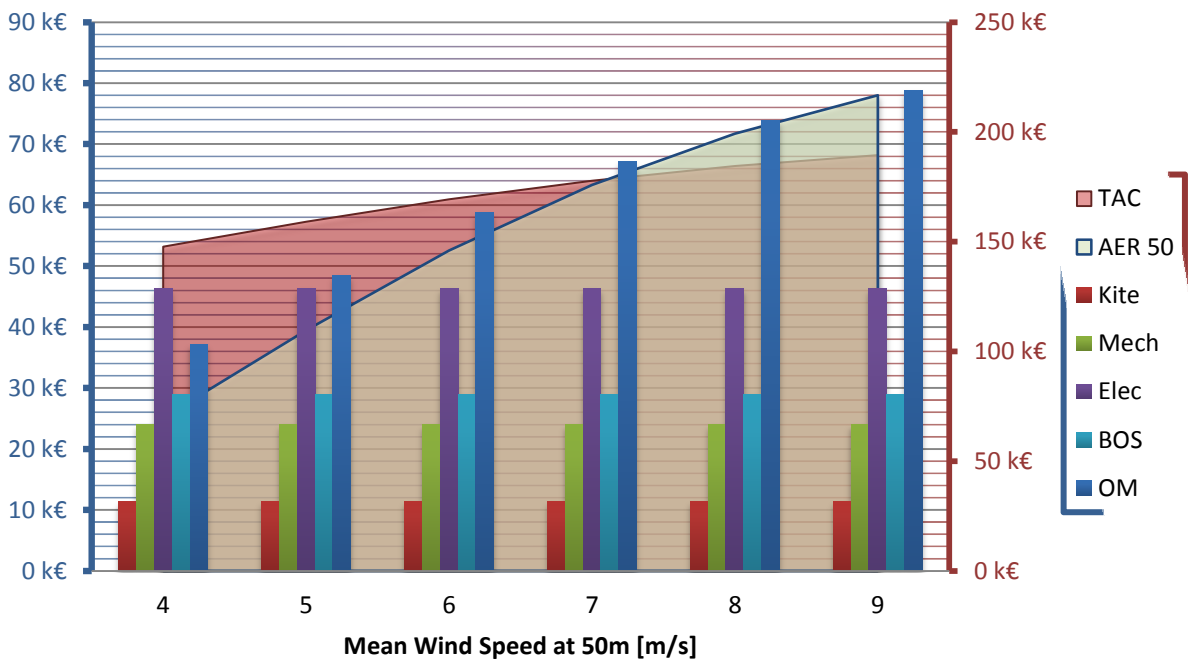


FIGURE 6-3 COST AND REVENUES FOR DIFFERENT MEAN WIND SPEEDS

Figure 6-2 and Figure 6-3 show the outcomes of a simulation with the baseline design, a wind shear exponent of 0.143 and different average wind speeds. The capacity factor can be doubled by increasing the wind speed from 4 to 7 m/s. The result is a strongly decreasing cost of energy, but for higher mean wind speeds, the cost does not decrease that much anymore. Such an analysis is however of limited use, because the baseline is optimized for mean wind speeds around 7 m/s and optimization for the other wind speeds might actually yield much more favorable LCOE's. To illustrate this effect, different kite areas were tested for the baseline machine at 4 m/s mean wind speed (see Figure 6-4).

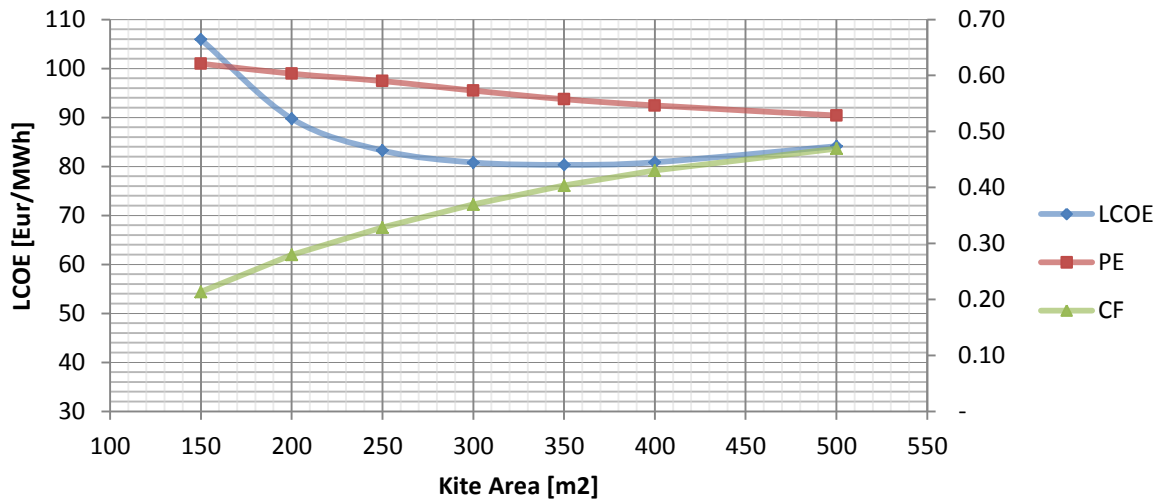


FIGURE 6-4 KITE AREA OPTIMIZATION AT MEAN WIND SPEED OF 4 M/S

Replacing the 150m²-kite from the baseline design by a kite of 300 m² brings the LCOE down to about 80 €/MWh. The capacity factor can even be doubled by increasing the kite size. Note that the same ground station is used and only the kite has to be changed. As mentioned above, it might even be possible to just add more kites on the same tether (see Figure 1-11). Such options could make it very easy to adjust a PKG design to many different wind conditions at relatively low cost.

6.3 SWISS MOUNTAIN SITE

The weather model cosmo2 (see 3.4) is used to calculate the performance of the baseline machine at the mountain Chasseral in western Switzerland. This site is currently used for prototype testing and is one of the windier spots in Switzerland. Data for the year 2008 is used to calculate the annual energy production. The annual mean wind speed is 3.9 m/s at 50 meters and 7.2 at 300 meters altitude (Those are average values for an area of about 4 km², on the mountain top wind speeds are probably much higher). The kite is operated at 30 degrees tether angle and thus at an altitude of about 300 meters. As the kite size of the baseline design is likely to be too small for this site, other sizes are tested as well.

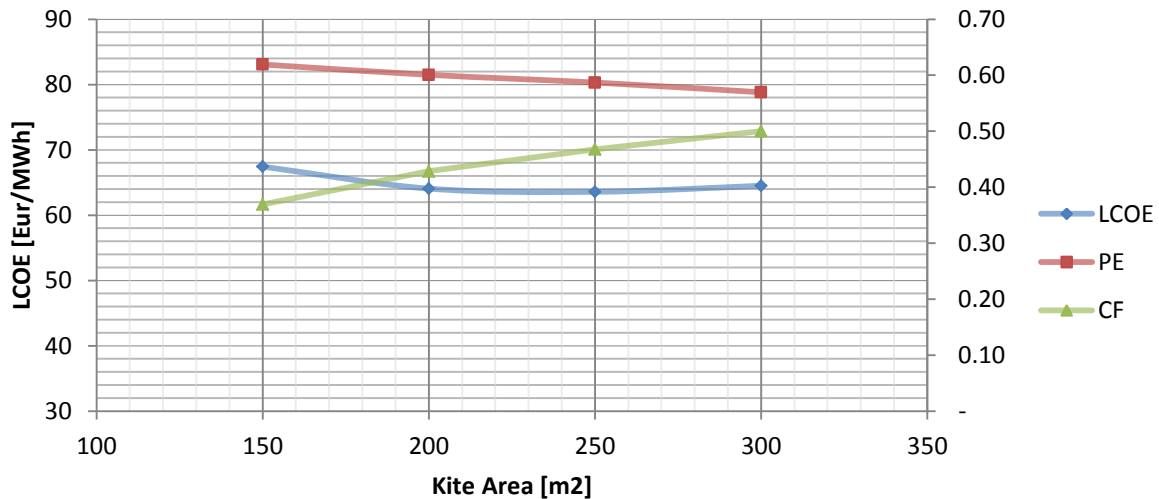


FIGURE 6-5 KITE AREA FOR CHASSERAL

The LCOE can be reduced by about 4 €/MWh when using a 250 m² kite instead of the baseline kite area of 150 m². The capacity factor even goes up by 10 percentage points. The LCOE for the larger kite area is 63.57 €/MWh.

6.4 VARIABLE TETHER ANGLE

One advantage of pumping kite generators is that they can change their altitude easily by changing their tether angle or tether length. If the wind profile changes, they can adjust to it and maximize their energy production. A conventional wind turbine always operates at a constant height. However, the advantage of a variable altitude only occurs if the wind profile changes significantly over time. For a given wind profile, there is an optimal altitude which is the result of a trade-off between small tether angles for better efficiency (see 4.2.1) and large tether angles for generally higher wind speeds at higher altitudes. The average tether length is assumed to be always equal to 90% of the maximum length to allow for pumping motion over 20% of the tether length. Actually, it could also make sense to operate with shorter average tether length occasionally, to further decrease tether drag (e.g. when the wind speed does not increase much with height). This option is not considered here.

In order to measure the effect of a variable tether angle, the levelized cost of energy of one system is calculated for different operating modes:

- A system with fixed angle throughout the year (10,20,30,40 and 50 degree)
- A system with variable angle between 10 and 50 degree

This analysis cannot be done with a probability density function (PDF) for the wind speeds. A PDF can give information only on wind speeds at a certain altitude or on an average wind profile, but not on actual wind profiles for each hour. These profiles are necessary to make a decision on the optimal operation altitude for each hour (The decision process is described in 3.4). The weather model cosmo2 (see 3.4) can be used to create such hourly profiles by interpolating the wind speed data of the available altitudes.

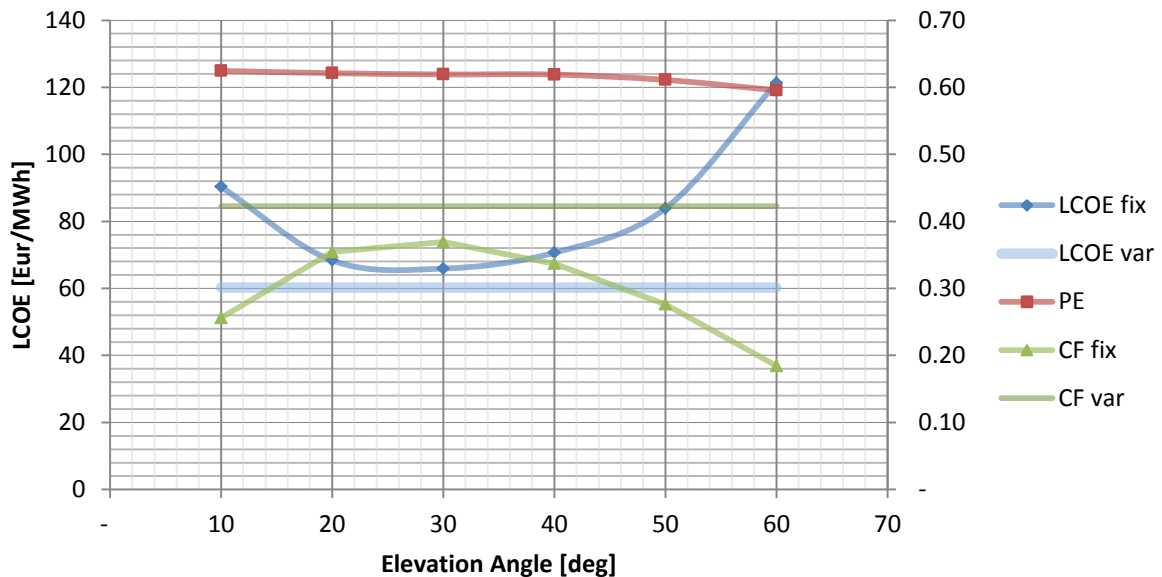


FIGURE 6-6 COMPARISON OF FIXED-ANGLE AND VARIABLE-ANGLE OPERATION

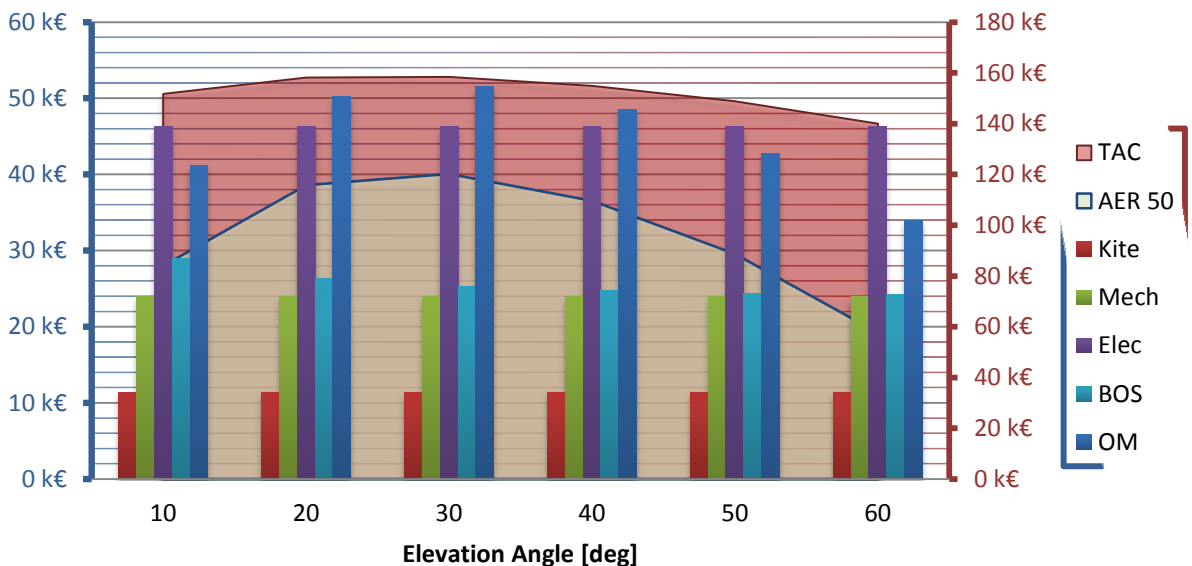


FIGURE 6-7 COST AND REVENUES FOR DIFFERENT ELEVATION ANGLES

A PKG farm that is designed to always operate kites at relatively high angles has somewhat cheaper balance-of-station (BOS) cost, because the ground station can be put closer together (see 0). The O&M cost varies based on capacity factor as it is very dependent on energy

production. The best LCOE for fixed-angle is 65.44 €/MWh for 30 degree. The pumping efficiency is almost constant – the changing LCOE results mainly from different capacity factors ranging from 18 and 37 % for the fixed-angle options. The capacity factor for the variable angle mode is 42%. However, this does not translate directly to an equally large decrease of the LCOE: Higher cost for kite replacement and other variable O&M costs result in an LCOE of 60.04 €/MWh.

The high capacity factor of the system with variable angle mode is possible, because the kite can be operated at the ideal wind speed much more frequently than in fixed angle mode. It operates at 11 and 12 m/s wind speed much more often than a Rayleigh distribution would predict.

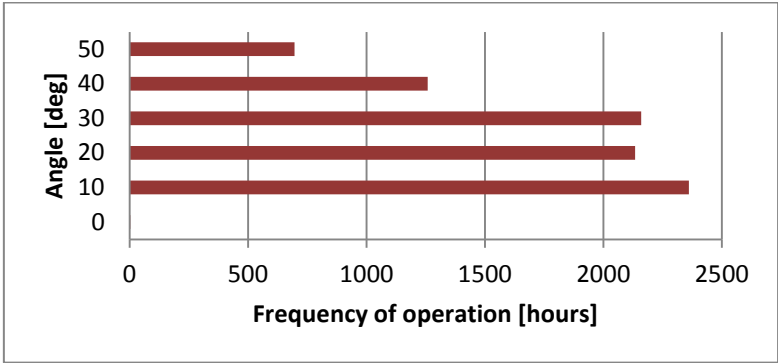


FIGURE 6-8 OPERATION IN VARIABLE ANGLE MODE

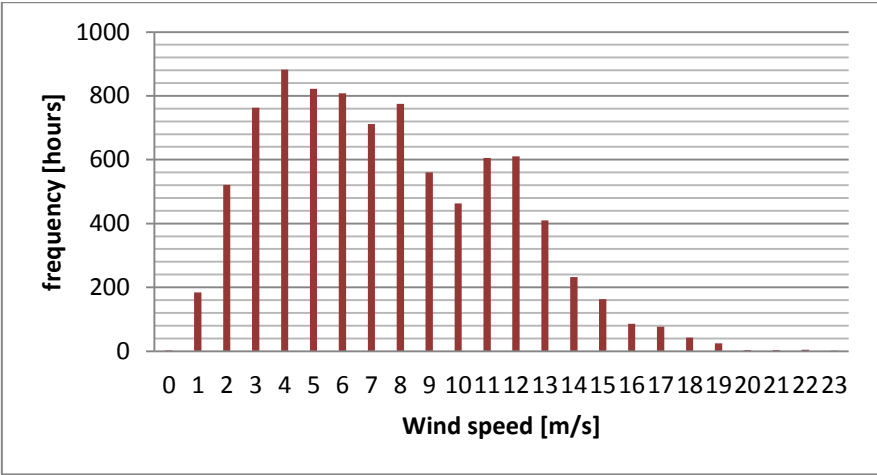


FIGURE 6-9 WIND SPEED DISTRIBUTION FOR VARIABLE ANGLE MODE

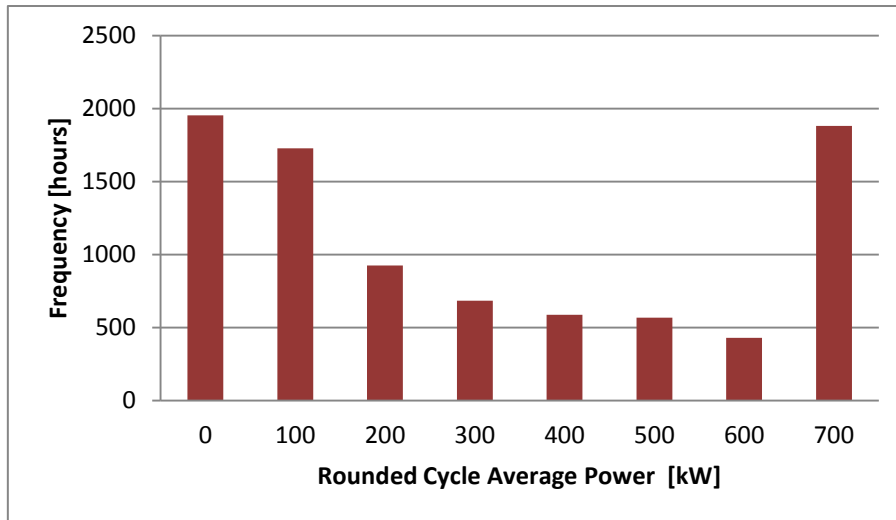


FIGURE 6-10 CYCLE POWER FREQUENCY DISTRIBUTION FOR VARIABLE ANGLE MODE

7 EXPERIMENTAL RESULTS

The performance simulation described above has to be validated against experimental data in order to find out how well it can describe the actual power output of future systems. With the prototype developed at FHNW some power cycles have been flown last autumn (2011). Although it does not make sense to use the results from those flights to predict the performance of future systems, because the kite and the control strategies are still far from optimized, we will make a first comparison to the outputs of the above used simulation. The prototype has a generator with rated power of 10 kW and the nominal force of the system is 2.88 kN. The reel-in speed is about the same as the nominal traction speed, so the asymmetry factor is 1. The tether diameter is 4mm.



FIGURE 7-1 LEFT - FHNW KITE TEST BENCH. RIGHT - KITE AND KITE CONTROL UNIT (KCU)

The kite that was used for this analysis has a projected area of 10 m² and a lift-to-drag ratio of about 4. C_L and C_D are assumed to be 1 and 0.25, respectively. These values are not given by the manufacturer, are dependent on the operation and cannot be measured accurately yet. The kite was steered by a kite control unit (KCU) that is connected to the tether a few meters away from the kite. It can vary the angle-of-attack of the kite and the relative length of the right and left steering line. The KCU also adds significant weight to the kite and thus decreases its performance. This effect is not taken into account by the simulation.

Figure 7-2 shows some data from a typical pumping cycle. At a relatively constant wind speed of around 10 m/s, the tether length varies between 100 and 200 meters, producing significantly more energy during the traction phases than consuming during the reel-in phases. The net energy production over the first thousand seconds amounts to about 1200 kJ, which corresponds to about 1.2 kW average power.

The parameters of the prototype were used to calculate its theoretically obtainable power production with the performance model that was used throughout the thesis for performance estimation (see chapter 3.2.1). A direct comparison of the theoretical and the experimental results is shown in Figure 7-3. For the three lower wind speeds, significantly more than half of the theoretic potential is already reached and the shape of the power curve corresponds well to the theoretic one. At the higher wind speed (~ 11 m/s) the power cannot be increased as much as predicted by the simulation. It has to be noted that apart from a number of other shortcomings, the experimental flight path is fundamentally different from the theoretic one: The kite is flown out of the wind window to be retracted at a large elevation angle, while in the simulation the tether is reeled in and out at the same angle.

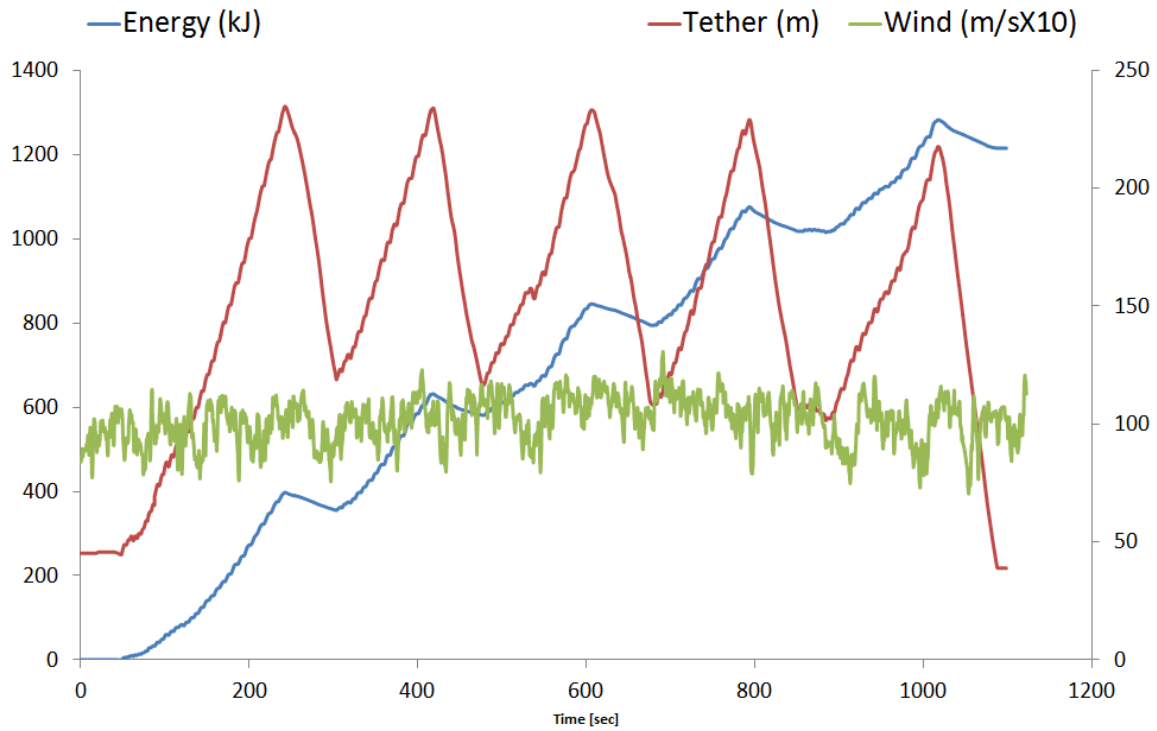


FIGURE 7-2 TETHER LENGTH, ENERGY AND WIND SPEED DURING PROTOTYPE OPERATION

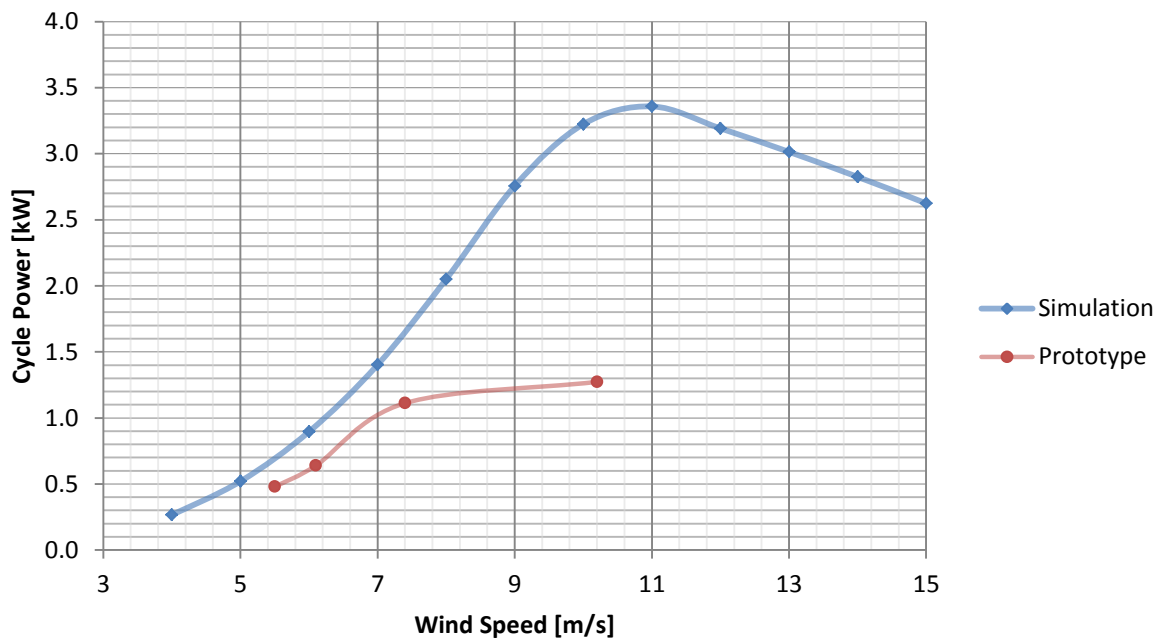


FIGURE 7-3 POWER CURVE: COMPARISON OF PROTOTYPE AND SIMULATION RESULTS

8 SUMMARY OF RESULTS

In Figure 8-1, the percentage by which the parameters were changed and the resulting range of energy cost is depicted. Only one parameter was changed at a time, all others being equal to the baseline value.

Concerning a change of the pumping fraction, there is no visible effect, because it is not considered in the performance calculation. The parameters C_{L_max} , C_D and kite lifetime carry a large uncertainty at the current state of the research and also have a strong impact on the LCOE. The drivetrain efficiency during traction and the asymmetry factor also strongly influence the LCOE, but they can relatively easily be predicted and optimized. Although there is still a rather big uncertainty concerning the cost of several system components (see appendix 11.4) the resulting uncertainty for LCOE is relatively small. Factors like wind shear and mean wind speed can actually be estimated fairly well for a given location. The LCOE range for these factors does not represent a project's specific uncertainty, but it shows the influence of the location. At a very windy spot with 9 m/s wind speed, the cost of energy can be lower by as much as 62 €/MWh compared to a poor spot with 4 m/s average wind speed. However, the performance of a PKG at such a location can be improved amongst others by increasing the kite size as shown in chapter 6.2.

A comparison of different fixed tether angles used throughout the year showed that if reasonable tether angles between 20 and 40 degrees are used, the LCOE varies only by a maximum of 5 €/MWh. In the example of a Swiss mountain site, a continually adjusted tether angle could drop the cost by about 7 €/MWh compared to the best fixed tether angle (65,91€/MWh). The capacity factor could be increased from 37 to 42 %.

It seems thus necessary to use hourly wind data and simulate a continuous optimization of the tether angle in order to obtain an accurate estimation for the LCOE of a PKG.

A comparison with a conventional wind turbine showed that pumping kite generators can be cost competitive. Even when taking the assumed uncertainties into account, a PKG installed at a good site has a large probability of being feasible under current subsidy schemes of for instance Germany. It might even be economical without subsidies. However, the analysis also showed, that PKGs will (if at all) only be slightly cheaper and not by orders of magnitude cheaper than HAWTs.

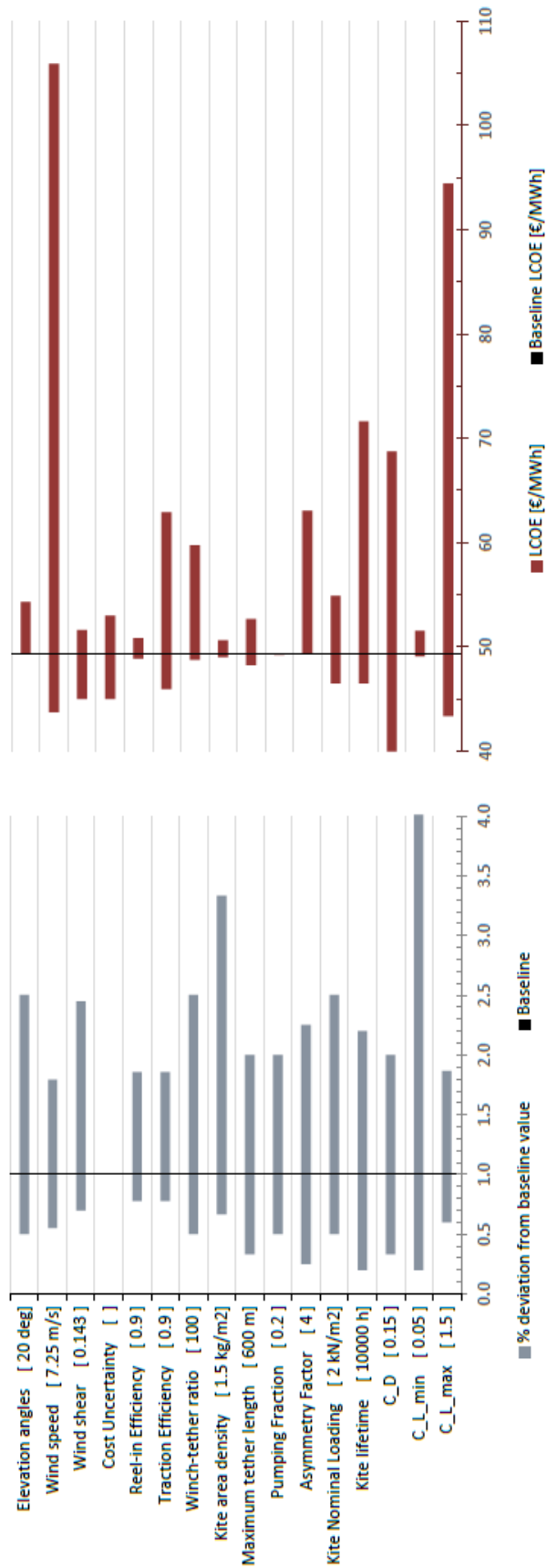


FIGURE 8-1 PARAMETER CHANGES FROM BASELINE VALUE [IN BRACKETS]

9 CONCLUSIONS

9.1 RESEARCH QUESTIONS

The research questions stated in chapter 1.6 will be related to the results of the study. The following question was treated in this thesis: “How can the cost of energy produced by a PKG be calculated and how does the outcome depend on the point of use, the machine design, the operation and the cost?”

In order to answer this question, a method has been developed to calculate the LCOE of a PKG, including a cost model, a performance model and two approaches for estimating the annual energy production: Rayleigh distributions or hourly wind data from a weather model where used.

The influence of the location of the system was analyzed by varying the mean wind speed and the wind shear exponent, using a Rayleigh distribution. An increase of mean wind speed from 4 to 9 m/s showed to result in an improvement of the LCOE from 106 to 44 €/MWh for the baseline system. It was furthermore shown that by increasing the kite size, the LCOE at a low wind speed site with 4 m/s can be decreased to 80 instead of 106 €/MWh. A change in the wind shear exponent showed to have a smaller impact – the LCOE changed by 7 €/MWh at most.

The machine design was analyzed in detail. Primary and secondary parameters were varied around their baseline value to see the resulting change in LCOE. The kite properties have a large influence on the LCOE. Especially the drag and the maximum lift coefficient of the kite as well as its lifetime are important. The primary parameters, generator rating, nominal tether force and kite area, were varied around their baseline value and it was shown that the baseline design lies within a quite robust optimum range. Up scaling of the system leads to some benefit initially, but from 200 kN tether force, there is no significant change of LCOE for larger systems.

Different modes of operation have been compared. When keeping the tether angle constant throughout the year, angles between 20 and 30 degrees lead to the lowest LCOE values for the considered site in Switzerland. It has been shown that an hourly adjustment of the tether angle can increase the capacity factor and decrease the LCOE by about 7 €/MWh.

It became apparent that the uncertainty in the cost of components has a relatively small impact on the uncertainty in the resulting LCOE. The standard deviation of the LCOE was 4 €/MWh for the baseline design.

9.2 CONSEQUENCES

The analysis of the kite properties and their impact on the cost of energy showed that the efficiency and the lifetime of the kite determine to a large degree how competitive a pumping kite generator can be as a large scale, grid-connected energy source. Those topics should thus be researched in more detail.

Under the assumptions made in this thesis, it is possible to build PKGs in the next 5 to 10 years, which are competitive with medium scale current wind turbines. Those PKGs could be profitable under current subsidy schemes and the LCOE would be close to current market prices.

The expectation that PKGs will not clearly outperform conventional technology in the short term implies that for a successful market introduction, niche markets should be found, where PKGs have significant advantages or where HAWTs cannot be used at all. Those might be found in offshore applications or hardly accessible locations. Also, PKGs might be especially cost competitive in the market of 50 to 500 kW turbines, because their hub height is usually rather low and PKGs can operate at much greater altitudes at only small cost.

Another advantage of PKGs is the possibility to increase their capacity factor significantly at relatively low extra cost. This can be of great use when a reliable power source is required or when the electricity is to be marketed on an electricity market with high wind energy penetration. In the absence of feed-in tariffs, also the cost structure of a pumping kite wind farm could become interesting: Depending on the kite cost and lifetime, the operational costs and replacements might become the dominant cost factor. This would be a very uncommon situation for a renewable power source. The financing might become easier because the cost is spread over the lifetime.

9.3 LIMITATIONS

The quality of the performance simulation used in this thesis is difficult to estimate at the moment. The first results from the prototype built at FHNW seem promising, but many more measurements have to be taken. Eventually, a kite with higher performance has to be tested. The simulation is expected to show limited accuracy, because it does not take the weight of the kite or the weight and shape of the tether (tether sag) into account. Nor does it model the actual flight path and the limitations of controllers.

The optimization of the system was done only for three parameters and separated for each parameter, keeping the others constant. Also the sensitivity analysis was done for each parameter separately and a combined change of several parameters might have unexpected effects.

One shortcoming of the cost model is that the O&M cost is too strongly related to energy production. This could increase the cost too much when energy production is increased and the benefit from higher capacity factors might in that way be underestimated.

10 FUTURE RESEARCH

Concerning the point of use, it is interesting to find out if (compared to terrestrial wind generators):

- PKGs are more or less sensitive to a decrease in average wind speed
- the optimal wind conditions for PKGs are different

In order to do these kinds of comparisons, a simple (scalable) cost and benefit model for a conventional wind turbine should be developed.

The performance model for the PKG used in this research should be further validated against experimental data as soon as possible. Also the comparison to other performance models could yield more insights on its accuracy. Deeper analysis into farm arrangement and operation should be done. Especially the aerodynamic interference between kites that could potentially cause an aggregate decrease in farm productivity must be considered. Such effects could significantly change the spacing method. Also the launching and landing method and its consequences for annual energy production and LCOE should be analyzed in more detail.

Also the assumptions concerning cost functions must be further improved, especially for the kite. Realistic values for the CL have to be found and good estimates on the lifetime of the kite have to be made. Many cost functions in this thesis were based on numbers from large wind turbines. Alternatively, quotes directly from the industry could serve as a basis for cost estimates. Considering a step-by-step up-scaling of the technology, it would make sense to also develop cost functions for smaller machines in the 10 to 500 kW range.

Apart from the hard facts (that can in the end be described by the LCOE), the more soft factors should be considered:

- What are the regulations for using the airspace?
- How does the public acceptance of kite power compare to that of HAWTs?
- What are the subjective and objective risks of kite operation and how can they be tackled?

In the present thesis, only one specific concept was considered. There are various other ways to realize a pumping kite generator and even more options to build a device for airborne wind energy; for instance an airborne wind turbine. A comparison between different concepts should be done to find out more about their specific strengths and weaknesses.

In addition more research should be done on niche markets where pumping kite generators can make use of their specific advantages.

11 APPENDIX

11.1 PERFORMANCE MODEL

11.1.1 MATLAB FILES

```
function [Psurf Parameters] = ...
    MakePowerSurface(P,F,L,A,C_D,CLmax,CLmin,AF,...
    trajdim8orEfficienciesRT,winds,angles,index_simulation,varname,varval)
% Calculates power surface of given system design
% using the values varval for the variable varname
warning off
rho=1.225; %sea level , about 10% lower per 1000m height

effReelin=trajdim8orEfficienciesRT(1)
effTraction=trajdim8orEfficienciesRT(2)

evalin('base', 'clear all')

Psurf=zeros(length(winds),length(angles),size(varval,1));
assignin('base','P',P)
assignin('base','F',F)
assignin('base','L',L)
assignin('base','A',A)
assignin('base','CLmin',CLmin)
assignin('base','CLmax',CLmax)
assignin('base','cd0',C_D)
assignin('base','AF',AF)
assignin('base','dim8',trajdim8orEfficienciesRT)
assignin('base','effReelin',effReelin)
assignin('base','effTraction',effTraction)
assignin('base','winds',winds)
assignin('base','angles',angles)
assignin('base','index_simulation',index_simulation)
assignin('base','rho',rho)

C_L=CLmax;
Pcol=ones(size(varval,1),1)*P;
Fcol=ones(size(varval,1),1)*F;
Lcol=ones(size(varval,1),1)*L;
Acol=ones(size(varval,1),1)*A;

v_R_log=zeros(length(winds),2);
v_R_log(:,1)=winds';
assignin('base','v_R_log',v_R_log)
assignin('base','v_T_log',v_R_log)

F_out=(1+(C_L/C_D)^2)*C_L;
F_in =C_D;
```

```

Fout2Fin=F_out/F_in;

for i=1:size(varval,1)
    assignin('base','thevar',varname)
    assignin('base',strcat(varname,'_range'),varval)
    assignin('base',varname,varval(i,:))
    assignin('base','varvalindex',i)
    eval([varname '=' mat2str(varval(i,:))])
    eval([strcat(varname,'col(') mat2str(i) ')=' mat2str(varval(i,:))])

    for wi=1:length(winds)
        for ai=1:length(angles)
            timen=tic;
            assignin('base','wconst',winds(wi))
            assignin('base','v_w',winds(wi))
            assignin('base','theta',angles(ai))

            if index_simulation==1

                PmeanvectPS=P_C_opt()

            elseif index_simulation==2
                % Set variables
                assignin('base','wconst',winds(wi))
                % elevation angle in degree
                elevation_in_degree=angles(ai);
                theta = deg2rad(90-elevation_in_degree);
                % [phi theta] of center position
                pos8 = [0,theta] ;
                assignin('base','pos8',pos8)
                if winds(wi)==0
                    PmeanvectPS=0
                else
                    % Run Simulation
                    % Param2Design is automatically run by Init-function
                    sim('System_1MW',500);
                    PmeanvectPS=evalin('base','Pmeanvect')
                end
            end

        end

    end

    % Display information
    message1=strcat('finished: wind: ',num2str(winds(wi)),...
        ' m/s  angle: ',num2str(angles(ai)), ' deg');
    message2=strcat('P = ',num2str(P),'F = ',num2str(F),...
        ' L = ',num2str(L),' A = ',num2str(A));
    message3=strcat('Power Production:',num2str(max(PmeanvectPS)));
    message4=strcat('time spent:',num2str(toc(timen)));
    disp(message1)
    disp(message2)
    disp(message3)
    disp(message4)

    Psurf(wi,ai,i)=max(PmeanvectPS);
    disp('_____')
end

```

```

    end
end
assignin('base','Psurf',Psurf)
Parameters=[Pcol Fcol Lcol Acol];
assignin('base','Parameters',Parameters)

relPsurf=Psurf/F_out;

% Plot Power Curve for first angle
colormap(Jet(size(Psurf,3)))
cmap=colormap;
for i=1:size(Psurf,3)
    Fout2Fin=F_out/F_in;
    plot(winds,Psurf(:,1,i),'Color',cmap(i,:),'Marker','.')
    xlabel('wind speed [m/s]')
    ylabel('P_c [W]')
    hold on
end
end

```

```

function [ P_C ] = fun_P_C( x)
% Average cycle power
% without tether weight and kite weight
% tether drag must be included in overall drag C_D

v_R=x(1);
v_T=x(2);

P_R=fun_P_R( v_R) ;
P_T=fun_P_T_limCL( v_T) ;
P_C =-( (P_T./v_T - P_R./v_R) ./ (1./v_T + 1./v_R) );

end

```

```

function [ P_R ] = fun_P_R( v_R )
% Power consumption during reel-in

% Drivetrain efficiency during reel-in
effReelin=evalin('base','effReelin');

global C_L_min
C_L=C_L_min;
global theta
global v_w
global A
global rho
global C_D

% No power zero for wind speed
if v_w==0; P_R=0; return;end;

% Calculate power consumption during reel-in
P_R=C_D.*0.5*rho*A.*v_R.*v_w.^2.*(C_L.^2/C_D.^2 +
1).^ (1/2).*(v_R.^2./v_w.^2 + (2.*v_R.*cosd(theta))./v_w + 1);

% Include efficiency
P_R=real(P_R)/effReelin;
end

```



```

function [ P_T] = fun_P_T_limCL( v_T)
% Power production during traction
global v_w
global theta
global rho
global P
global F
global A
global C_D
global C_L_max

C_L=C_L_max;
Pnom=1000*P;
Fnom=1000*F;
vnom=Pnom/Fnom;
effTraction=evalin('base','effTraction');

% No power zero for wind speed
if v_w<=0; P_T=0; return;end;

% Calculate force during traction phase (formula splitted in two sub-parts)
part1=( (cosd(theta)-v_T./v_w).* ...
        ((C_L./C_D).^2+1)+ 2.*v_T./v_w.*sind(theta).*(sind(theta)-1) );
part2=sqrt(cosd(theta)-v_T./v_w);
T_T=0.5*rho*A.*v_w.^2.*C_D.* part1.^(3/2).* real(part2);

P_T=real(T_T.*v_T);

% Limit traction force by decreasing C_L
F_T=P_T/v_T;
if F_T>Fnom
    P_T=Fnom*v_T;
end

% Include efficiency
P_T=P_T*effTraction;
end

```

```

function [ v_R_v_T ] = opt_v_R_v_T()
% Calculates the optimum traction and reel-in speeds
% to maximize average cycle power
global P
global F
global AF
vnom=P/F;

v_R_max=vnom*AF;

x0=[0.01  0.01]; a=[]; b=[]; Aeq=[]; beq=[]; lb=[1  0.01];ub=[v_R_max
vnom]; nonlcon=[];
options=optimset('Algorithm','interior-point');
v_R_v_T=fmincon(@fun_P_C,x0, a, b,Aeq,beq, lb,ub,nonlcon,options );

end

```

```

function [ P_C P_T P_R ] = P_C_opt( )
% Average cycle power
% without tether drag and weight and kite weight

global v_w
global P
global F
global L
global A
global C_D
global C_L_max
global C_L_min
global AF
global rho
global theta
v_w=evalin('base','v_w');
P=evalin('base','P');
F=evalin('base','F');
L=evalin('base','L');
A=evalin('base','A');
C_D=evalin('base','cd0');
C_L_min=evalin('base','CLmin');
C_L_max=evalin('base','CLmax');
AF=evalin('base','AF');
rho=evalin('base','rho');
theta=evalin('base','theta');

% Find optimal speeds
[ v_R_v_T ] = opt_v_R_v_T( );

% Determine maximum possible cycle power
P_C =-fun_P_C(v_R_v_T);

end

```

11.1.2 ALTERNATIVE PERFORMANCE MODEL

The simulation developed by Jérôme Marchand (Marchand, 2011) could be used to estimate the effect of suboptimal conditions on the average power output. As opposed to the simple model introduced above, it takes into account:

- Mass of kite and tether (using a point mass approximation)
- Suboptimal control of flight trajectory
- Suboptimal traction speed and reel-in speed

A trial has been made to make this simulation suitable for a parameter study. A major change was done on the kite trajectory control. As explained above (2.6), the controller used two inputs with two manually chosen gains to derive a roll angle that can bring the kite back to the trajectory. This controller cannot be used for a parameter study because its performance depends strongly on parameter values like kite area or maximum traction force. It would thus be difficult to find out if a poor performance is due to suboptimal parameters or due to poor controller performance. A controller that performs well for all kinds of parameter combination had to be developed.

The new controller uses the distance d to the closest point on the set trajectory (green dot in FIGURE 11-1) to define a target point (red) which is at a distance L further on the trajectory:

$$L = \text{round} \left(\frac{5d - \frac{d^2}{10} + 6}{1000 * dtraj} \right)$$

The trajectory consists of points that are $dtraj$ apart from each other, so L is an integer that stands for the number of points between the green and the red dot. When the kite is very close to the trajectory, L is 1. For somewhat larger distances, L increases about linearly. When the distance d becomes very large, it is made sure that the kite returns to the trajectory as quickly as possible by again decreasing L . In order to steer the kite in the direction of the red dot, the angle between the red line (kite to target) and the grey arrow (kite velocity vector) is calculated. This angle is called the error angle as it describes the difference between actual direction and target direction. The roll angle of the kite is then related to this error angle:

$$\psi = k \alpha_{err}$$

where k is usually 1, but becomes .1 when the kite becomes very slow. This is done in order to prevent rapid oscillations at low speeds.

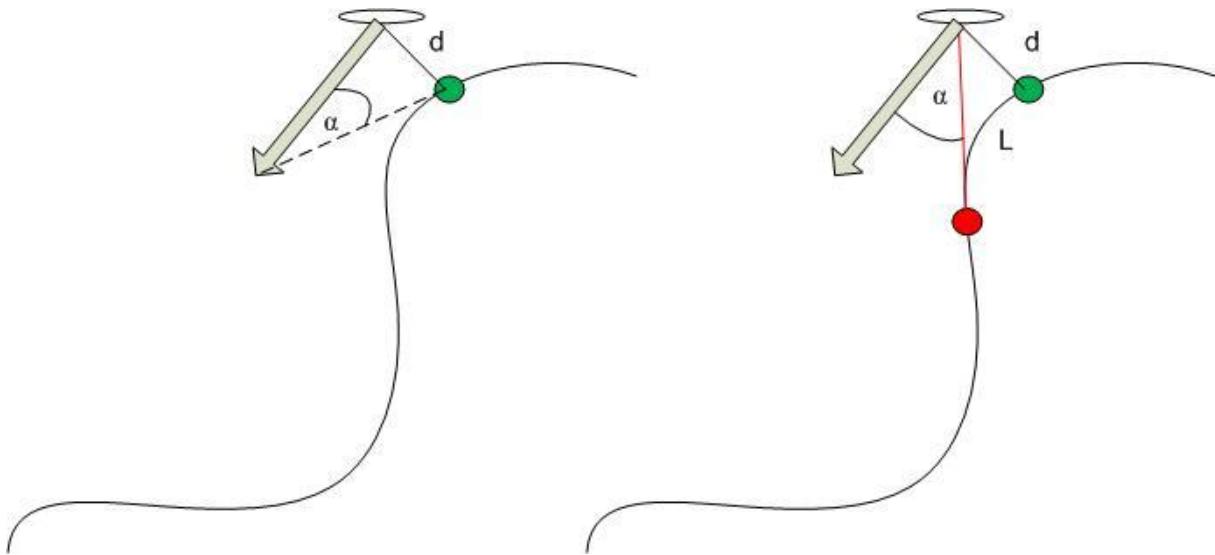


FIGURE 11-1 KITE TRAJECTORY CONTROLLER

The new controller is able to keep the kite on the trajectory for all realistic parameter combinations.

Furthermore, the five phases of the power cycle were reduced to only two. This was possible because according to the assumptions made above, there are no transition phases between traction and reel-in phase. A positive side effect of this approach is a significantly improved computation time.

This simulation now takes about 20 seconds to simulate a full pumping cycle and the corresponding power production. This means a full description of a pumping kite generator for 20 wind speeds and 5 elevation angles takes about half an hour.

The above described adjustments were made using a 10kW system similar to the prototype at FHNW. When trying to use the simulation for a larger system with different parameters, some controllers turned out not to work properly anymore. It seems that the torque controller and the CL-controller have to be manually tuned for each new set of parameters. They are both responsible for limiting the traction force and at the same time optimize power production. If they do not work properly, the power production is lower and most of the times, the kite even crashes. There was not enough time to fix those problems and the simulation was thus not used to estimate the performance of the baseline design. This should be done when the above described problems are fixed. A comparison can then be done, between the two simulations described in this thesis.

11.2 ANNUAL ENERGY CALCULATION

11.2.1 MATLAB FILES

```
function [EnergyProduction CF PE Operation] =
Calculate_EnergyProduction(StartDateAsString,ntestdays,PowerSurfaces,Parameters,winds,angles,M,dates,hlevels)
% Calculates the energy production for a given time frame
% and the capacity factor based on the maximum cycle average on the power
% surface
% The Operation is logged as power, wind speed, operating angle and date
% StartDateAsString in the format yyyyymmddHHMM

testhours=0:1/24:ntestdays;
startdate=datetime(StartDateAsString,'yyyyymmddHHMM');

disp('Starting new Energy Production file')
P=Parameters(:,1)*1000
nsize=size(Parameters,1);
Pmax=zeros(nsize,1);
PE= zeros(nsize,1);
EnergyProduction=zeros(nsize,3);
Operation=zeros(length(testhours),4,nsize);
CF=zeros(nsize,1);

for n=1:nsize
    timen=tic;

    % Let the design run under real wind conditions
    [PowerPerHour wopt aopt date] = ...
        P_optim(winds,angles,PowerSurfaces(:,:,n),...
            Parameters(n,3),startdate+testhours,M,dates,hlevels);
    % Calculate total energy production of the testing period
    Energy=sum(PowerPerHour)
    Operation(:,:,n)=[PowerPerHour wopt aopt date];

    Pmax(n)=max(max(PowerSurfaces(:,:,n)))
    Pnom=P(n)
    PE(n)=Pmax(n)/P(n)

    hours=length(PowerPerHour);
    CF(n)=Energy/(Pmax(n)*size(PowerPerHour,1))

    EnergyProduction(n,:)=[startdate startdate+ntestdays Energy];

    time_spent=toc(timen);
    disp(strcat('time spent for this power surface:',num2str(time_spent)))
end
```

```

function [ Popt_out wopt_out aopt_out date_out ] = P_optim(
winds,angles,Psurf,R, datenumber ,M,dates,hlevels)
% Calculates the maximum obtainable power
% in a given wind data hour
% with a given power surface
% and tether length R

Pmax=zeros(length(datenumber),1);
wopt=zeros(length(datenumber),1);
aopt=zeros(length(datenumber),1);
match=0;

for di=1:length(datenumber)
    for ai=1:length(angles)
        % actual_date=datestr(datenumber(di))
        w=angle2wind(datenumber(di),R,angles(ai),M,dates,hlevels);
        if isempty(w); disp('no data for this date in M'); return; end
        for wi=1:length(winds)
            % Within the values in winds, find the wind speed which is
            % closest to the found wind speed w at angle ai
            wstep=winds(2)-winds(1);
            if and(w>winds(wi)-wstep/2, w<winds(wi)+wstep/2)
                match=1;
            elseif and(wi==max(winds), w > max(winds)); match=1;
            end
            if match
                P=Psurf(wi,ai);
                if P > Pmax(di)
                    Pmax(di)=P;
                    wopt(di)=winds(wi);
                    aopt(di)=angles(ai);
                end
            end
            match=0;
        end
    end
end

end
Popt_out=Pmax;
wopt_out=wopt;
aopt_out=aopt;
date_out=datenumber';
end

```

```

function [ wi ] = angle2wind( datenumber, R, angled,M,dates,hlevels )
% This function determines the wind speed
% for a given altitude given by elevation angle and tether length
% and for a given date and time

dindex= find(dates==datenumber);
if length(dindex)>1; disp(dindex); disp('too many dates');return;end;
w=M(:,dindex);

% for downloading data from server
% datestring=datestr(datenumber,'yyyymmddHHMM');
% [m height d hour]= getdata(datestring);
% w=m(:,1+hour);

wi=interp1(hlevels,w,R*sind(angled));

end

```


11.3 MACHINE SPACING

A formula for the spacing of pumping kite machines is derived by assuming that two neighboring kites always move in cones of identical orientation. The cones have a length L (the maximum tether length) and an opening angle γ (defined by the flight trajectory) and are elevated by an angle α (the elevation angle of the tether). The red triangle in Figure 11-2 is used to derive a formula for the distance between the machines (grey squares).

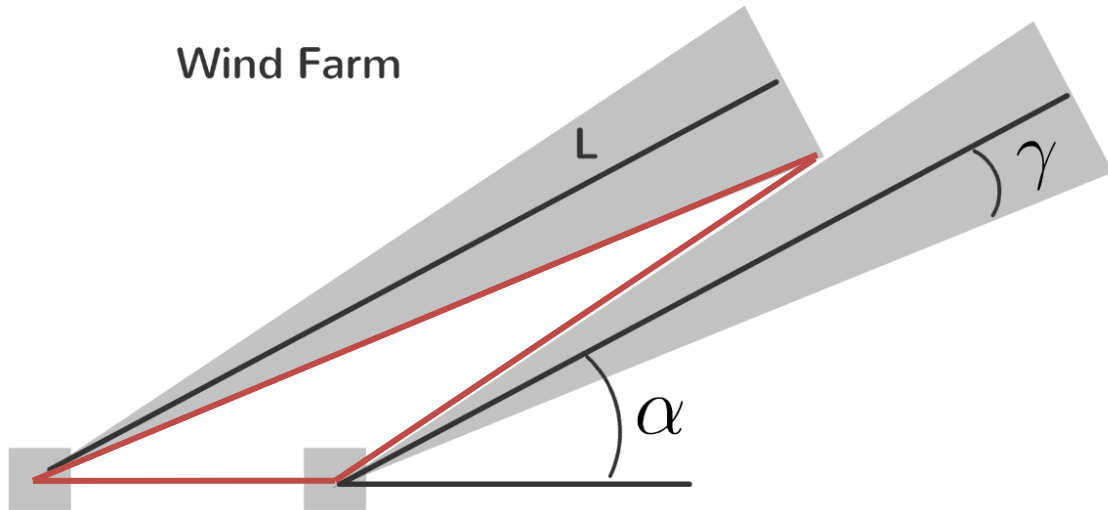


FIGURE 11-2 MACHINE SPACING ASSUMPTIONS

The angles and distances in this triangle are depicted in Figure 11-3.

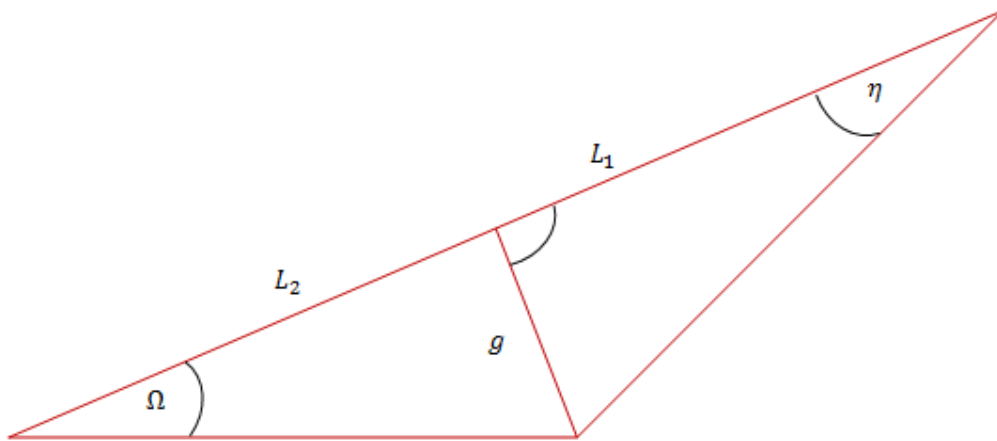


FIGURE 11-3 DERIVATION OF MACHINE SPACING

The maximum tether length L can be expressed by:

$$L = L_1 + L_2 \quad , \text{ with}$$

$$L_1 = \frac{g}{\tan(\Omega)} \quad \text{and} \quad L_2 = \frac{g}{\tan(\eta)}$$

and the distance g is then:

$$g = \frac{L}{\frac{1}{\tan(\Omega)} + \frac{1}{\tan(\eta)}}$$

The distance between the machines can then be described by:

$$dist = \frac{g}{\sin(\Omega)} = \frac{g}{\sin(\Omega) * \left(\frac{1}{\tan(\Omega)} + \frac{1}{\tan(\eta)} \right)}$$

The angles from Figure 11-2 are related to those from Figure 11-3as follows:

$$\Omega = \alpha - \gamma$$

$$\eta = \alpha + \gamma - \Omega = 2\gamma$$

So the distance between neighboring machines can be expressed as a function of the elevation angle, the angle of the flight trajectory and the maximum tether length:

$$dist = L / \left(\sin(\alpha - \gamma) \left(\frac{1}{\tan(\alpha - \gamma)} + \frac{1}{\tan(2\gamma)} \right) \right)$$

11.4 COMPONENT COST MODEL

11.4.1 KITE

In order to calculate the cost of the kite, formulas were developed that can relate the total annual kite cost to its size and loadings. The basis for this analysis is a kite concept developed by EMPA. The assumptions are based on discussions with Roland Verheul (EMPA). As the concept is still in an early development stage, all assumptions will be subject to significant change and can only be seen as a first estimate.

The kite includes a wing and a kite control unit (KCU). The production cost of a kite consists of costs for material and labor. Replacement of the Kite is treated in the chapter on Levelized Replacement Cost. The KCU is assumed to be replaced every 5 years, while the launch and recovery system should survive the whole lifetime of the system.

WING

The cost of the wing will be expressed as a function of its area. The difference between total area and projected area will be neglected, because the wing is assumed to be almost flat. The maximum load it can take will be assumed to be 50 kg (or 200 for the future scenario) per square meter for all sizes. Also the aspect ratio and the thickness ratio will be assumed to not change for different sizes but only for different drag and lift coefficients (which are not treated here). The material cost is assumed to rise linearly with the width of the wing.

Using a one-dimensional scaling factor f , which could for example be the width of the wing, and a constant aspect ratio and thickness ratio, we get the following relationships:

$A \sim f^2$ (twice the width makes twice the length and thus twice the area)

$C \sim f^3$ (cost depends on the volume of the kite)

$C/A \sim f$ (the cost per area increases linearly with the scaling factor)

$C \sim A^{3/2}$

PRESENT SCENARIO

The material currently used for surf kites costs about 4 Euros per sqm for kites up to 30 sqm. It has a lifetime of about 100 full load hours. Slightly improved, already available material can have a lifetime of about 1000 hours and costs about four times more. In the current process that is used by kite manufacturers, four layers of material are used. The material cost of a 30 sqm kite would thus be:

$$4 * 4 * 4 \text{ Euros/m}^2 * 30 \text{ m}^2 = 1920 \text{ Euros (for a 30m}^2 \text{ kite)}$$

For larger areas the cost increase can be estimated from the relationships above:

$$1920 \text{ Euros} = k * 30^{3/2}$$

$$k = 1920 \text{ Euros} / 30^{3/2} \text{ m}^3 = 11,68 = 12$$

For the higher cost boundary, it is assumed that the labor cost adds a factor 2:

$$k=24$$

The lower cost boundaries is based on a slightly lower material cost factor of $k=8$ and significantly decreased labor cost (factor 1.25), due to mass production. The resulting total cost factor is:

$$k=10$$

The total cost for one kite is:

$$\text{Cost (A)} = k * A^{3/2}$$

Example: A 10 m² kite would cost 316 to 760 Euros. Per year (2000 full load hours), about 2 of those kites would be required. So the annual cost would be around 630 to 1520 Euros

Example: A 200 m² kite would cost 28,000 to 68,000 Euros. Per year, about 2 of those kites would be required. So the annual cost would be around 56,000 to 136,000 Euros.

The cost is converted to Euro with a conversion factor of 1.3.

	Minimum Cost	Maximum Cost
Wing Cost [€]	Cost (A) = 10 * A ^{3/2}	Cost (A) = 24 * A ^{3/2}

TABEL 11-1

FUTURE SCENARIO

In the future, new materials have to be used in order to build kites that last longer than 1000 hours. They will most likely be more expensive, but the lifetime increase might make up for this. Carbon fiber seems to be a good choice for reaching lifetimes of more than 10000 hours with semi-rigid, lightweight wings. More research on this topic will be done in the next few years. However, for the present study, some simple assumptions will be made to arrive at a cost function for future kite designs that are more economical than current technology. The assumptions can be seen as a reference point for this research. For somewhat higher area loadings scenario (200 kg/m²), the lifetime of a semi-rigid carbon fiber wing is assumed to be 10,000 hours. The cost factor is assumed to be twice as much as for the currently used material. The resulting lower bound estimate is:

$$k= 20$$

and the higher bound:

$$k= 48$$

	Minimum Cost	Maximum Cost
Wing Cost [€]	Cost (A) = 20 * A ^{3/2}	Cost (A) = 48 * A ^{3/2}

TABEL 11-2

KITE CONTROL UNIT

The kite Control Unit (KCU) is responsible for controlling the kite's angle-of-attack and direction of flight. The angle-of-attack could be changed by a small winch system. The direction could be changed by changing the roll angle or applying an asymmetric drag with small turbines or using a yaw ruder. For the present analysis, a small winch system is considered, that can both control the angle-of-attack and the roll angle.

Estimates for the cost of a KCU were taken from the prototype that was built at FHNW (Marchand, 2011) and from Crosswind Power Systems. Marchand assumes based on Crosswind values a cost for the KCU of about 25,000 € for a 1 MW – 100 kN - machine and a kite of 300 m². The cost is most likely related to the nominal system force. From this cost, 5000 € is assumed to be a constant amount for the electronics and software, the rest is assumed to be linearly related to force:

$$20,000 \text{ €} = 100 \text{ kN} * k_{\text{KCU}}$$

$$k_{\text{KCU}} = 200$$

$$\text{KCU_Cost} = F \text{ [kN]} * 200 \text{ €} + 5000 \text{ €}$$

As this formula is derived from the cost of a prototype, it is assumed to be rather conservative. For a more optimistic formula, taking into account mass production and technological development, a cost reduction by a factor of 2 is assumed for both the constant and the variable part. The KCU is assumed to be replaced four times during the lifetime of the system.

	Minimum Cost	Maximum Cost
KCU Cost [€]	F [kN] * 100 € + 2500 €	F [kN] * 200 € + 5000 €

TABLE 11-1 KCU COST

11.4.2 MECHANICAL SYSTEMS

MAST

The options for launching and landing a kite can be divided into kite integrated and ground based mechanisms. A few examples are:

Kite integrated:

- One or more propellers
- Buoyant kite, e.g. filled with helium
- Wheels below the kite for rolling on the ground

Ground based:

- Fixed vertical tower
- Mast with fixed length but flexible angle
- Telescopic mast with fixed or flexible angle
- Robotic arm
- Rail to move the kite on

The concept with a mast of fixed length but flexible angle is used in this study. It can follow the tether direction, so it does not have to carry significant load. The only load it has to carry is the weight of the kite. Aerodynamic forces related to the kite's drag coefficient are neglected here. The cost function is thus not dependent on the systems nominal force, but only on the kite weight. Furthermore it is assumed that kites with bigger chord length require a longer mast. Mast length thus increases with the square root of the area.

Masts (15 m) for medium sized sailing boats cost about 5 to 10 k€. They are assumed to be able to carry 500 kg. Using the highest cost estimate and a kite area of 50 m² and assuming that the mast has to be able to carry at least 100 kg, even if the kite weight is zero, the cost factor K_m for the mast is:

$$10 \text{ k€} = K_m * (400 \text{ kg} + 100 \text{ kg}) * \text{sqrt}(50)$$

$$K_m = 10 \text{ k€} / (500 \text{ kg} * \text{sqrt}(50)) = 2.8 \sim 3$$

This value is used as the lower bound for the cost function and it is assumed that the mechanism (e.g. hydraulic) for moving the mast costs as much as the mast itself. For a more conservative cost function, the total cost is assumed to be twice as high.

	Minimum Cost	Maximum Cost
Mast Cost [€]	$6 \text{ €} * (\text{kite mass} + 100) * \text{sqrt}(A)$	$12 \text{ €} * (\text{kite mass} + 100) * \text{sqrt}(A)$

TETHER COST MODEL

It is likely that for the tether, some kind of Dyneema material will be used. This material can handle the same forces as wire rope at far lower weight per meter. It is already widely used for power kites and (with much larger diameters) in the offshore industry. So the cost per meter of tether can easily be found on supplier's websites for a large range of diameters.

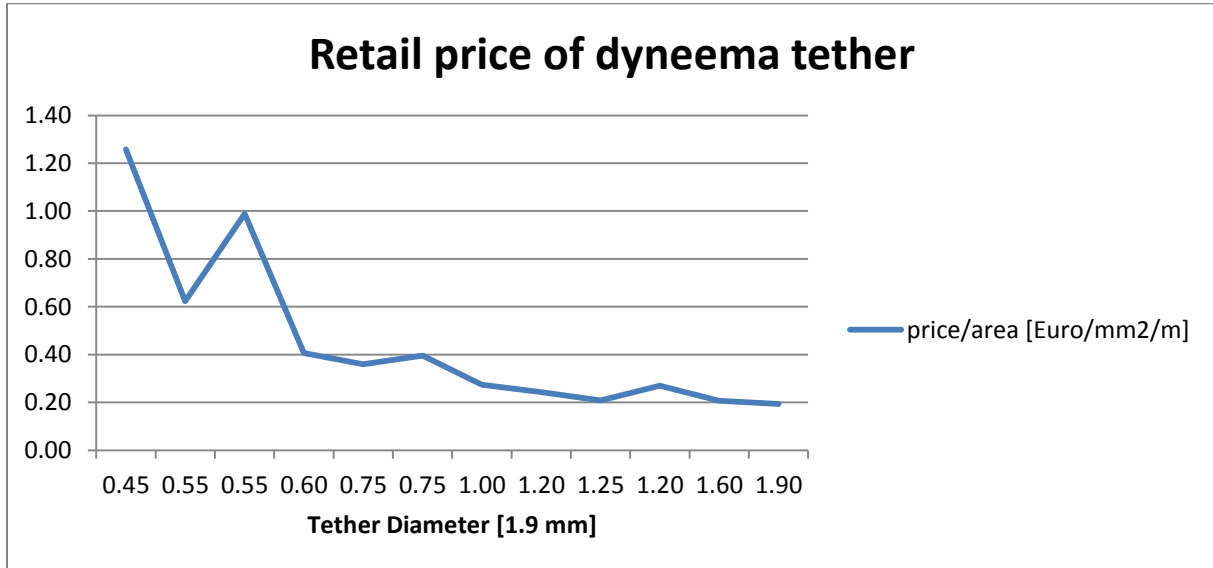


FIGURE 11-4 RETAIL PRICE OF DYNEEMA FOR SMALL DIAMETERS

The cost scales with sectional area rather than diameter. For small diameters up to 1.9 mm the price decreases to about 0.20 €/mm²/m. For larger diameters up to 10mm (about 11 tons load) the price stays at about 0.11 €/mm²/m for small quantities. A maximum price of 0.15 €/mm²/m is assumed for all tether diameters. The cost of a tether on which 200 N/mm² is applied at nominal operation, is:

$$\text{Cost [€]} = 0.15 \text{ €/mm}^2/\text{m} * L * 1/(200 \text{ N/mm}^2) * F_{\text{nom}}[\text{kN}] * 1000$$

Example 1: 200 m of tether with diameter 35 mm and sectional area 1000 mm² (for a 1MW /200kN machine) would cost about 30,000 €, would have specific force of 200 N/mm² and could be used as the pumping part of the tether on a 2.2 m drum for about a year (10,000 hours), with 100 cycles per hour (1.6 per min)(For details see Levelized Replacement Cost).

When buying larger quantities of rope with large diameters, the price will likely go down significantly. For the optimistic scenario, a cost factor of 0.04 €/mm²/m is used.

	Minimum Cost	Maximum Cost
Tether Cost [€/mm ² /m]	$0.15 * L * 1/200 * (F[\text{kN}] * 1000)$	$0.04 * L * 1/200 * (F[\text{kN}] * 1000)$
Spec. Tether Cost [€/kWh]	$\text{Cost_Tether} / \text{Exp}(7+0.1 * D/d) / P_{\text{max_cyc}} * \text{cycles_per_h}$	

TABEL 11-3

WINCH COST MODEL

The winch includes winch bearings, some means of line handling (lead-out sheaves) and the winch drum itself. The size and mass of the winch drum depends on the maximum force on the tether and the pumping length L_p. It is assumed that the tether needed for pumping is stored on the first layer and all the rest of the tether can be stored on top, because there is only little force

acting on the tether while launching or landing the kite. The diameter of the drum D needs to be a certain fraction of the tether diameter d in order to obtain a decent tether lifetime (see Levelized Replacement Cost). However, the drum diameter also defines the gear ratio between drum and generator. If no gearbox is to be used, the winch diameter has to be sufficiently small to match the generator speed. The wall thickness depends on the maximum tether force, but for simplicity, it is assumed to be a constant fraction of the diameter:

$$\text{thickness} = D \cdot 0.05$$

$$\text{mass of drum} = M_D = \pi/4 \cdot (D^2 - (0.9 \cdot D)^2) \cdot d \cdot L_p / (\pi \cdot D) \cdot M_{\text{Alu}}$$

The drum is assumed to be constructed out of aluminum. So the weight can directly be derived from thickness, radius and length. The cost of the drum is derived by using a material cost factor plus a factor for labor cost. Both are assumed to be equal to the market price of aluminum (currently around 1.6 €/kg) as an optimistic estimate. This estimate is based on the assumption that the drums are relatively easy to manufacture (and/or being manufactured on a large scale) and the material cost is thus a major factor.

$$\text{Cost_Drum_min} = 2 \cdot M_D \cdot \text{Cost_alu}$$

As different groups in the AWE sector report that the winch is currently a major cost driver for the total system cost, the upper limit is set much higher. It depends on the mass of the drum as well as on its diameter D . Larger diameters are assumed to make the manufacturing more complex.

$$\text{Cost_Drum_max} = 2 \cdot M_D \cdot \text{Cost_alu} + 20,000 \cdot D$$

The structure needed to guide the tether to the right place on the winch (level winds and lead-out sheaves) is largely dependent on the maximum force acting on the tether. As a large part of the cost is due to the complexity of the construction, cost is assumed to only increase as the square root of the force.

The bearings cost depends on maximum force as well. It is assumed that the drum weight is not the limiting factor here, because the maximum tether force is higher and both will never point in the same direction. A linear function of force is used. More accurate functions could be derived from (WindPACT Drive Train Study p52).

	Minimum Cost	Maximum Cost
Winch Drum [€]	$2 \cdot M_D \cdot \text{Cost_alu}$	$2 \cdot M_D \cdot \text{Cost_alu} + 20,000 \cdot D$
Line Handling [€]	$2000 \cdot \sqrt{F[\text{kN}]}$	$6000 \cdot \sqrt{F[\text{kN}]}$
Winch Bearings [€]	$50 \cdot F[\text{kN}]$	$100 \cdot F[\text{kN}]$

TABEL 11-4

11.4.3 ELECTRICAL SYSTEMS

All components that have mainly costs related to the generator's nominal power are called electrical systems. Some of those components are not directly connected to the generator power, but for conventional turbines, it has been found that they usually scale with nominal power (Fingersh et al., 2006).

The drivetrain for a pumping kite generator can be build similar to a drivetrain for conventional wind turbines. It should be able to deal with variable speeds and to be used in motor mode. Most modern wind turbines have these features. The nominal rotor speed of conventional wind turbine is around 20 to 30 rpm. For pumping kite systems, the nominal winch speed depends on

both the nominal tether speed and the diameter of the winch. It can be significantly higher than 30 rpm, especially for systems with small winches. For a system with 5 m/s (300 m /min) nominal tether speed and a winch diameter of 1 m (perimeter: 3.14 m), the nominal winch speed is about 95 rpm. Higher speeds usually lead to lower cost for the drivetrain, because generators or gear boxes can be smaller.

Most of the required figures for the following assumptions were taken from the NREL WINDpact Advanced Wind Turbine Drive Train Designs Study (Poore et al., 2003) or from the NREL Cost and Scaling Model (Fingersh et al., 2006). Those cost functions are given in 2002 U.S. Dollars. They will be converted to 2012 Euros later.

The nacelle of a conventional wind turbine contains the following parts:

- Low-speed shaft
- Bearings
- Gearbox
- Mechanical brake, high-speed coupling, and associated components
- Generator
- Variable-speed electronics
- Yaw drive and bearing
- Main frame
- Electrical connections
- Hydraulic and cooling systems
- Nacelle cover

For the proposed AWG drivetrain, it is assumed that a drive similar to a wind turbine **yaw drive** is used in order to maintain the winch's orientation to the wind direction.. The nacelle cover is assumed to be similar to a **ground station cover** for an AWG. The **main frame** cost is assumed to be equal to the cheapest option from the NREL study (multi-path drive) for all drivetrain options, because there is neither a space nor a weight restriction in AWG ground stations. Main frame and ground station cover are together called 'Ground Station Cover and Frame'. The **gearbox** is avoided by using a small enough winch or a generator with low speed (see below). For the **electrical connections**, 60 % is assigned to power wires. As PKGs do not have a tower, wiring can be limited to a minimum. It is thus assumed that the electrical connections cost is only 50%. The cost for electrical connections is combined with the variable speed electronics and called '**Power Electronics**'. Figures for hydraulic and cooling systems are directly taken over from conventional wind turbines. Some small parts were not considered, because the costs are negligible in comparison to the other costs (e.g. mech. brake, high speed bearings).

For some parts of the drive train, the cost function depends on the rotor diameter. The nominal power of the AWG will serve as a proxy for calculating a rotor diameter D. With a typical nominal wind speed of 14 m/s, air density of 1 and rotor efficiency of 0.5:

$$P = \frac{1}{2} 14^3 \pi (D/2)^2 * 0.5$$

$$RD = \sqrt{2 * P}$$

This relation is used to convert HAWT cost functions that depend on RD to PKG cost functions that depend on nominal power. The cost for yaw drive and bearing then becomes:

$$C_{YDB} = 2 * 0.0339 * RD^{3.314} = 0.0678 * (2 * P)^{1.657} = 0.2165 * P^{1.657}$$

Power electronics cost is the sum of reported figures for variable speed electronics and half of the cost for electrical connections (incl. switch gear) from conventional turbines:

$$C_{PE} = P \cdot 79 + 0,5 \cdot P \cdot 40 = P \cdot 99$$

The cost for ground station cover and frame are:

$$C_{CF} = 11.537 \cdot P + 3849.7 + 17.92 \cdot \sqrt[2]{2P}^{1.672} = 11.537 \cdot P + 32 \cdot P^{0.8360} + 3849.7$$

In general, the cost functions derived from conventional HAWTs is assumed to be on the optimistic side. The different properties of PKGs might lead to unexpected cost increases, but because both drive trains are very similar, the cost is assumed to increase only by 10% in the pessimistic scenario.

Generator	$P \cdot 1208 \cdot w_{nom}[\text{rpm}]^{-0.57}$ (see below)
Power electronics	$P \cdot 99$
Yaw drive and bearing	$= 0.2165 \cdot P^{1.657}$
Hydraulic and cooling systems	$P \cdot 12$
Ground station cover and frame	$11.537 \cdot P + 32 \cdot P^{0.8360} + 3849.7$

TABLE 11-2 ELECTRICAL SYSTEMS COST IN 2002 U.S. DOLLARS AS A FUNCTION OF P IN KW

The cost is converted to 2012 Euro with a conversion factor of 1.048 (see Methodology).

Generator	$P \cdot 1152 \cdot w_{nom}[\text{rpm}]S^{-0.57}$ (see below)
Power electronics	$P \cdot 94$
Yaw drive and bearing	$= 0.2065 \cdot P^{1.657}$
Hydraulic and cooling systems	$P \cdot 11.4$
Ground station cover and frame	$11 \cdot P + 30.5 \cdot P^{0.8360} + 3671.8$

TABLE 11-3 ELECTRICAL SYSTEMS COST IN 2012 EUROS AS A FUNCTION OF P IN KW

GENERATOR OPTIONS

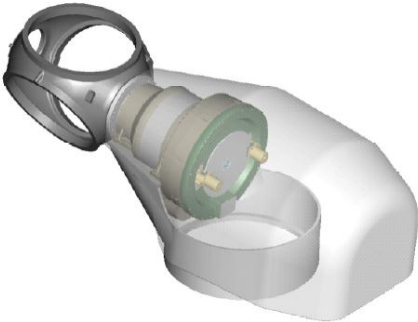


Figure 7-1. WindPACT single PM generator drive train

For small tether diameters (small forces), a small winch and a high-speed generator can be used without gearbox, but for larger systems the winch should not be built too small because the tether would wear out too quickly (see chapter 11.6.1). Generators with lower speeds could be used in order to still avoid using a gearbox. There are a few options described in the WindPACT

Drive Train Study. The generators or generator combinations all have a (total) nominal power of 1.5 MW. Cost curves for other sizes are given in the NREL Cost Study and are summarized below.

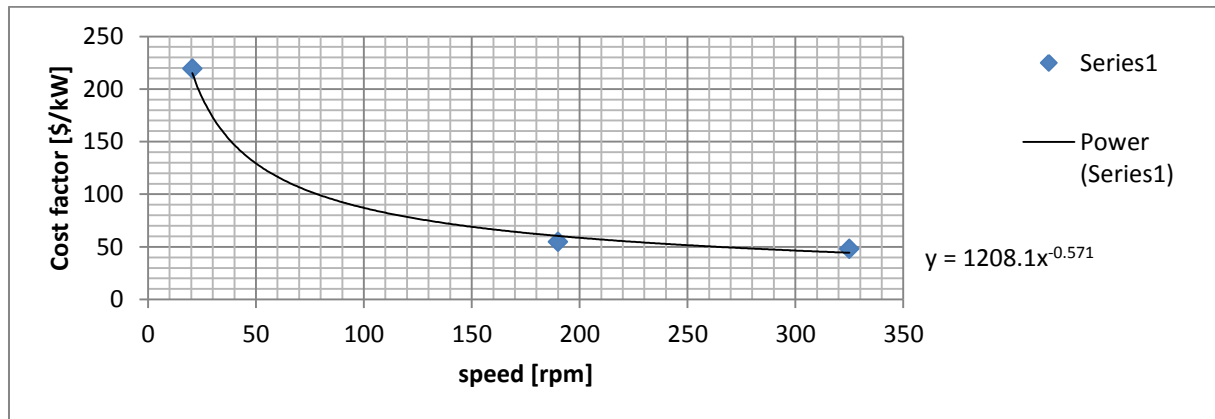
Another Generator option is a medium torque medium speed machine described in WindPACT Drive Train Study, Appendix K (p470). It has 164 rpm at nominal speed and a maximum speed of 266.4 rpm and a cost factor of 112 at its best efficiency of 97.15%.

	Nominal speed [rpm]	Cost factor
High Speed Generator	1500	65
Multi-Path PM	325 (after bull gear 20)	48.03
Medium Speed PM	190	54.73
Medium Speed PM (2)	164.4	112
Direct-Drive	20.5	219.33

TABEL 11-5

The Generator Cost is calculated by multiplying the cost factor with the nominal power in kW.

Generator cost factors for other nominal generator speeds can be estimated by interpolating in between the ones stated above. This allows sizing the drum independently (for example based on tether diameter) and still avoiding a gearbox, because a direct drive can be used.



The generator cost as a function of nominal generator speed w_{nom} [rpm] is:

$$Gen_cost_low = P * 1208 * w_{nom}^{-0.57}$$

This value is chosen as the lower cost limit, while the upper limit is 10% higher.

$$Gen_cost_high = P * 1.1 * 1208 * w_{nom}^{-0.57}$$

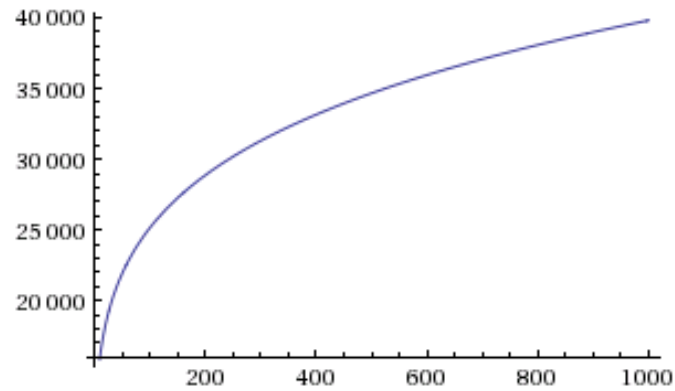
11.4.4 CONTROL AND MONITORING

As compared to conventional wind turbines, AWGs will likely require more sophisticated control and safety systems. It might however be that ground based installation makes it somewhat cheaper and both end up in a similar range. The NREL cost study uses a fixed rate of 35 k\$ per machine for all sizes from 750 kW to 10 MW. For offshore turbines, 55 k\$ is assumed. In order to get reasonable numbers also for small systems, a function that approaches the NREL values for large machines and decreases for small machines was used:

$$Cost\ per\ machine = 10000 \$ * P^{0.2} \quad \text{with } P \text{ in kW}$$

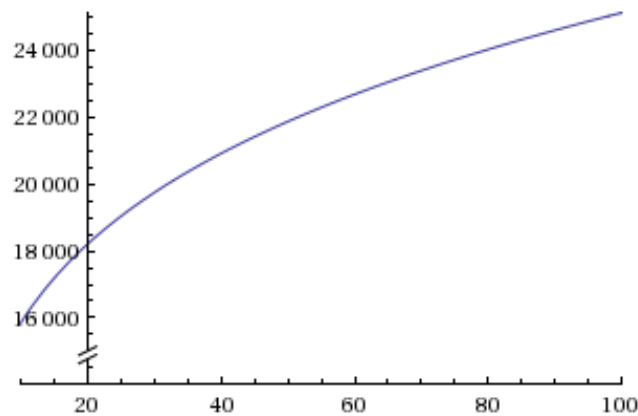
plot	$P^{0.2} \cdot 10\,000$	$P = 10 \text{ to } 1000$
------	-------------------------	---------------------------

Plot:



plot	$P^{0.2} \cdot 10\,000$	$P = 10 \text{ to } 100$
------	-------------------------	--------------------------

Plot:



As this function is very close to the values stated by NREL for onshore wind turbines, it is probably rather optimistic. A more conservative estimate would be 30% higher cost, resulting in a range close to what the system costs for offshore wind turbines.

A more bottom-up estimation should be done as soon as the required cost data is available.

The cost is again converted to 2012 Euros with a conversion factor of 1.048 (see 3.3.3).

	Minimum Cost	Maximum Cost
Control, Safety, Monitoring [€/machine]	$9538 \cdot P^{0.2}$	$12400 \cdot P^{0.2}$

TABEL 11-6

11.5 BALANCE-OF-STATION COST

This document is based upon the WindPACT Turbine Design Scaling Study on Balance-of-Station (BOS) Cost (Technical Area 4) by NREL. In the study, cost estimates for the BOS cost of conventional wind turbines with installed power of 750 kW to 10 MW in a wind farm of a total 50 MW installed power, are made.

In the following it will be discussed as to how far those estimates can be taken over for a similarly sized wind farm consisting of pumping kite systems.

All costs are in 2002 U.S. Dollars. They are converted to 2012 Euros in the end, in order to use them in the cost model.

11.5.1 SUMMARY

The Balance-of-station Cost includes foundations, transportation, roads and civil works, assembly and installation, electrical connections and engineering and permits.

The **foundation** cost of conventional turbines can serve as a rough orientation, but the forces acting on a kite ground station differ a lot from the overturning moment acting on a wind turbine. In case the vertical pulling force of the kite determines the foundation size, its cost would be negligible. The same is likely to hold for direct horizontal forces as the critical factor. However, this could be analyzed in more detail. When the overturning moment starts to become important, costs will be higher. This depends mainly on the system used for launch and recovery.

Transportation costs in the NREL reports are based on a location in the US. So they are of limited use concerning wind farm installations in Switzerland. All the other categories can be used for pumping kite wind farms. The issue of international differences in cost is less severe for those and might be solved by applying a general cost factor (which could for example be derived from IEA Wind Task 26: Cost of Wind Energy, by Hand & Lantz). The '**engineering and permits**'- cost formulas reported in different NREL studies show inconsistencies and should be verified by additional sources.

The cost for **roads** can be either calculated with the cost function by NREL that relates installed power to cost or with a function derived from that one, which relates costs to machine distance d and thus meters of road.

	Minimum [€]	Maximum [€]
Foundation	0	negligible
Transportation	9.5/kW	19/kW
Roads, Civil work	$d * 157$ /unit	$d * 157$ /unit
Assembly and Installation	0	negligible
Electrical Interface	76 / kW	95 / kW
Miscellaneous, Lighting	15 / kW	29 / kW
Engineering, permits	$0.95*(0.005 * P + 10)*P$	$2.86*(0.005 * P + 10)*P$

TABEL 11-7 COST FUNCTIONS IN 2012 EUROS

	Minimum [\$]	Maximum [\$]
Foundation	0	negligible
Transportation	10 /kW (US)	20 /kW
Roads, Civil work	$d * 165$ /unit	$d * 165$ /unit
Assembly and Installation	0	negligible

Electrical Interface	80 / kW	100 / kW
Miscellaneous, Lighting	16 / kW	30 / kW
Engineering, permits	$(0.005 * P + 10)*P$	$3*(0.005 * P + 10)*P$

TABLE 11-4 BOS COST FUNCTIONS IN 2002 U.S. DOLLARS

11.5.2 FOUNDATION/SUPPORT STRUCTURE

Two cost functions are given in the NREL rotor study (Malcolm, Hansen) on page 35. One is based on the machine rating in kW, the other on the load in kNm.

$$\text{Cost/kW} = 584 * (\text{Rating})^{-0.377}$$

$$\text{Cost} = 510 * (\text{load})^{0.465}$$

As kite systems do not have towers comparable to those of conventional turbines – increasing in height with increasing power rating – the second formula is far more useful for our purposes. The overturning moment can be calculated from the force acting on the tether. A tower height of a few meters will be realistic. For MW systems, forces around 1 MN can be expected. A cost comparison example for a conventional turbine and a kite system of each 1 MW shows that the costs and thus the loads are in the same order of magnitude:

$$1000\text{kW} * (584 * (1000\text{kW})^{-0.377}) = 45 \text{ k dollar}$$

$$510 * (500\text{kN} * 3\text{m})^{0.465} = 15 \text{ k dollar}$$

However, the overturning moment might not be the most important factor for the design of a pumping kite foundation. The kite does not pull only in the horizontal direction, but also in the vertical direction. In order to find out if the system can withstand those forces, the weight of the ground station has to be estimated and potentially measures have to be taken to keep the ground station from moving (e.g. anchoring or additional weight). Cost functions for this might be found in the WindPACT study ‘Technical Area 3’.

The foundations used in the formulas mentioned above are squared blocks made of concrete (24 kN or 2.4 tons per m³). The smallest foundation (for a 750 kW machine) is 260 m³ of concrete. It costs 78 k\$ and weighs 624 tons (about 6 MN). So it costs 78/6=13 \$ per kN. The foundation can be assumed sufficiently strong, if it can withstand five times the maximum tether force in vertical direction. The cost function would then be:

$$\text{Cost} = 13 \text{ \$/kN} * 5 * (\text{max tether force [kN]})$$

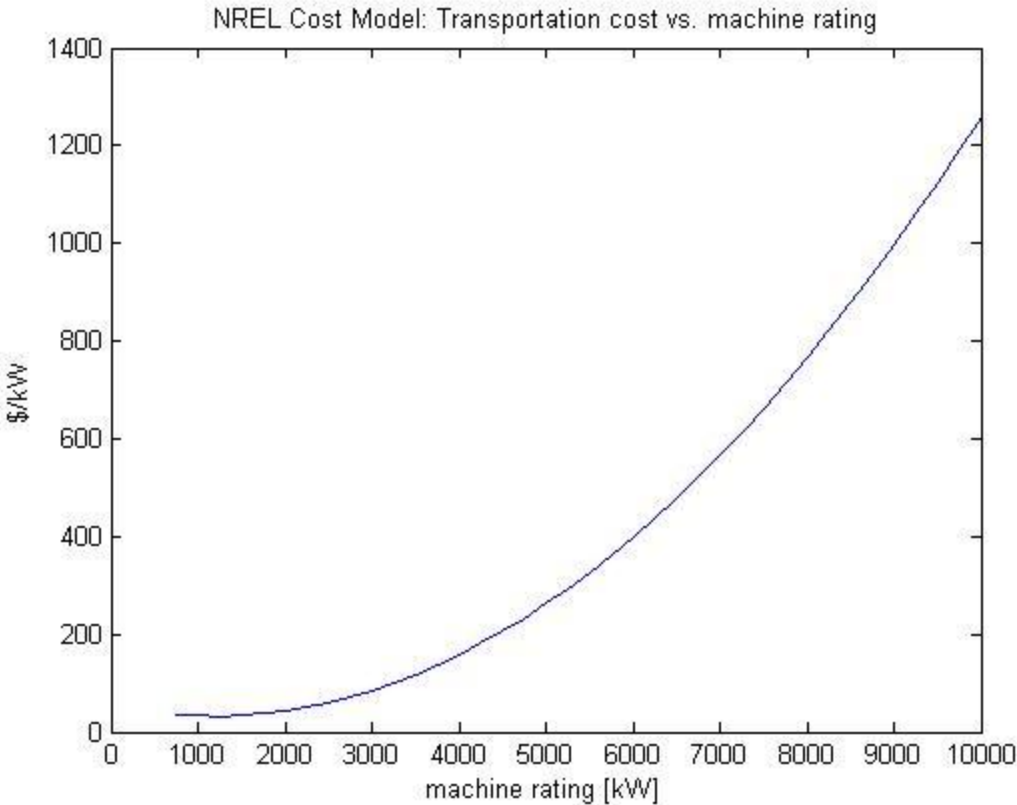
In this formula, it is assumed that the vertical force determines the foundation size and this structure will always be able to withstand the same force in horizontal direction. The associated cost would then be negligible as compared to all other components. To decide if the overturning moment or the vertical pulling force is most important, a decision on the launching/recovery system (height and function of mast/tower) has to be made first.

11.5.3 TRANSPORTATION

The WindPACT study ‘Technical Area 2’ treats logistics of all wind turbine components and compares three scenarios: a current practice scenario and two scenarios with different degrees of an increased on-site assembly of rotor and tower or nacelle components respectively. The third scenario can most likely serve as a basis for transportation cost calculation of pumping kite systems.

All calculations are based on a location in South Dakota, USA. As the analysis for pumping kite systems shall be conducted with wind data from Switzerland, the cost data cannot be directly used. However, it might be possible to derive a cost ratio (conventional/kite) or apply a cost factor (CH/US). Alternatively, one could look for transportation cost data for wind turbines in Switzerland.

The NREL Cost and Scaling Model uses an aggregated cost function for the transportation of all components. It uses rated power as an indicator and rises very quickly with turbine size:



The WindPACT logistics study applies cost curves to each component (Blades, Hub, Nacelle, Tower). Tower transportation contributes the largest part of total cost.

TURBINE RATING (KW)	750	1500	2500	3500	5000
Scenario 1	\$16	\$27	\$519	\$663	\$693
Scenario 2	\$16	\$27	\$35	\$48	\$51

Figure 3-7. Scenario 1 and Scenario 2 tower transportation cost comparisons
 Costs based on transport from Shreveport, Louisiana (see Appendix P, page 4)

Instead of using conventional turbine transportation as a reference, one could also use standard container shipping costs.

11.5.4 ROADS, CIVIL WORK

For conventional wind farms, the two major cost factors in this category are crane pads and roads. In WindPACT ‘Technical Area 4’, three options for roads were considered (cost for 1 to 3 MW):

1. Six meter wide gravel road; assembly at the site (10 to 20 \$/kW)
2. Eight to ten meter wide, paved road; small cranes and maintenance equipment can be moved (20 to 40 \$/kW)
3. Nine to twelve meter wide, paved road; largest cranes can be moved from site to site (30 to 60 \$/kW)

For the operation of large cranes, a crane pad is needed (24 to 28 \$/kW).

A wind farm for pumping kites would need only gravel roads and no crane pads, because no tower has to be erected. The gravel road is stated to cost 1290 \$ per 7.8 m (165 \$/m). Each machine has to be connected via a road to its closest neighbor at distance d:

$$\text{Total Cost} = d \cdot 165 \$ = d \cdot 165 \$$$

For a distance d of 100 meter, this would result in costs for roads of 16.5 k\$.

11.5.5 ASSEMBLY AND INSTALLATION

In WindPACT ‘Technical Area 2’ (Logistics), turbine assembly was treated together with crane relocation. Three scenarios are considered with pre-assembled parts, on-site tower assembling and on-top-of-tower gearbox and generator assembling. The first scenario was chosen as a basis of comparison. The assembly costs per turbine range from 13 k\$ to 70 k\$ (0.75 to 10 MW) - driven mainly by ‘the height increase and to a lesser extent the increase in component sizes’. As pumping kite ground stations do not increase significantly in height for increasing machine ratings and are significantly less tall than a 750 kW wind turbine, 13 k\$ per machine could be seen as an upper limit for MW size systems. Cranes are not required. The cost for assembly and installation will thus not be higher than 13 \$/kW.

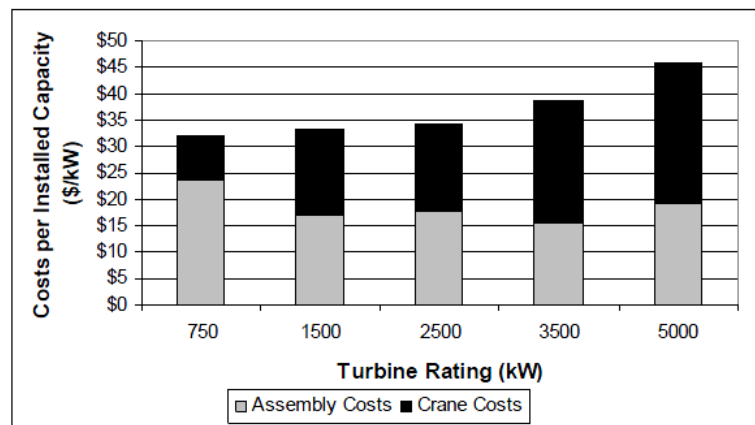


Figure 4-6.Scenario 1 assembly and crane costs
(See Appendix P, page 6)

FIGURE 11-5 COST FOR ASSEMBLY AND CRANE

The NREL Cost and Scaling Model (Fingersh et al., 2006) uses a cost function based on hub height and rotor diameter. This seems not to be a very practical tool to use for pumping kite systems, because they have no tower or rotor.

If the ground station is transported as one piece, assembly cost can be avoided completely.

11.5.6 ELECTRICAL INTERFACE, CONNECTIONS

In the WindPACT BOS cost study (Technical Area 4), two different voltage levels for each turbine size were considered – 25 kV for all sizes and 15 kV for the smallest and 35 kV for the larger ones. The 25 kV option for 2.5 MW turbines was the one with lowest cost (3762 k\$ for the 50 MW wind farm). The resulting specific cost can be directly applied to a pumping kite wind farm of similar size. As machines around 1 MW are considered, the cost is assumed to be 80 \$/kW for the lower limit and 100 \$/kW for the upper limit.

750 kW machines	91 \$/kW
2.5 MW machines	75 \$/kW
10 MW machines	74 \$/kW

TABEL 11-8

11.5.7 MISCELLANEOUS INFRASTRUCTURE

This category includes communications, lighting, meteorological towers an administrative building. The cost estimates are taken over from the WindPACT BOS cost study.

System Component	Plant Size			
	750 kW	2,500 kW	5,000 kW	10,000 kW
Communications	823	380	335	209
Tower Lighting	660	200	100	50
Meteorological Towers	74	88	106	160
Maintenance Building	156	156	156	156
Subtotal Misc. (\$x1,000)	\$ 1,713	\$ 824	\$ 697	\$ 575

For 2.5 MW systems in a 50 MW wind farm the specific costs are 16 \$/kW. The cost for lighting on kites could be similar to the costs for tower lighting. It might however increase to 30 \$ / kW because for instance the weight of the installation has to be decreased drastically.

11.5.8 ENGINEERING, PERMITS

This category includes land, overhead and contingency. In the WindPACT Turbine Study (Technical Area 4) a total of 4.6 and 4.4 M\$ for a 50 MW wind park with small (<1MW) or large (>5MW) turbines, respectively, is assumed. For the overhead cost, only BOS-items are considered. Land costs only concern the land needed for transmission lines, maintenance building and substation, but not the land for the wind farm itself.

The NREL Cost Model uses a cost function that would lead to a total of 3.5 M\$ and refers to the Turbine Study described above.

$$$/kW = 9.94 \cdot 10^{-4} \cdot P + 20.31$$

The specific cost (\$/kW) increases with increasing machine rating. This might be due to increasing complexity for larger machines. In the NREL Cost Model, for an example of a 1.5 MW machine in a 50 MW wind farm, 32 k\$ is stated for engineering and permits. This does not fit with the formula stated above. It seems, the cost for a single turbine (not in a farm) was calculated.

In order to take the large uncertainties for engineering and permits costs for pumping kite wind farms into account, a rather big range around the above stated value is chosen:

$$\text{Cost for Engineering and Permits} = C_{EP} * (0.005 * P + 10) * P$$

with $C_{EP} = 1$ for the lower limit and $C_{EP} = 3$ for the upper limit. This results for instance for a 1 MW machine in a range from 15000 to 45000 \$.

11.6 LEVELIZED REPLACEMENT COST

The Levelized Replacement Cost (LRC) is the cost factor associated to replacements and overhaul of major parts of an installed system. The LRC of a pumping kite wind farm differs significantly from that of a conventional wind farm, because kite and tether have to be replaced regularly and on the other hand, there is no work that has to be done in great heights.

Cost formulas will be developed for the tether and the wing, because those wear out quickly and the wear depends strongly on their usage.

11.6.1 TETHER

The tether wears out due to UV-light and due to the repeated bending over the drum. The latter affects only the lower part of the tether – a length that corresponds to the applied pumping length. It is assumed that there is no additional bending that significantly affects tether wear.

In the following analysis, it is assumed that UV degradation is not an issue because the tether first wears out due to bending. The combination of both effects should be researched in more detail, but for this study, the simple approach seems sufficient.

There has been done some research on bending cycles of Dyneema at Stuttgart University (Vogel & Wehking, 2004). For calculating cost, the number of bending cycles has to be known. In general, it depends on the specific tether force S/d^2 in N/mm^2 and the diameter ratio D/d between drum and tether.

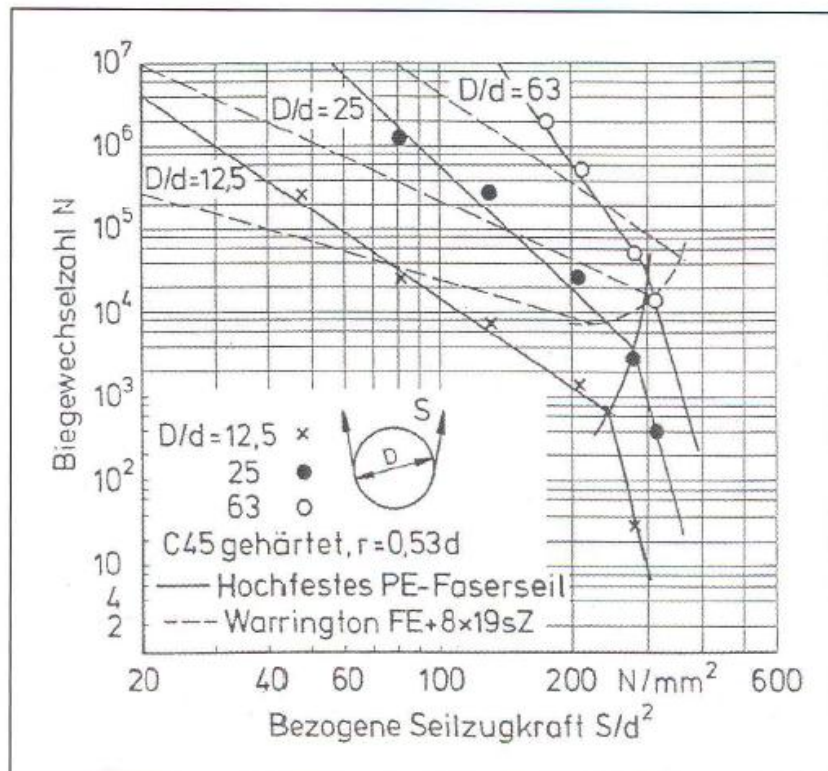


Bild 3 Bruchbiegewechselzahlen eines Faserseils mit hochfesten Polyethylenfasern Dyneema SK60, [2]

The graph from (Vogel & Wehking, 2004) shows this relationship for tether diameter $d=8\text{mm}$ Dyneema SK60. An optimization considering tether cost and all possible diameter ratios and specific tether forces could be conducted. Instead, the analysis could be kept simple by just choosing reasonable numbers for both of the parameters (S/d^2 and D/d) and keeping them constant for all different machine designs. The resulting bending cycles N can be derived from the graph above and would also be constant for all machines.

Example 1: $D/d=25$; $S/d^2=90$; $N=10^6$

Example 2: $D/d=63$; $S/d^2=200$; $N=10^6$

In order to do this, the gear ratio would have to be changed for each design. Another option is to choose a value for the specific tether force (e.g. 200 N/mm^2) and calculate the bending cycles as a function of the diameter ratio. This would allow keeping the gear ratio constant and choosing a drum diameter according to the desired tether speed. The number of bending cycles as a function of D/d can be estimated by looking up three values at 200 N/mm^2 from the graph above and interpolating in between:

$$D/d = [12.5 \quad 25 \quad 63]$$

$$\log N = [1.5 \quad 20 \quad 600] \cdot 1000$$

$$\log N = 7 + 0.1 \cdot \frac{D}{d}$$

We assume that only the bending over the winch affects the tether life and line handling has no effect. This can be realized approximately by using very small forces and/or very large wheels for the line handling. In that case, the number of bending cycles is equal to the number of power cycles when assuming a constant force throughout all cycles. A more accurate proxy would be considering also the actual power production at each hour. An increase in power production is approximately equal to either an increase in tether force or an increase in tether speed. Both relate approximately linearly to the lifetime of the tether. One can thus assume that each tether can produce a certain amount of energy before it has to be replaced, no matter at which wind speed it operates. Using the nominal average cycle power P_{cyc} as an indicator for traction power, the energy that one tether can produce becomes:

$$E = P_{\text{cyc}} / \text{cycles_per_h} * N$$

And the levelized cost of tether replacement is then:

$$\text{Cost/kWh} = \text{Cost_tether} / (N / (\text{cycles per h}) * P_{\text{cyc}})$$

The cycles per hour at nominal operation can be estimated once the nominal speed v_{nom} , pumping length L_P and the asymmetry factor AF are known:

$$\text{Cycles per hour} = 3600 * v_{\text{nom}} / L_P * AF / (1 + AF)$$

Example 2: 200 m of tether with diameter 35 mm and area 1000 mm^2 (for a $1\text{MW} / 200\text{kN}$ machine) would cost 8000 € (see Component Cost Model), would have specific force of 200 N/mm^2 . On a 2.2 m drum it could do about $6 * 10^5$ bending cycles. The LRC would be: $8000\text{ \$} / (10^6 / 100\text{ h} * 0.6\text{ MW}) = 2.2\text{ \$} / \text{MWh}$.

There is an upper part of the tether that is airborne most of the time and is only coiled up on the winch for landing the kite. This part is likely to wear out much slower and more due to UV-light than due to loading. It might be beneficial to use a smaller diameter tether for this part to reduce

weight and drag. However, it is assumed, that the upper part has the same diameter and is replaced together with the lower part of the tether.

	Minimum Cost	Maximum Cost
Tether Cost [\$/kWh]	$\text{Cost_tether} / (N / (\text{cycles per h}) * P_{\text{cyc}})$	
Cycles per hour	$3600 * v_{\text{nom}} / L_P * AF / (1 + AF)$	

TABEL 11-9

11.6.2 KITE

The kite is likely to wear out relatively quickly. It is made of thin material that is exposed to UV-light, rain, frost and heat. Before it degrades to a point where it cannot withstand the required forces anymore, it has to be replaced. At the moment, it is hard to tell, what such a kite will look like. So only some very rough assumptions can be made.

Some issues to be solved:

- What is the critical factor for wear-out? (UV, loading, frost, ...)
- Will the complete kite be replaced or only parts?
- Will the kite be flexible, semi-rigid or rigid?

VARIABLE LOADING

The kite cost per year depends on the frequency of replacement and thus on the operation of the kite. If it is used very frequently and high loads are applied, it wears out quicker. The available airborne hours per kite depend on the materials used and their resistance against UV-radiation and loading induced wear. It is assumed that loading will be the crucial factor and UV-stability will not be an issue. Furthermore it is assumed that any kite has a maximum area loading of 0.5 kN/m² or 2 kN/m² in the current and future scenario respectively.

A simple way of estimating the frequency of replacement would be to assume constant loading and consider all hours the kite is airborne as equivalent. Alternatively, the average power production could be taken as a proxy for the loading and the cost for kite replacement could then directly be related to the produced power. The most important shortcomings of this approach are: At low wind speeds the loading might already be at its maximum while the reel-out speed and thus the power production is still below nominal. At high wind speeds, the nominal power is already reached during reel-out, but the average power gets lower as the power consumption during retraction increases. Despite these facts, the described approach is used because it is simpler than relating the frequency of replacement to the force on the tether and the error is most likely rather small. Taking into account that a system might use only a fraction of the maximum possible kite loading at nominal production:

$$\text{kite loading factor} = \text{klf} = \text{system nominal area loading} / \text{kite maximum area loading}$$

the energy produced in 1000 hours of operation at maximum area loading can be approximated by:

$$P_{\text{max_cyc}} / \text{klf} * 1000 \text{ hours} = \text{energy produced in 1000 maximum area loading hours}$$

Using the kite loading factor, the energy that one kite can produce is dependent on the force-to-power ratio of the system it is used on: A higher nominal reel-out speed leads to a lower force and thus less wear-out of the kite at the same power production level. The levelized cost of replacement for the wing is:

$$\text{Cost/MWh} = \text{Cost_wing} / (1000 \text{ h} * \text{P_max_cyc}[\text{MWh}]) * \text{klf}$$

$$\text{Cost/MWh} = 20 * A^{3/2} / (1000 \text{ h} * \text{P_max_cyc}[\text{MWh}]) * \text{klf}$$

e.g.: $600 \text{ \$} / 1,000 \text{ h} / 10 \text{ kW} * 1 = 60 \text{ \$} / \text{MWh}$ (for a 10 m² Kite)

e.g.: $56.5 \text{ k\$} / 1,000 \text{ h} / 1 \text{ MW} * 1 = 56 \text{ \$} / \text{MWh}$ (for a 200 m² Kite)

or with the optimistic formula (see Component Cost Model):

e.g.: $1.2 \text{ k\$} / 10,000 \text{ h} / 10 \text{ kW} * 1 = 12 \text{ \$} / \text{MWh}$ (for a 10 m² Kite)

e.g.: $113 \text{ k\$} / 10,000 \text{ h} / 1000 \text{ kW} * 1 = 11 \text{ \$} / \text{MWh}$ (for a 200 m² Kite)

	Minimum Cost	Maximum Cost
Wing Cost [€]	Current: 10; Future: 20	Current 24; Future 48
Wing Cost [€/kWh]	$\text{Wing_cost} / (\text{Lifetime}[\text{h}] * \text{P_max_cyc}) * \text{klf}$	

TABEL 11-10

11.7 OPERATION AND MAINTENANCE COST

In the NREL Cost Model the cost for O&M is assumed to be 7 \$/MWh. It is however mentioned that this value can differ a lot, even for identical machines, depending on wind farm size, tower height or other operational factors. Values from 5 to 10 \$/MWh have been reported. The kite makes a pumping kite generator more vulnerable and probably leads to higher O&M cost. On the other hand, the whole drivetrain is ground based and easily accessible. Furthermore, the avoidance of a gearbox makes the drivetrain much more reliable. Also, replacing the kite or the tether is rather easy. Still it is assumed that there are one to two people who look for 20 machines at all times (150,000 to 400,000€/year). Additionally, a variable cost factor of 5 to 10 Euro/MWh is assumed in order to cover the whole range of possible cases seen in conventional wind farms.

		Minimum Cost	Maximum Cost
Annual	O&M	12,150	32,400
[€/a/machine]			
Variable	O&M	5	10
[€/MWh]			

TABEL 11-11 O&M COST IN 2012 EUROS

11.8 LAND LEASE COST

In general, land lease costs vary strongly for different locations. Important influencing factors can be the local wind resource, potential electricity prices, the current use of the land and the accessibility of the site. The land lease cost have been directly taken over from (Fingersh et al., 2006):

$$\text{LLC cost} = 1.08 \text{ \$/MWh}$$

Expressing land lease costs in \$/MWh appears inappropriate because they do not change with energy production, however, using this value allows to compare results for the LCOE directly to the results from (Fingersh et al., 2006) for conventional wind turbines, without the influence of land lease costs. In 2012 Euros, the land lease cost would be 1.03 €/MWh

The land lease cost must be expressed in \$ or €/m² when doing an analysis of optimal turbine spacing. In this case it might also be sense to use a limited (fixed) area, because this is closer to reality. The important factor is then probably rather the limited space than the cost per square meter of land.

11.9 CALCULATING LEVELIZED COST

The following formula is used to calculate the Levelized Cost of Energy:

$$LCOE = \frac{(ICC * FCR)}{AEP} + LRC + O\&M + LLC$$

The initial capital cost (ICC) consists of all component costs and the balance of station costs (BOS). Levelized replacement cost (LRC), operating and maintenance cost (O&M) and land lease cost (LLC) are expressed in €/MWh.

An FCR of **11.85 %** is used, the same as in the *NREL Wind Turbine Design Cost and Scaling Model*. In this way the results can be compared to the results for horizontal wind turbines calculated in this study. The FCR includes construction financing, financing fees, return on debt and equity, depreciation, income tax, and property tax and insurance. Subsidies are not considered. They would be a crucial factor when assessing the feasibility of a specific project, but for comparing pumping kite technology to conventional wind farms, subsidies are not so important, because we can assume that they would be similar for both. The FCR is based on a typical economic lifetime of **20 years**, which is realistic for pumping kite generators as well.

11.10 ELECTRICITY MARKET

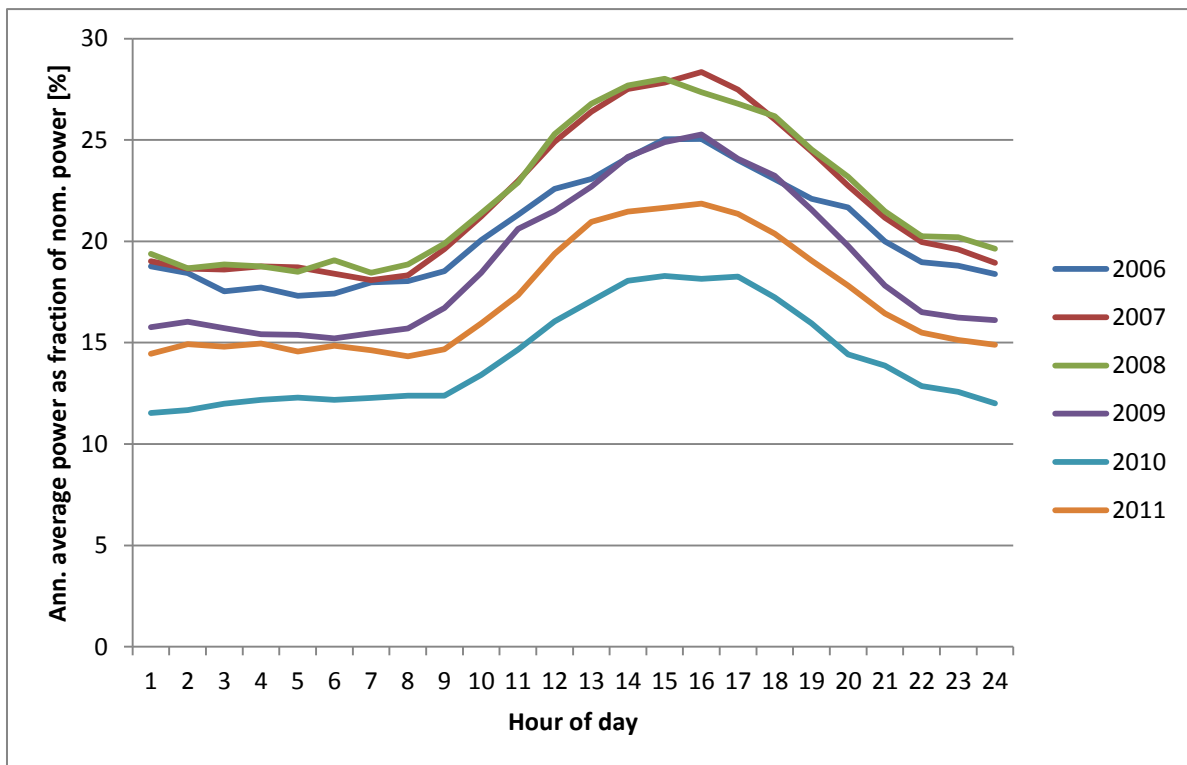


FIGURE 11-6 POWER PRODUCTION PER HOUR OF DAY, TYPICAL WIND TURBINE IN NL

The data for Figure 11-6 has been collected by Windunie Trading BV. The turbine statistically produces significantly more power during daytime than at night. As electricity demand is higher during daytime, the market price usually also is higher. This means that the difference between the average market price of electricity and the wind weighted average (see chapter 2.5) is unlikely to be a result of not coinciding electricity demand and wind power supply. On the contrary, it probably even counteracts the average price decrease resulting from coinciding power production of all Dutch wind farms.

12 REFERENCES

- Archer, C. L., & Caldeira, K. (2009). Global Assessment of High-Altitude Wind Power. *Energies*, 2(2), 307–319. doi:10.3390/en20200307
- BMU. (2012). EEG 2012, Vergütungsdegression. BMU.
- BTMConsult. (2008). Windfarm management. Retrieved from http://www.btm.dk/news/wind+turbine+prices+soar/?s=9&p=1&n=22&p_id=1
- Bolinger, M., & Wiser, R. (2011). *Understanding Trends in Wind Turbine Prices Over the Past Decade*.
- Breuer, J. C. M., & Luchsinger, R. H. (2010). Inflatable kites using the concept of Tensairity. *Aerospace Science and Technology*, 1–14.
- Bywaters, G., John, V., Lynch, J., Mattila, P., Norton, G., & Stowell, J. (2005). *Northern Power Systems WindPACT Drive Train Alternative Design Study Report Northern Power Systems WindPACT Drive Train Alternative Design Study Report*.
- Consortium for Small Scale Modeling. (2011). Operational Applications within COSMO. Retrieved from <http://www.cosmo-model.org/content/tasks/operational/meteoSwiss/default.htm>
- Corotis, R. B., Sigl, A. B., & Klein, J. (1978). VELOCITY MAGNITUDE AND PERSISTENCE, 20(v), 483–493.
- Fingersh, L., Hand, M., & Laxson, A. (2006). Wind Turbine Design Cost and Scaling Model Wind Turbine Design Cost and Scaling Model. *Contract*, 29(December), 1–43. doi:10.1016/j.advwatres.2006.01.003
- GWEC. (2009). Global Wind Energy Council. Retrieved May 21, 2012, from <http://www.gwec.net/index.php?id=148>
- Global Energy Concepts. (2001). *WindPACT Turbine Design Scaling Studies Technical Area 3 – Self-Erecting Tower and Nacelle Feasibility*. *Energy*. Retrieved from <http://scholar.google.com/scholar?hl=en&btnG=Search&q=intitle:WindPACT+Turbine+Design+Scaling+Studies+Technical+Area+3+?+Self-Erecting+Tower+and+Nacelle+Feasibility#1>
- Griffin, D. A. (2001). WindPACT Turbine Design Scaling Studies Technical Area 1 – Composite Blades for 80- to 120-Meter Rotor WindPACT Turbine Design Scaling Studies Technical Area 1 – Composite Blades for 80- to 120-Meter Rotor. *National Renewable Energy Laboratory*, (April). Retrieved from <http://www.nrel.gov/docs/fy01osti/29492.pdf>
- Hennessey, J. P. (1977). Some Aspects of Wind Power Statistics, Hennessey.pdf. *Journal of Applied Meteorology*, 16(2).
- Houska, B. (2007). *Robustness and Stability Optimization of Open-Loop Controlled Power Generating Kites*. Ruprecht-Karls-Universität Heidelberg.
- IEA. (2010). Key World Energy Statistics.

- Junginger, M., Sark, W. van, & Faaij, A. (2010). *Technological Learning in the Energy Sector: Lessons for Policy, Industry and Science* (p. 333). Edward Elgar Publishing.
- Kempton, W., Archer, C. L., Dhanju, A., Garvine, R. W., & Jacobson, M. Z. (2007). Large CO₂ reductions via offshore wind power matched to inherent storage in energy end-uses. *Geophysical Research Letters*, 34(2), 1–5. doi:10.1029/2006GL028016
- Loyd, M. L. (1980). Crosswind Kite Power. *Energy*, 4(3), 106–111.
- Luchsinger, R. (2012). Pumping Kite Power Optimization, Internal Report.
- Luchsinger, R. H. (2010). Weight matters : Tensairity kites, (September).
- Malcolm, D. J., & Hansen, A. C. (2006). WindPACT Turbine Rotor Design Study. *National Renewable Energy Laboratory*, (April), 164–167. Retrieved from <http://www.nrel.gov/docs/fy02osti/32495a.pdf>
- Manwell, J. F., McGowan, J. G., & Rogers, A. L. (2009). *Wind Energy Explained. Theory, Design and Application* (Second.). Wiley.
- Marchand, J. (2011). *Master Thesis MSE Energy production with kite*. Fachhochschule Nordwestschweiz.
- MeteoSwiss. (2012). COSMO. Retrieved from <http://www.meteoswiss.admin.ch/web/en/weather/models/cosmo.html>
- Miller, L. M., Gans, F., & Kleidon, A. (2011). Jet stream wind power as a renewable energy resource: little power, big impacts. *Earth System Dynamics*, 2(2), 201–212. doi:10.5194/esd-2-201-2011
- Poore, R., Global, T. L., & Concepts, E. (2003). *Alternative Design Study Report : WindPACT Advanced Wind Turbine Drive Train Designs Study Alternative Design Study Report : WindPACT Advanced Wind Turbine Drive Train Designs Study*.
- Risø National Laboratory. (2011). Wind Atlas. Retrieved June 24, 2012, from <http://www.windatlas.dk/europe/landmap.html>
- Robertson, A. N., & Jonkman, J. M. (2011). Loads Analysis of Several Offshore Floating Wind Turbine Concepts, (October).
- Shafer, D. A., Strawmyer, K. R., Conley, R. M., Guidinger, J. H., Wilkie, D. C., & Zellman, T. F. (2001). WindPACT Turbine Design Scaling Studies : Technical Area 4 — Balance-of-Station Cost. *National Renewable Energy Laboratory*, (July). Retrieved from <http://www.nrel.gov/docs/fy01osti/29950.pdf>
- Sky Windpower. (2012). Sky Windpower. Retrieved June 3, 2012, from http://www.skywindpower.com/science_generators.htm
- Smith, K. (2001). *WindPACT Turbine Design Scaling Studies Technical Area 2 : Turbine , Rotor , and Blade Logistics WindPACT Turbine Design Scaling Studies Technical Area 2 : Turbine , Rotor , and Blade Logistics*.

Street, M. (2004). INNOVATIVE DESIGN APPROACHES FOR LARGE WIND TURBINE BLADES
WindPACT Blade System Design Studies. *National Renewable Energy Laboratory*, (May), 48.

U.S. Department of Energy. (2011). Wind Powering America. Retrieved June 1, 2012, from
http://www.windpoweringamerica.gov/wind_maps_none.asp

Vogel, W., & Wehking, K. (2004). Hochfeste, laufende Faserseile in der Fördertechnik und
Logistik. *Euroseil*, (3), 1–5.

Windunie. (2012). Windmaand 155.